Imaging with PET and SPECT

Thorsten Poethko

Nuklearmedizinische Klinik und Poliklinik
und
Institut für Radiochemie
Technische Universität München

Basics of Radionuclide Production

Knowledge of production process

Purification

Recovery of target material

Analytical methods (quality control)

Radionuclide Production

(A) **Cyclotron** **(ca. 250 world-wide)**

(Ion accelerator)

(B) **Reactor** **(ca. 250 Research reactors world-wide)**

(C) **Generators**

General Aspect

Cyclotron-nuclides:
mostly neutron pure

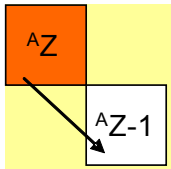

Positron emission: ß+-decay

Electron capture: EC-decay

Reactor-nuclides:
neutron rich

Emission of electron ß⁻-decay

Production of commonly used PET-Nuclides via Compact Cyclotron

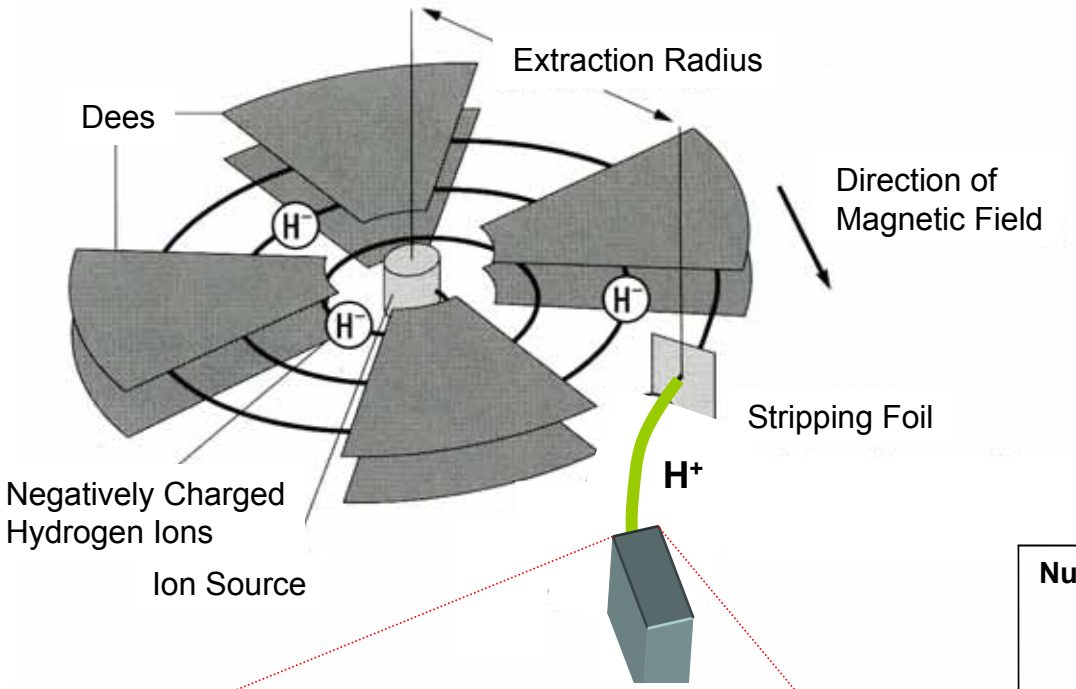

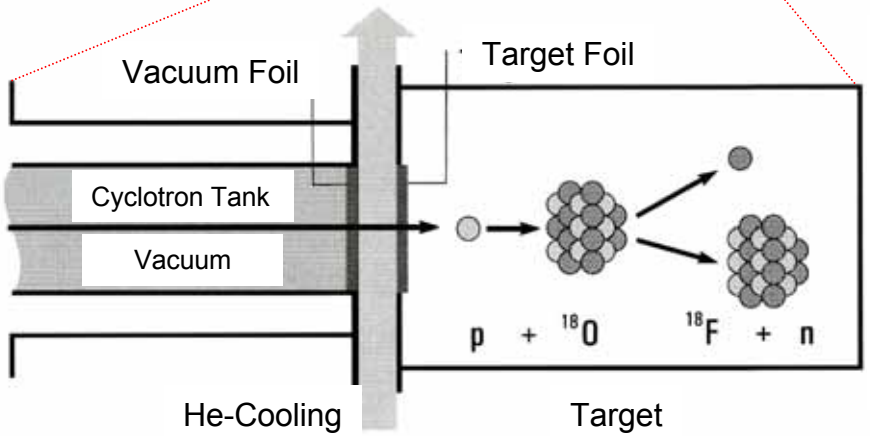

Nuclide	$T_{1/2}$ (min)	Nuclear-Reaction	Energy (MeV)	Mode of decay [%]	Target product
^{11}C	20.4	$^{14}N(p,\alpha)$	13 → 3	β^+ (99.8)	$^{11}CO_2$ ^{11}CO
^{13}N	10.0	$^{16}O(p,\alpha)$	16 → 7	β^+ (100)	$^{13}NO_2^-$ $^{13}NO_3^-$
^{15}O	2.0	$^{15}N(p,n)$	10 → 0	β^+ (99.9)	$^{15}O_2$
^{11}C	109.6	$^{18}O(p,n)$	16 → 3	β^+ (97)	$^{18}F_{aq}^-$ $^{18}F_2$

Selection of Radionuclide

Half-life comparable with kinetics of physiological process ?
(too short, too long)

Do the nuclear and physical properties fulfill the special demands ?
(e.g. pure β^+ - Emitter)

Labeling chemistry compatible with targeting ?
(e.g. metalated CNS-ligands)

Patient dose acceptable ?
(CNS-ligands: C-11 or F-18)

Nuclide availability ?
(Generator, cyclotron, energy range)

PET-Radionuclides

Isotope	Half-life [h]	Positron percentage branching $\%\beta^+$	Maximum positron energy [MeV] $E\beta^+_{max}$	Intrinsic spacial resolution loss [mm]	Comments
^{18}F	1,8	96,9	0,63	0,7	
^{55}Co	17,5	76	1,50	1,6	$T_{½,D}$ = 2,6 y
^{61}Cu	3,4	61	1,22	1,5	
^{64}Cu	12,7	18	0,65	0,7	
^{66}Ga	9,5	57	4,15	-	
^{68}Ga	1,14	89	1,90	2,4	G: ^{68}Ge / 271d
^{75}Br	1,6	71	1,72	2,2	$T_{½,D}$ = 120 d
^{76}Br	16,2	54	3,94	5,3	
^{86}Y	14,7	33	3,14	1,8	
^{110m}In	1,15	62	2,20	3,0	G: ^{110}Sn / 4,1 h
^{120g}I	1,35	56	4,59	5,4	
^{124}I	100,3	23	2,14	2,3	

Resolution Limitation due to Positron Energy

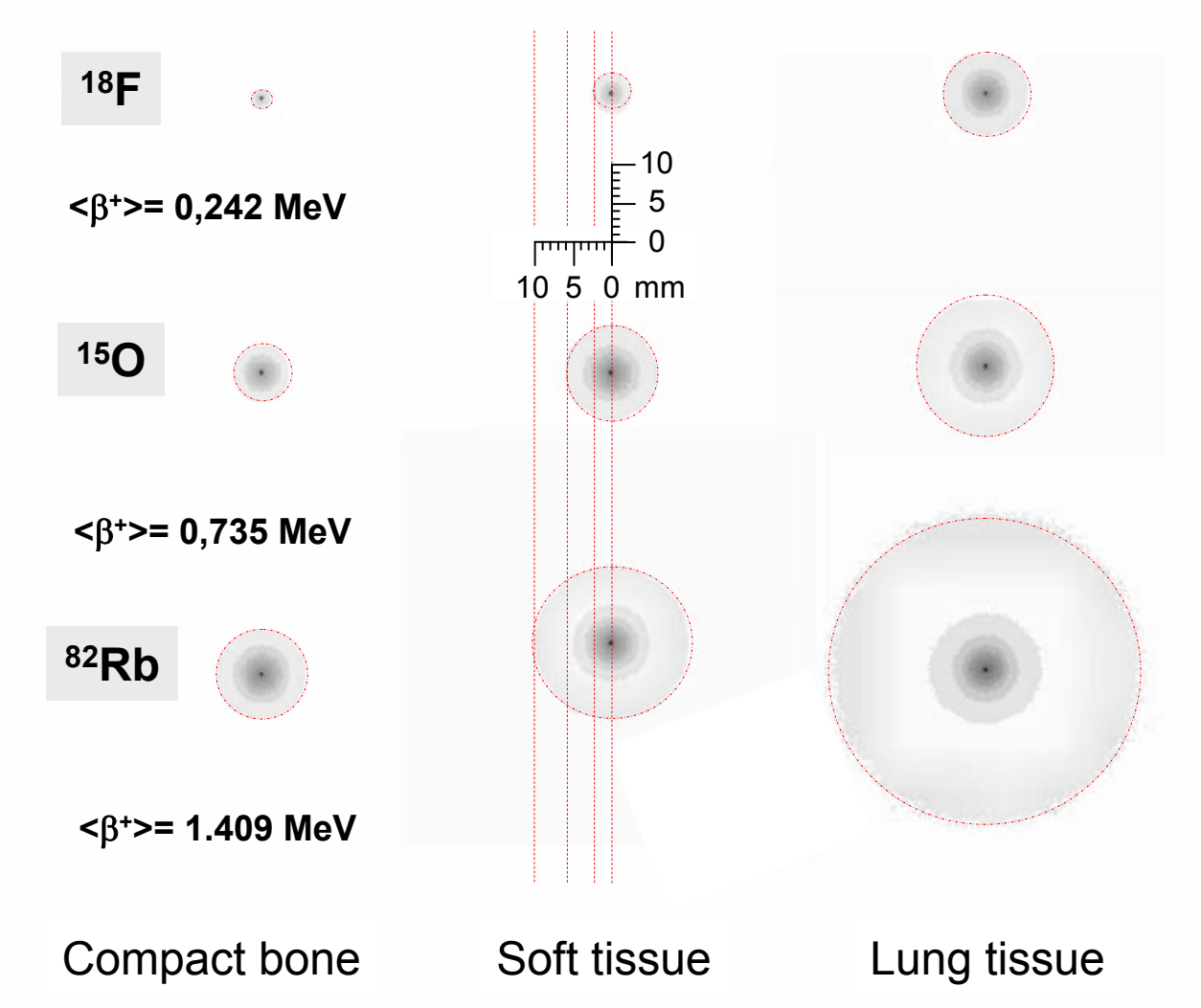

Positron-Emission

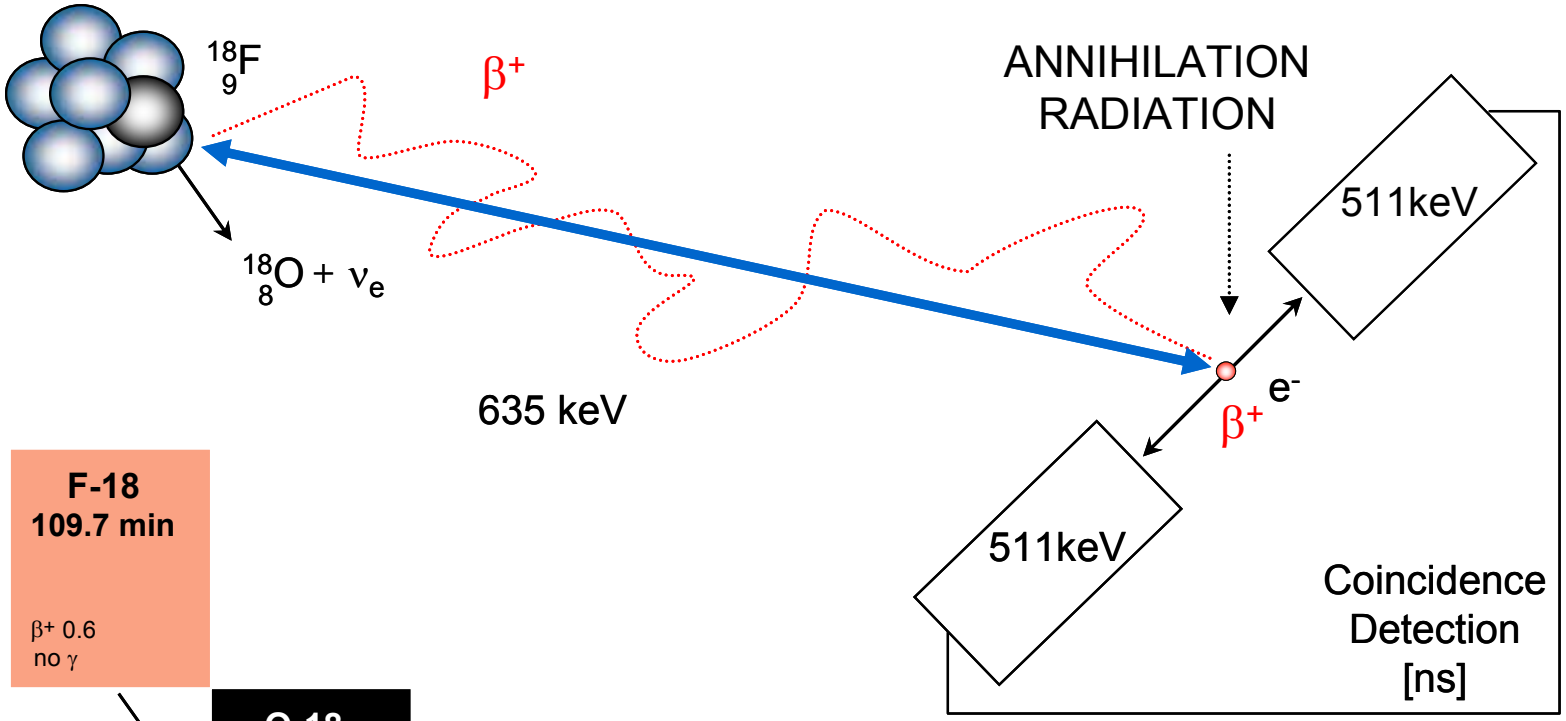

F-18
109.7 min

β^+ 0.6
no γ

O-18
0,200

σ 0.00016

Production of F-18

Nuclear reaction	$^{18}O(p,n)^{18}F$	$^{16}O(^{3}He,n)^{18}F$	$^{20}Ne(d,\alpha)^{18}F$	$^{18}O(p,n)^{18}F$
Target	$H_2{}^{18}O$	H_2O	Ne (0.1-0.2% F_2, 18 bar)	$^{18}O_2$ (20 bar) (2. + 0.1% F_2)
Energy range of bombarding particle [MeV]	16 → 0	36 → 0	11.2 → 0	10 → 0
Chemical form	$[^{18}F]F_{aq}^-$	$[^{18}F]F_{aq}^-$	$[^{18}F]F_2$	$[^{18}F]F_2$
Thick target yield [MBq $\mu A^{-1} h^{-1}$]	2.200	250	350-450	~350
Specific activity [TBq $mmol^{-1}$]	40×10^3	40×10^3	0.04–0.4	0.04-2

- **Mainly produced via $^{18}O(p,n)^{18}F$-reaction**
- **Product:** **$^{18}F_{aq}^-$ with high specific activity and up to 100% radiochemical yield, compared to $[^{18}F]F_2$ with low specific activity and max. 50% radiochemical yield**

^{18}F-Fluoride Chemistry

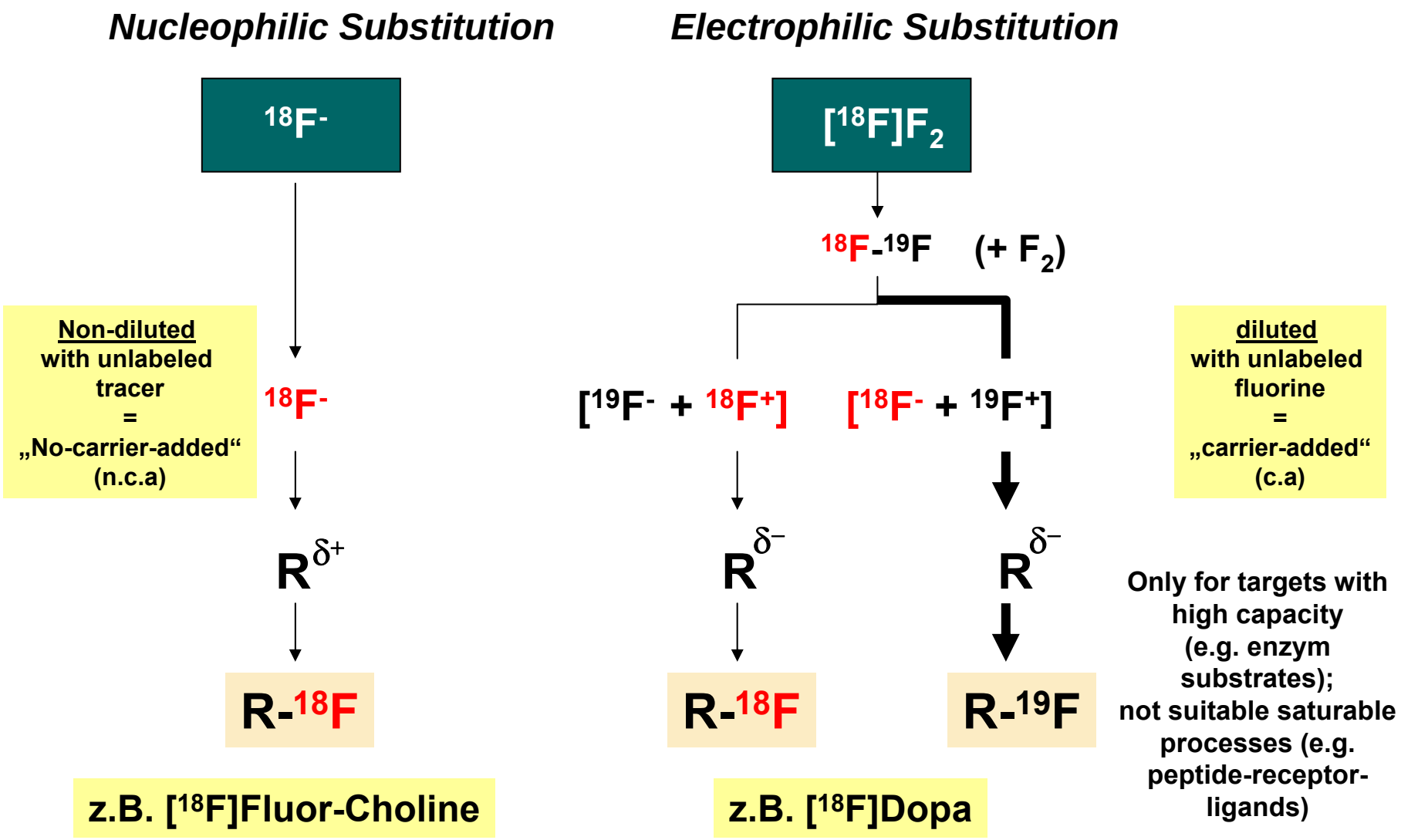

Production Scheme: Radiopharmaceutical Production

Cyclotron und on-line synthesis

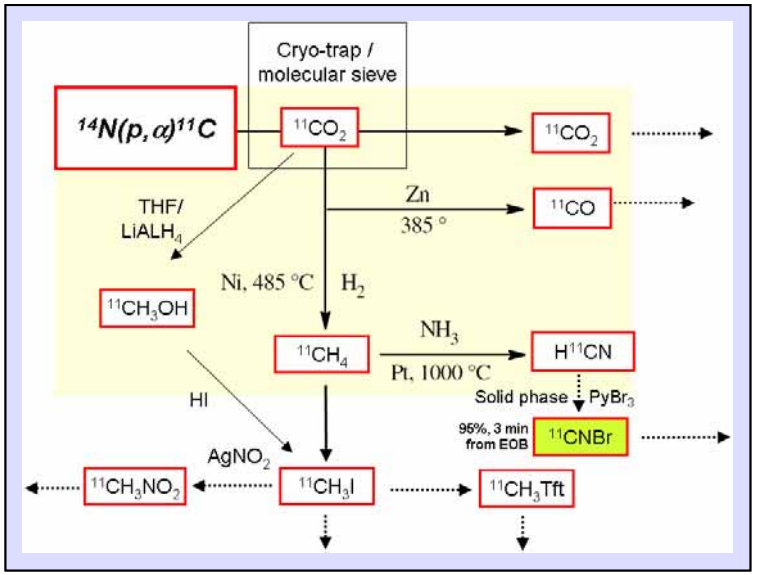

Automatic production

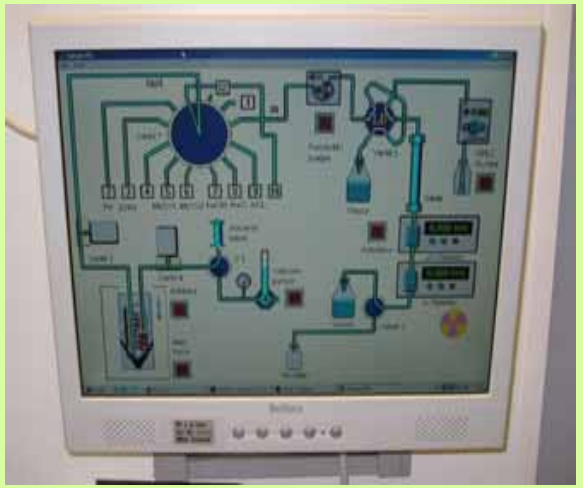

Quality control

Application

Automatic Synthesis

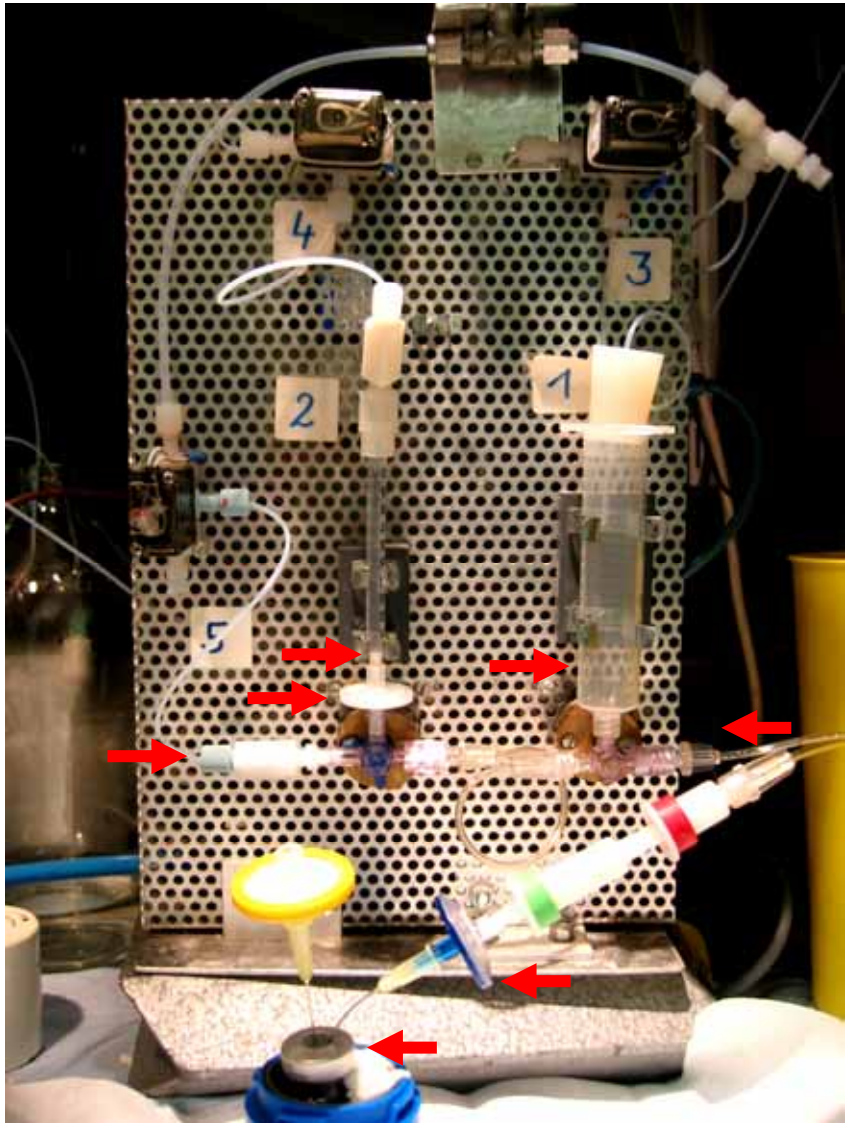

^{11}C-Methionine Production

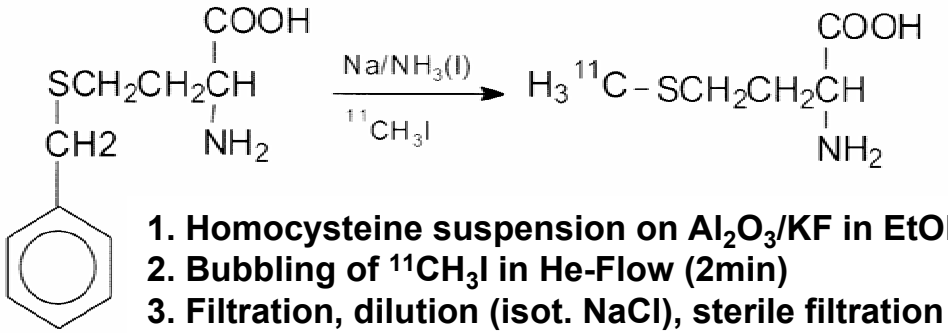

1. Homocysteine suspension on Al_2O_3/KF in EtOH
2. Bubbling of $^{11}CH_3I$ in He-Flow (2min)
3. Filtration, dilution (isot. NaCl), sterile filtration

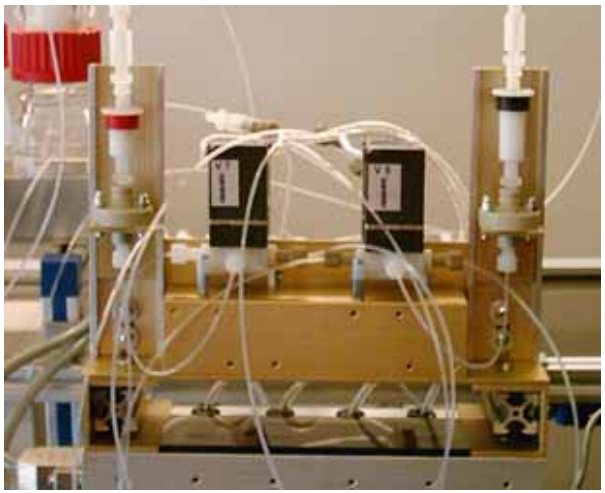

Generators for Positron Emission

Isotope	Half-life	Mode of decay	E_{β^+} [keV]
^{68}Ge	271 d	EC (100%)	
↓			
^{68}Ga	68 min	β^+ (90%), EC (10%)	1900
^{62}Zn	9.2 h	β^+ (93%), EC (7%)	660
↓			
^{62}Cu	9.7 min	β^+ (98%), EC(2%)	2930
^{82}Sr	25 d	EC (100%)	
↓			
^{82}Rb	1.3 min	β^+ (96%), EC (4%)	3350

Structure of „non-isotopic“ Radiopharmaceuticals

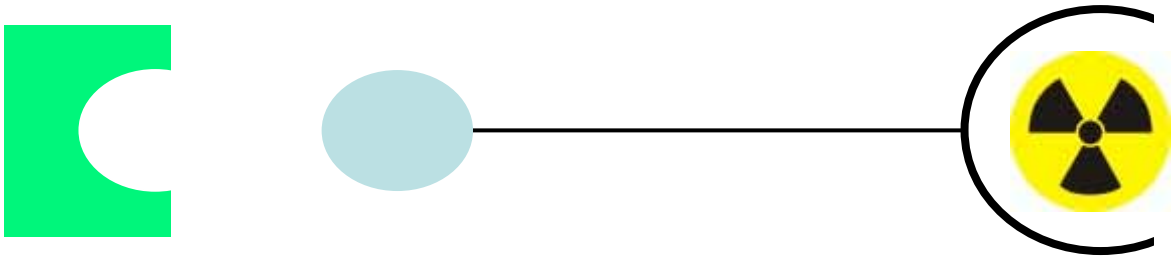

Address, Target	**Pharmacophor, biospecific binding**	**Spacer, Linker**	**Labeling, Label**
Intra-/Extracellular Receptors Transporter Enzyme Antigens RNA …	Small org. Molecules Peptidomimetics Peptide Protein Antibody Complex (Ions)	Metabolic stabile Metabolic labile Enzymatic cleavable Hydrolytic sensitive pH sensitive	Covalent Complex Statically distributed Defined bondage No-carrier-added Carrier-added

Peptide, Protein and Macromolecule Labeling with Radiometals

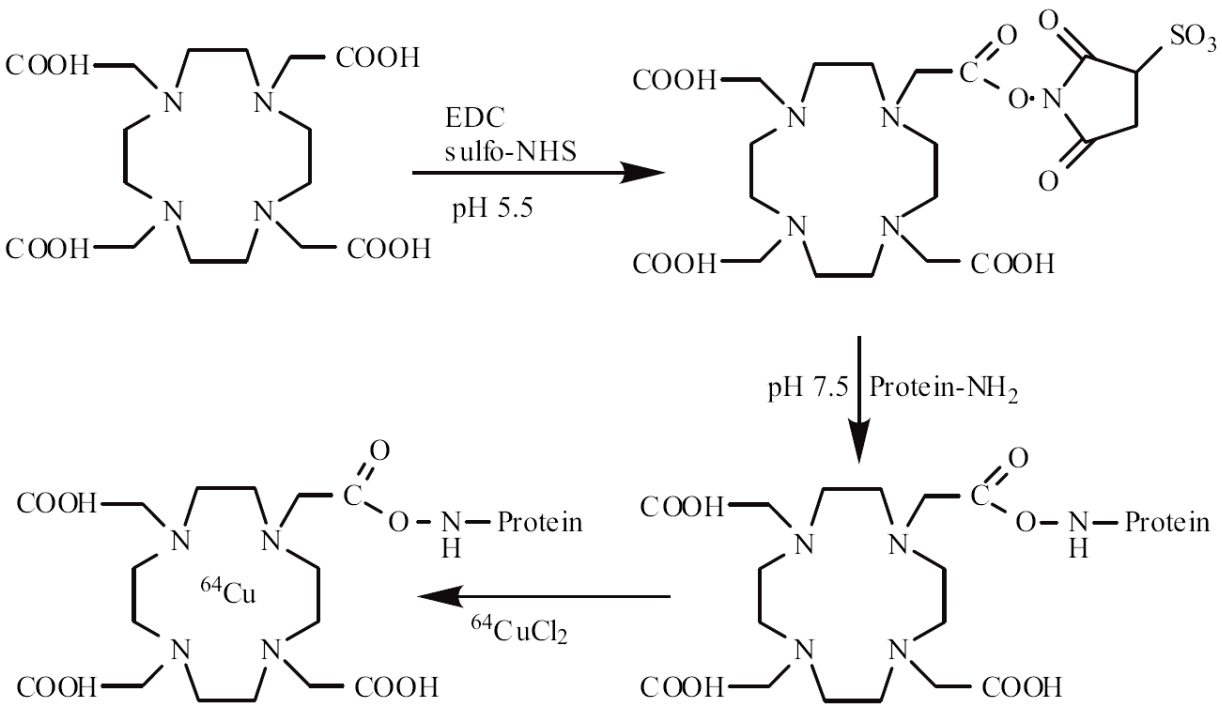

In, Ga, Cu …
Lu, Y, Bi, Ac …
Fe, Gd, …..

Radionuclide Production for SPECT

SPECT = Single-Photon-Emission-Computer Tomography

All these nuclides are commercially produced and sold

as radionuclide,

generators

or readily-prepared radiopharmaceuticals

Most important SPECT-Isotope is Technetium (^{99m}Tc) !

SPECT - Isotopes

Radio nuclide	$T_{1/2}$	Mode of decay	Main-γ-Lines	Productions data		
				Nuclear reaction	Energy range [MeV]	Yield [MBq/µAh]
^{67}Ga	3.26 d	EC (100)	93 (27%)	^{68}Zn(p,2n)	26→18	185
^{99}Mo	2.75 d	b- (100)	181 (6%) 740 (12%)	^{235}U(n,f) ^{98}Mo(n,g)	σ_{th}= 0.14b	
↓						
^{99m}Tc	6.0 h	IT (100)	141 (87%)			
^{111}In	2.8 d	EC (100)	173 (91%) 247 (94%)	^{112}Cd(p,2n)	25→18	166
^{123}I	13.2 h	EC (100)	159 (83%)	^{123}Te(p,n) ^{124}Xe(p,x)^{123}Xe ^{127}I(p,5n)^{123}Xe	14.5→10 29→23 65→45	137 414 777
^{201}Tl	3.06 d	EC (100)	68-82 (RL) 166 (10.2%)	^{210}Tl(p,3n)^{201}Pb	28→20	

^{99m}Tc-Generator (1)

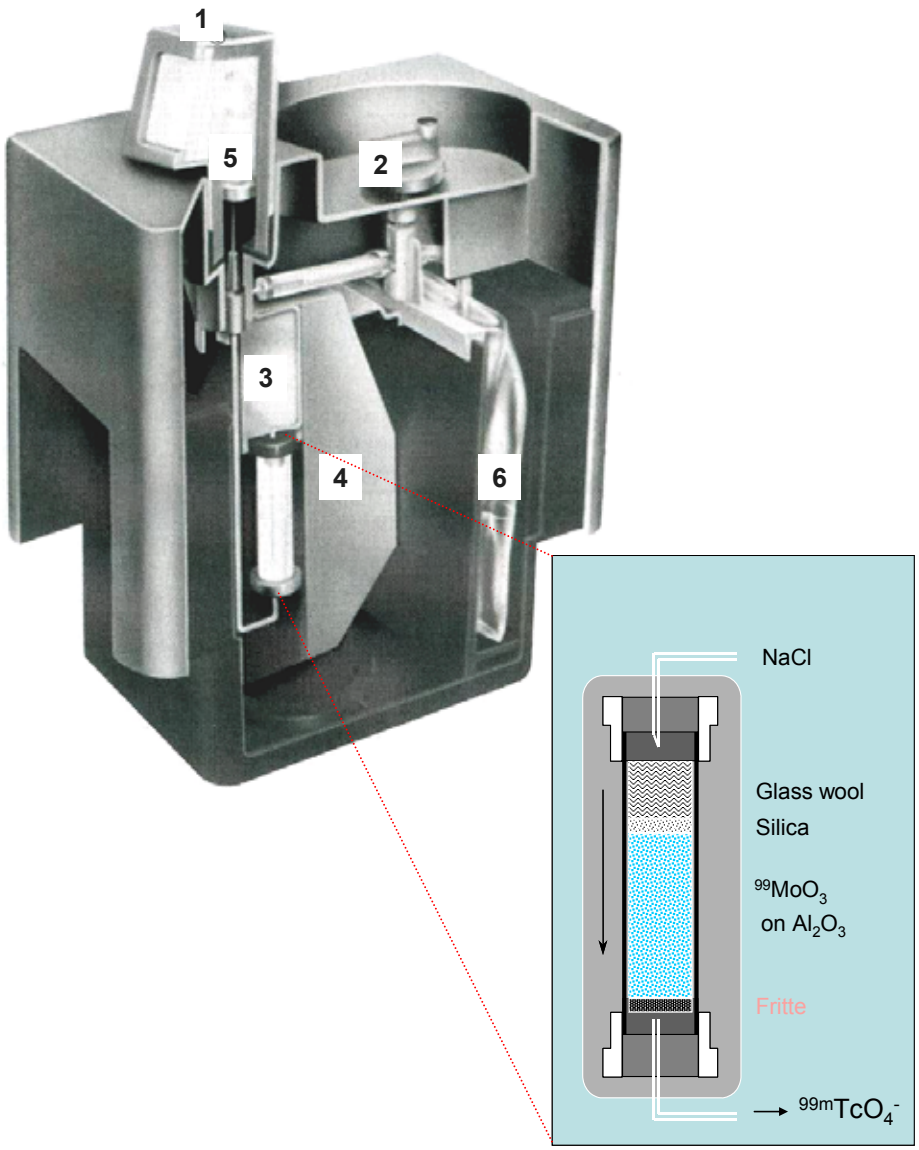

(1) Simple Handling

Insert vacuum flask and elute desired volume.

(2) Transport-Security-valve

Prevent an elution after production and during transport

(3) Shifted needle

Reduction of energy rich Mo-radiation

(4) Max. protection against radiation

Protection from all side.
^{99}Mo-column is covered at least with 52 mm Pb.
Supplementary shielding with overall 98 mm Pb.

(5) High concentrated activity

Total ^{99m}Tc-activity is less than 5 mL volume.

(6) Ready for use

Sterile, closed system.

Labeling of Tc-Radiopharmaceuticals

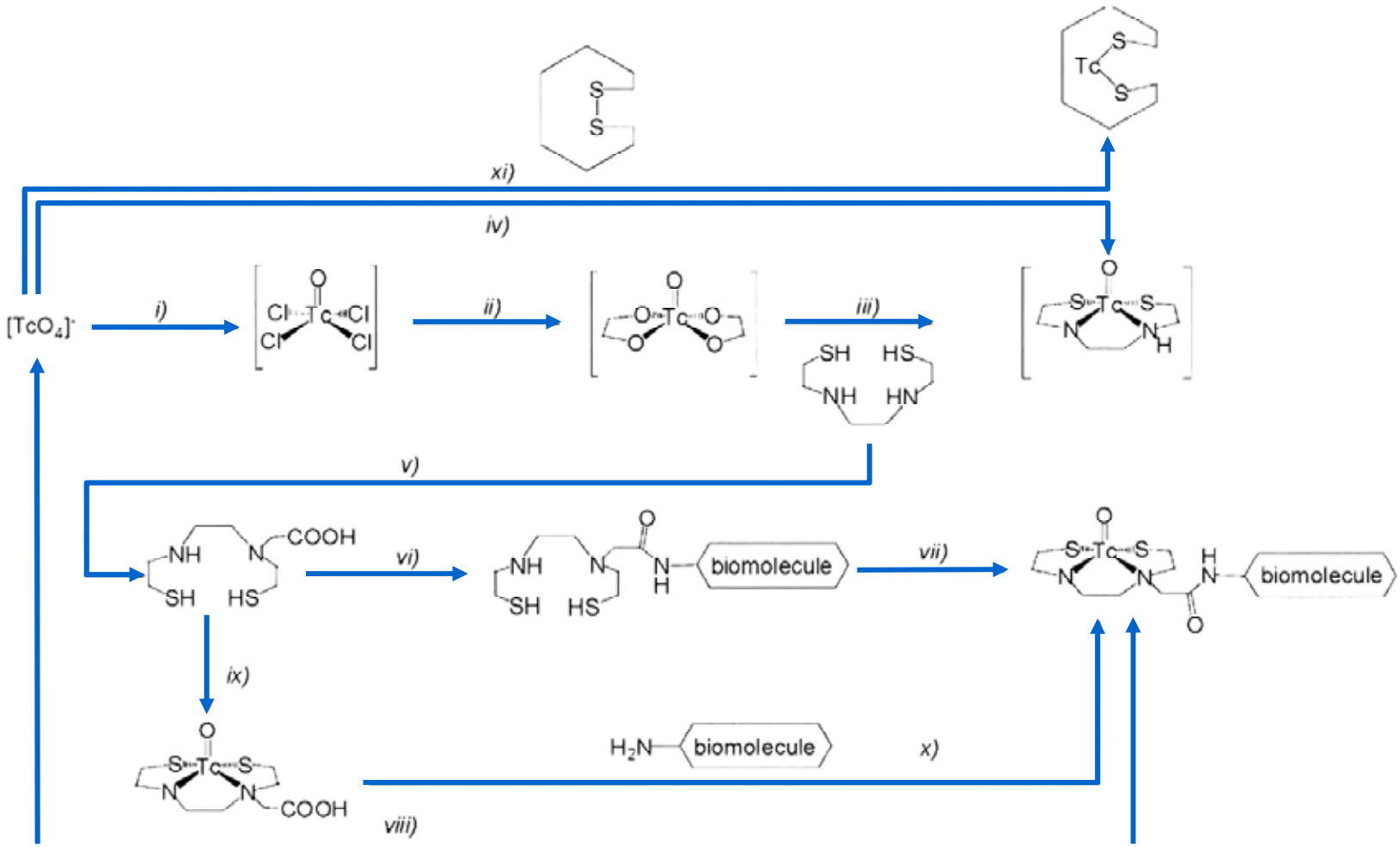

Tracer Properties: Influence of the Nuclide

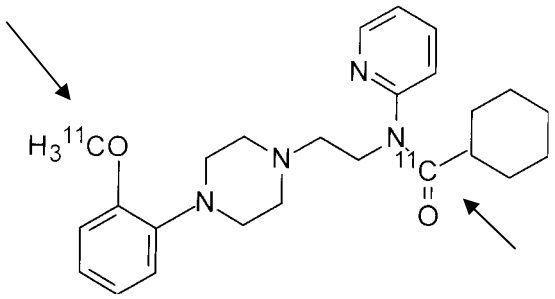

WAY 100638 (5-HT_{1A}-receptor ligand)

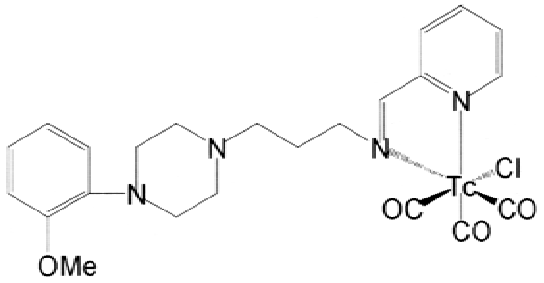

^{99m}Tc-WAY 100638-analog
(as 5-HT_{1A}-receptor ligand)

^{11}C **^{18}F** **^{123}I** **^{99m}Tc** **^{68}Ga / ^{111}In**

Change in structure

Predictability of biological integrity

Complexity of radiopharmaceutical development

Molecular Imaging by Radiotracer

Targeting biochemical processes in living organism
on basis of molecular interaction between tracer und target

by **radiolabeled, „molecular probes**“, changing their concentration at the target in a specific way

and suitable **detection systems** for non-invasive, quantitative and repetitive measurement

with the aim of **exploring** physiological processes,
diagnostics und therapy as well as **therapy monitoring**

Target Structures in Oncology

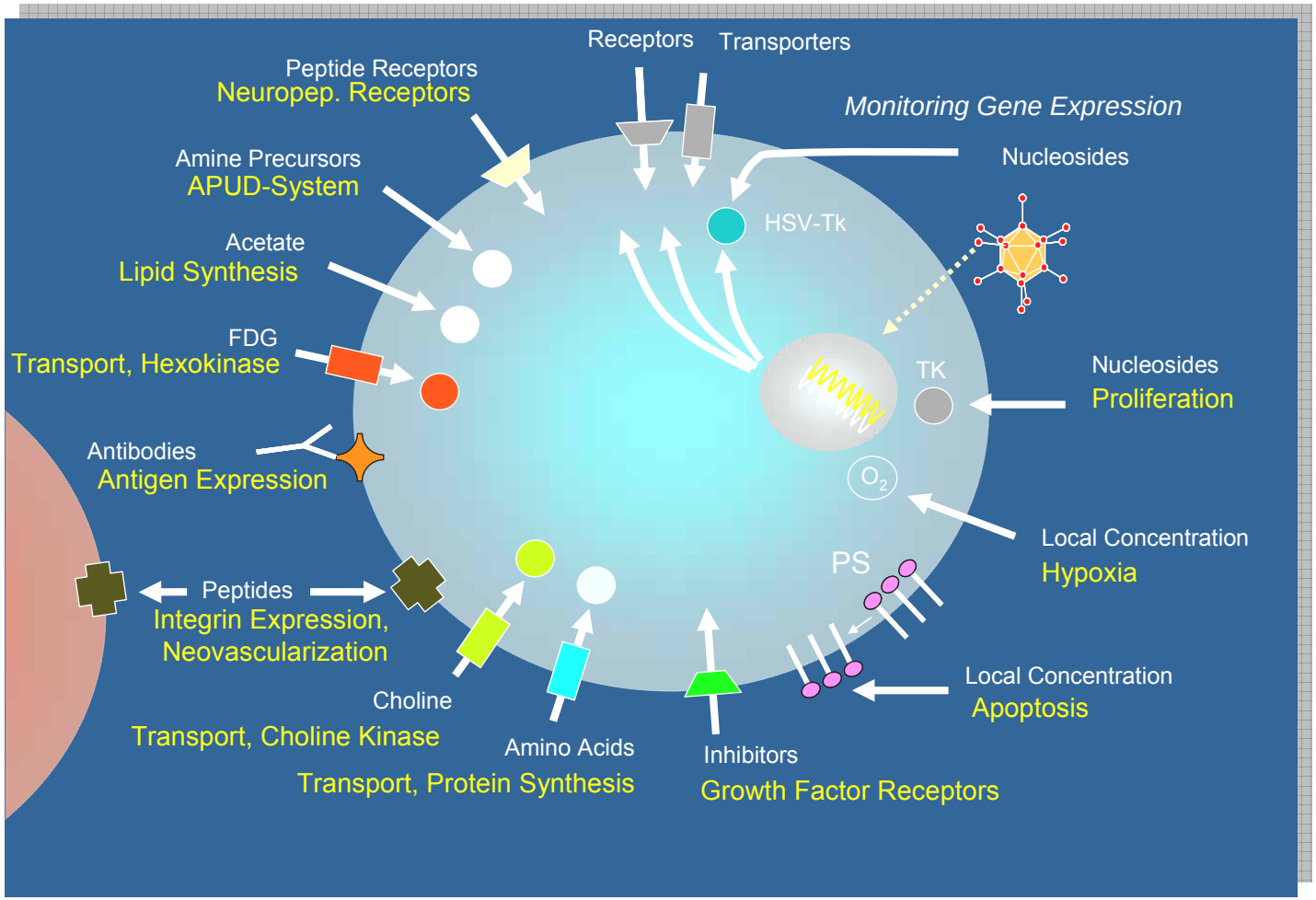

Characterization of the tumor biology by molecular imaging

2-[^{18}F]Fluoro-2-Deoxy-Glucose-Synthesis ([^{18}F]FDG)

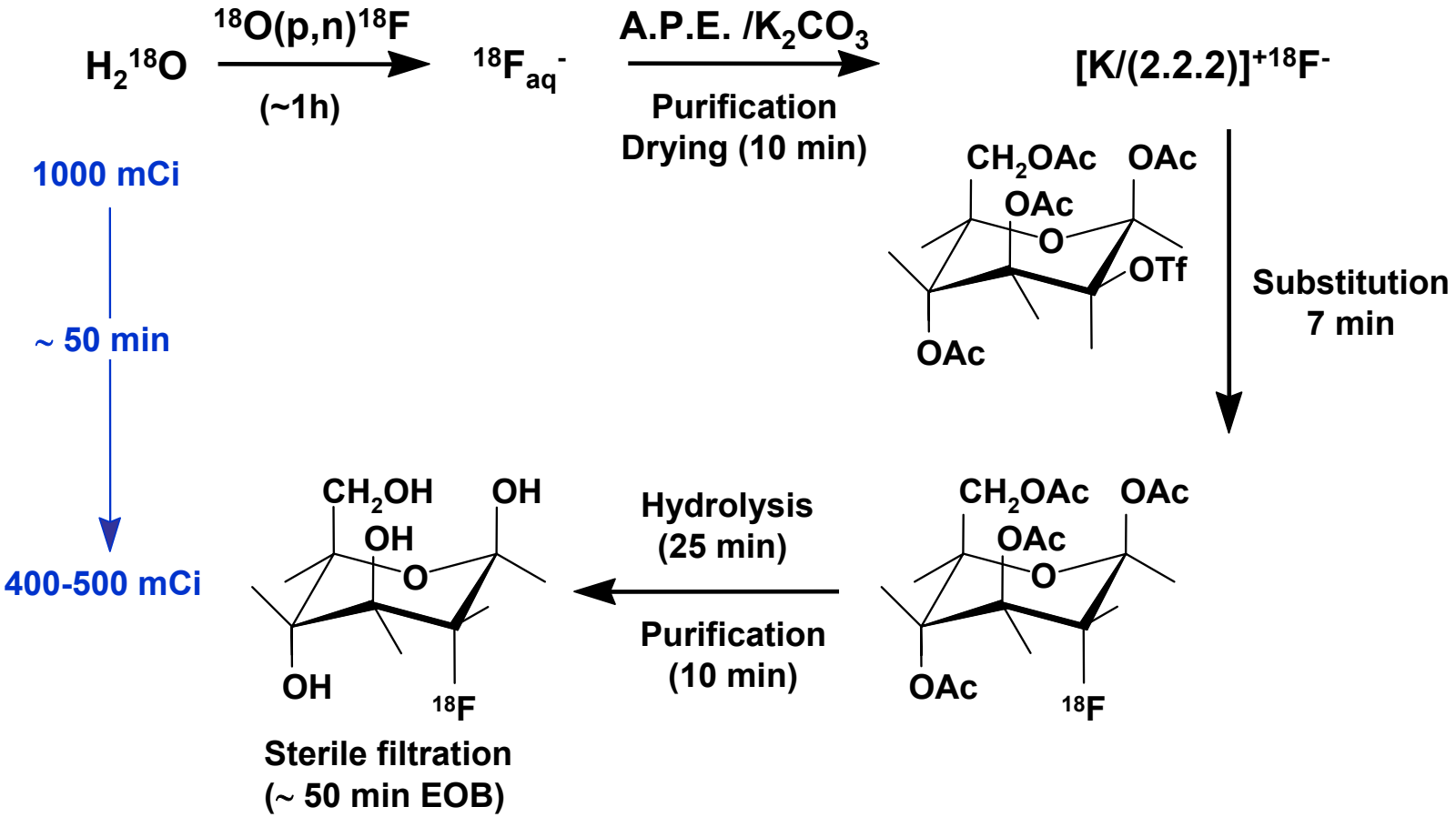

GMP Production of FDG
2-[^{18}F]Fluor-2-deoxy-D-Glucose, TU Munich

Scheme of [^{18}F]FDG Uptake

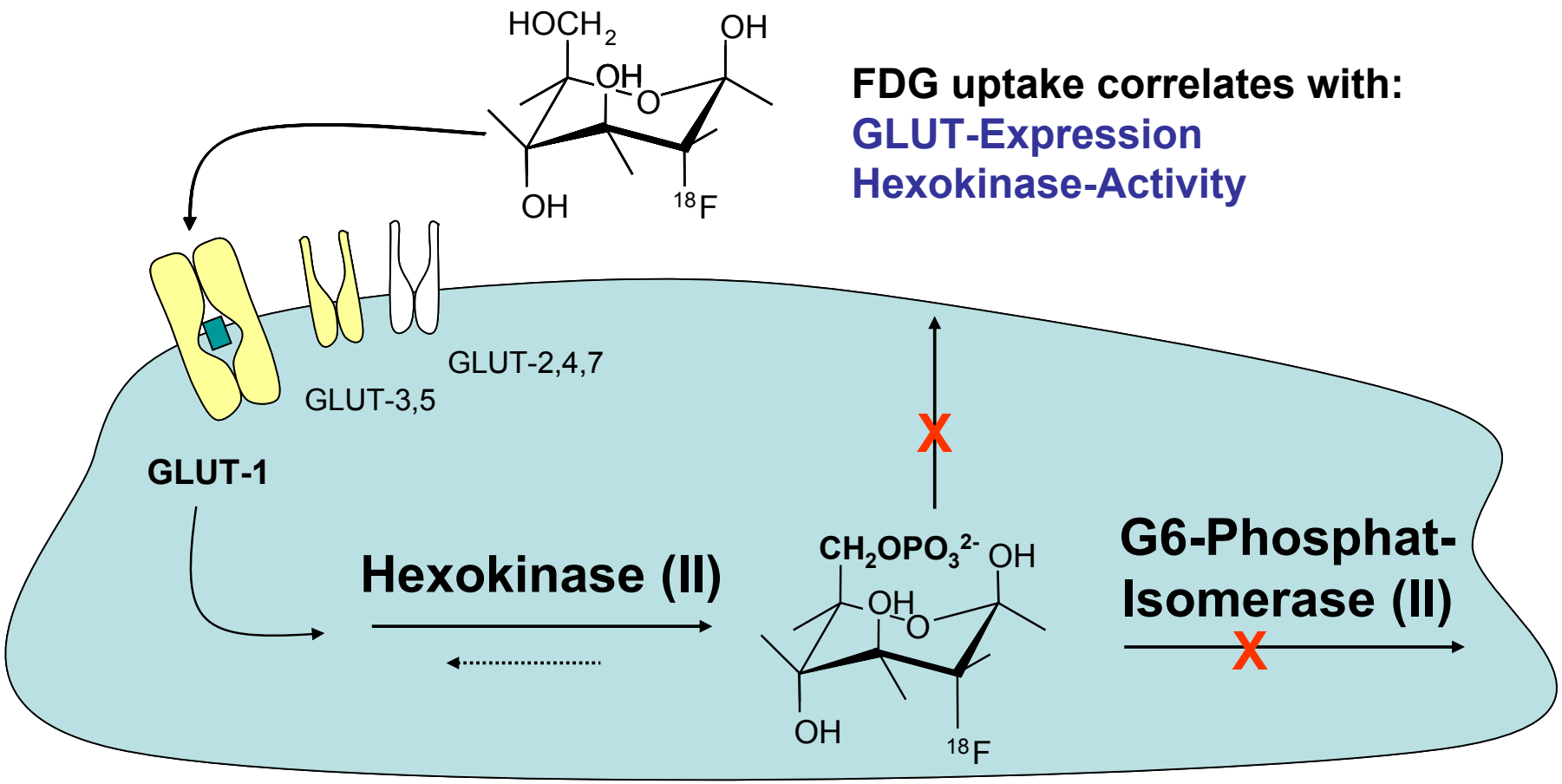

[^{18}F]FDG:
Therapy control –gastric carcinoma-

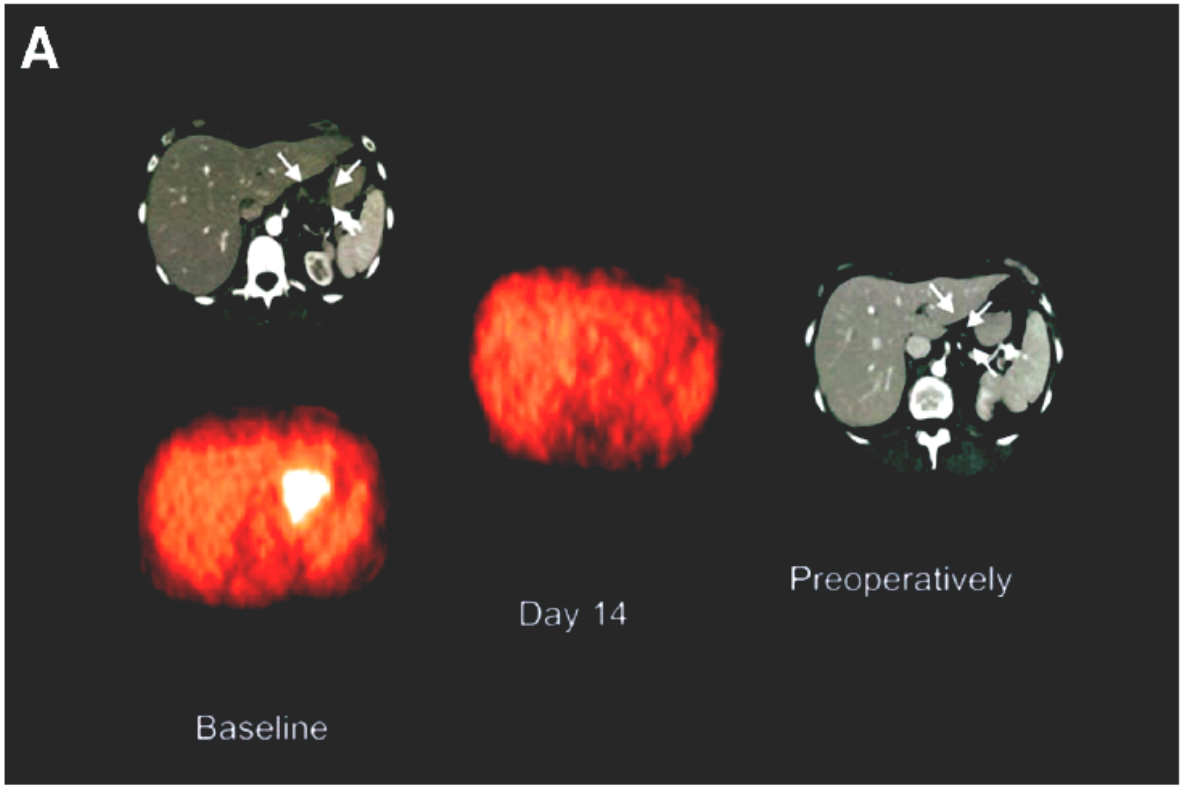

Amino Acid Transport

Primary target: Rate measurement of regional protein synthesis
But: During the short time period after injection the accumulation of tracer represent only the accumulation of amino acid by special transport systems

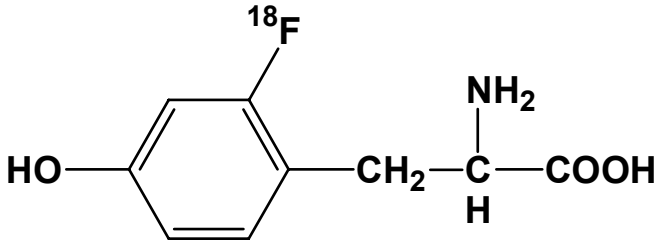

2-Fluoro-L-Tyrosin **2-[^{18}F]Tyr**

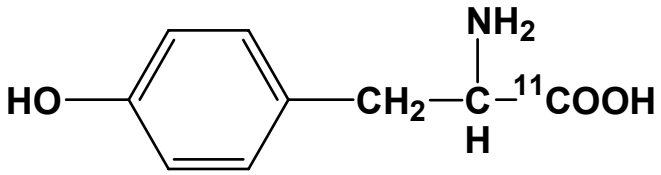

L-Tyrosin **1-[^{11}C]Tyr**

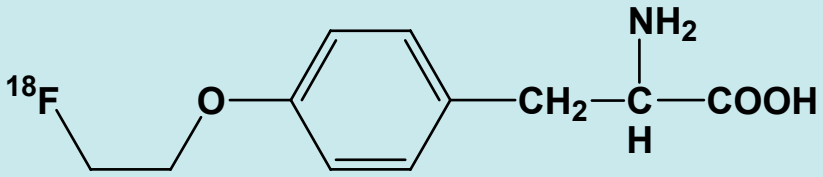

O-(2-Fluoroethyl)-L-Tyrosin **[^{18}F]FET**

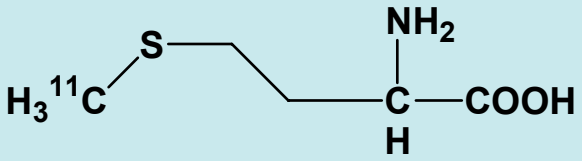

L-Methionine **[^{11}C]MET**

[^{18}F]FDG-PET versus [^{11}C]MET-PET
-Brain Tumor-

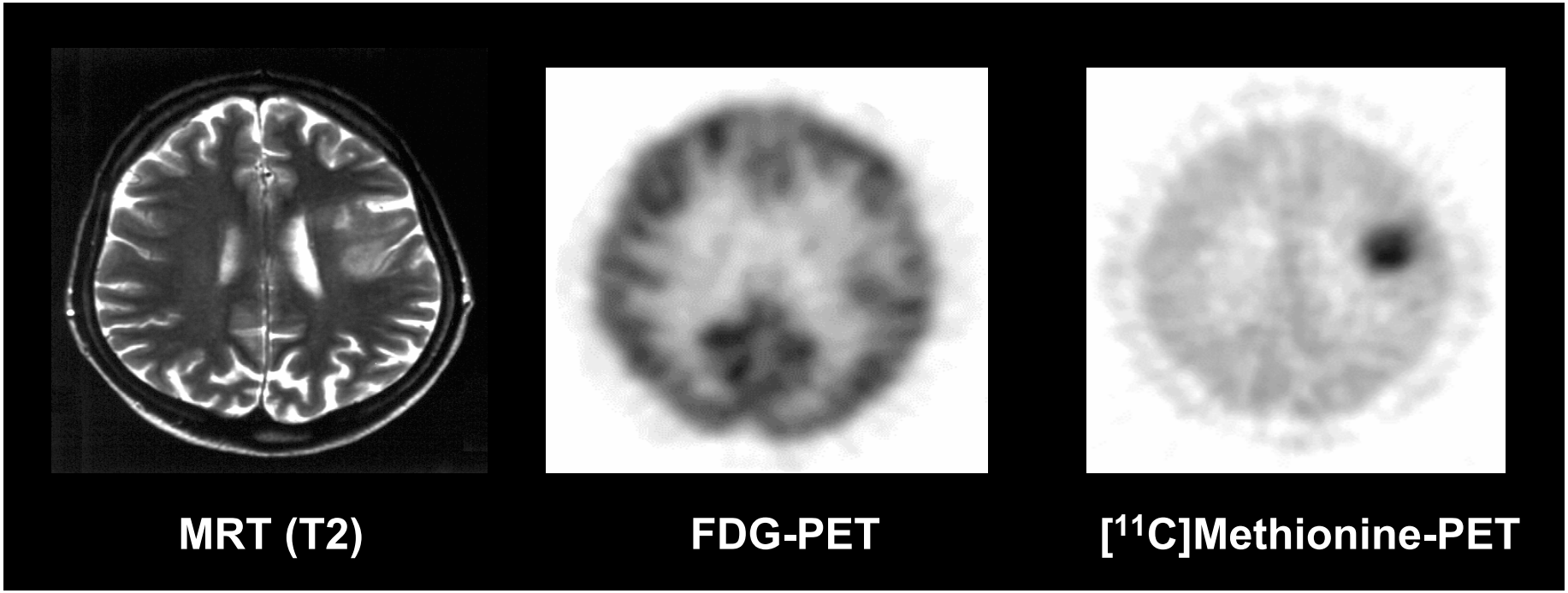

O-(2-[^{18}F]Fluoroethyl)-L-Tyrosin: [^{18}F]FET (2)

FDG also accumulates in inflammation,
amino acids and especially FET does not accumulate in inflammation.

Squamous cell carcinoma

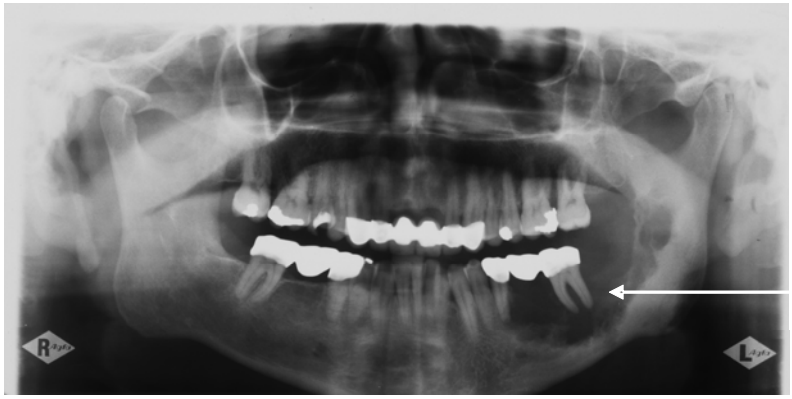

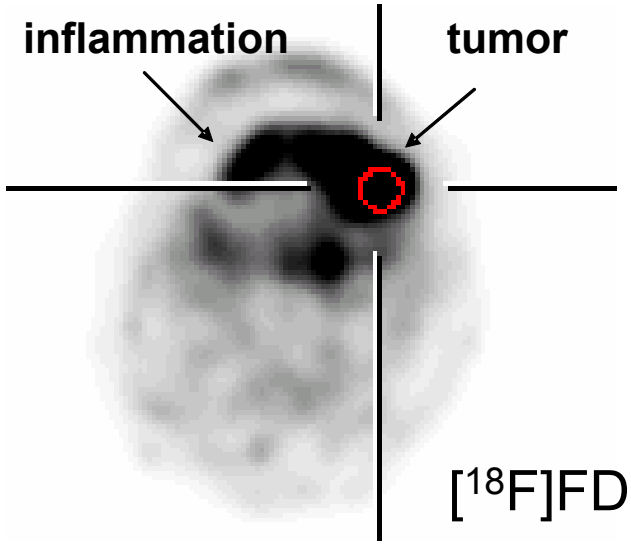

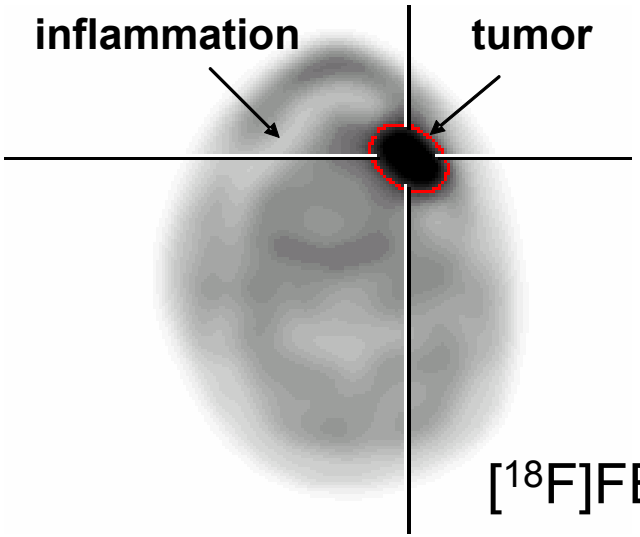

Imaging of Metastatic Prostate Cancer

^{11}C-Acetate:	**Prostate cells undergo metabolic transformation from citrate producing normal cells to citrate oxidizing malignant cells (Costello LC et al. *Urology* 1997)**
^{18}F/^{11}C-Cholines:	**malignant transformation is associated with induction of choline kinase activity (e.g. Kotzerke et al. and refs herein; J Nucl Med. 2002)**
(^{18}F-Fluoide):	**(for bone metastasis)**

Biochemical Model: Choline

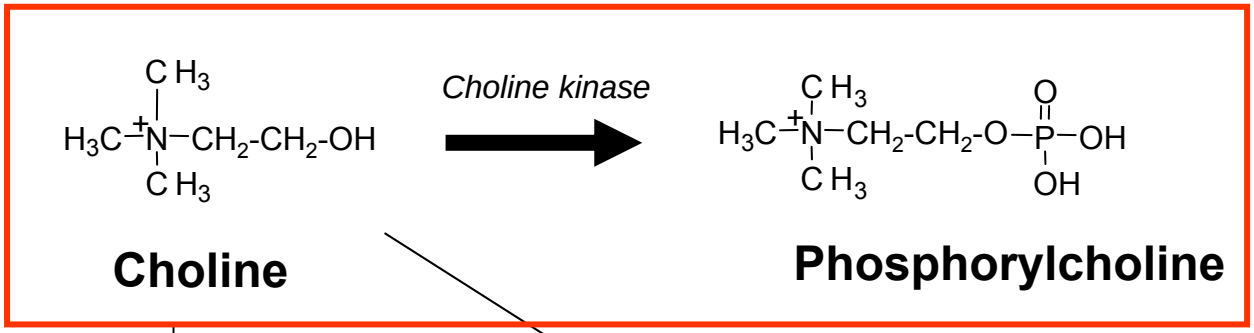

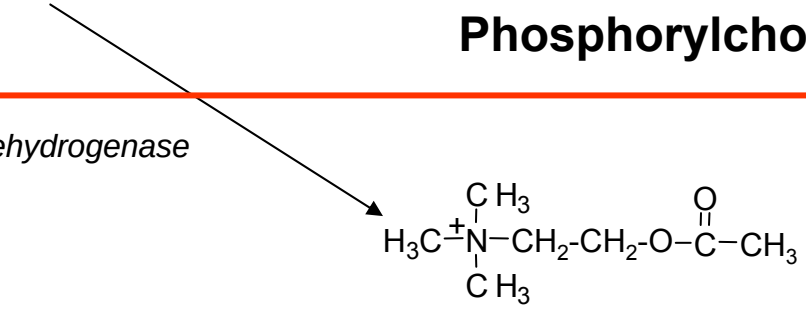

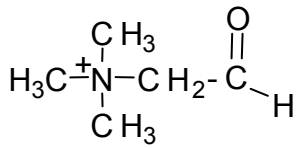

Betain-aldehyde

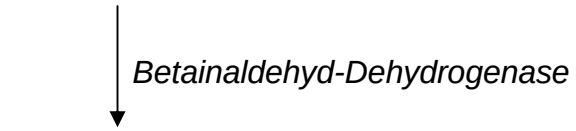

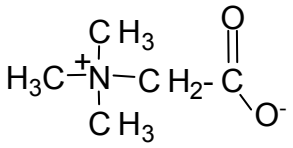

Betain

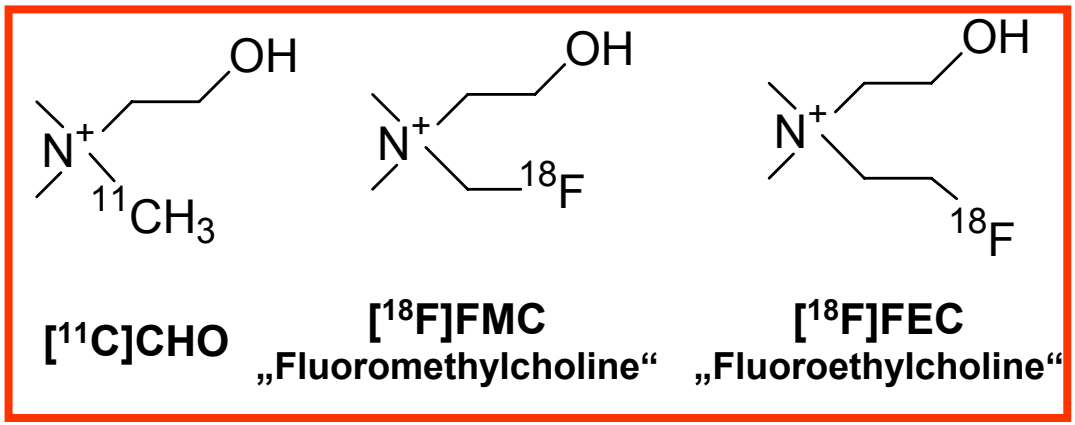

^{11}C-Choline-PET

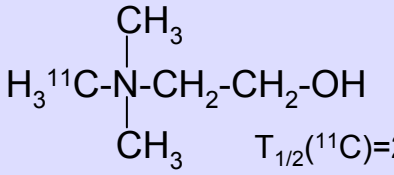

$T_{1/2}(^{11}C)$=20 min

^{18}F-Choline-PET

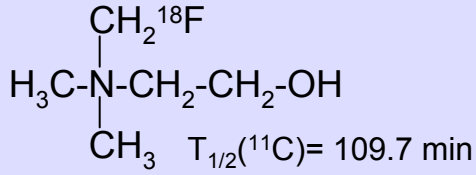

$T_{1/2}(^{11}C)$= 109.7 min

Bladder cancer metastasis

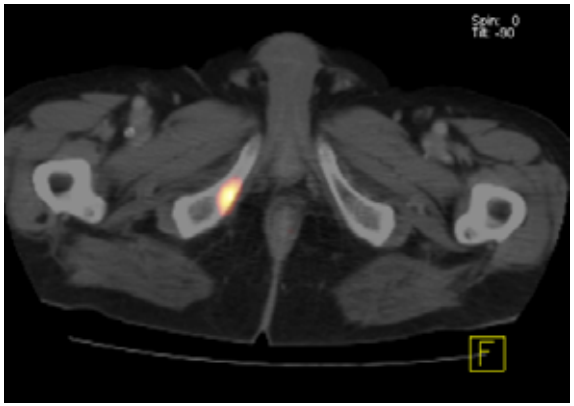

PET/CT

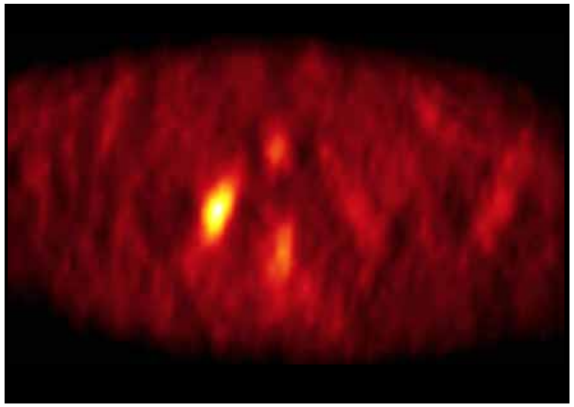

PET

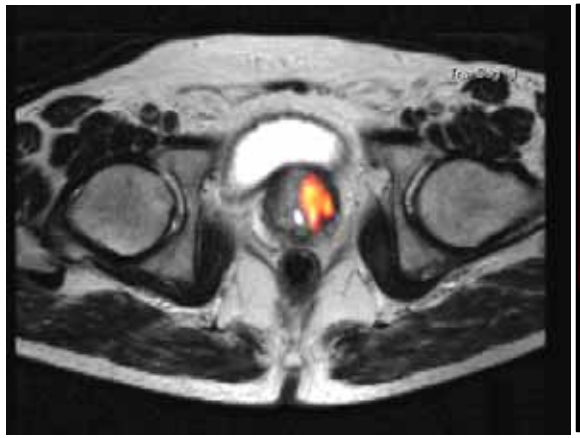

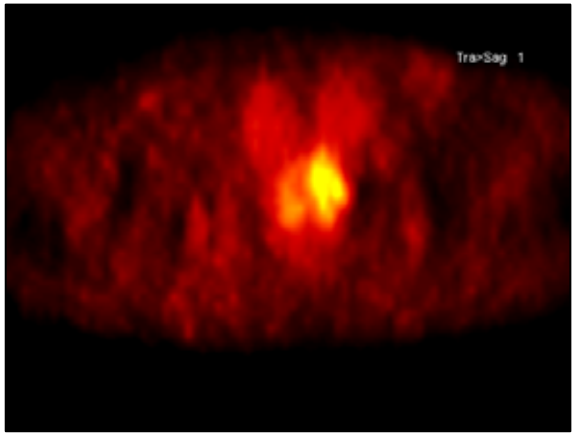

Prostate carcinoma

Tracer accumulation with:

1. Cellular accumulation by choline transporter;
(Signal in the first minutes after injection)

2. and followed by phosphorylation by choline kinase.
(Signal by late imaging)

3´-[^{18}F]Fluoro-3´-Deoxy-Thymidine: [^{18}F]FLT

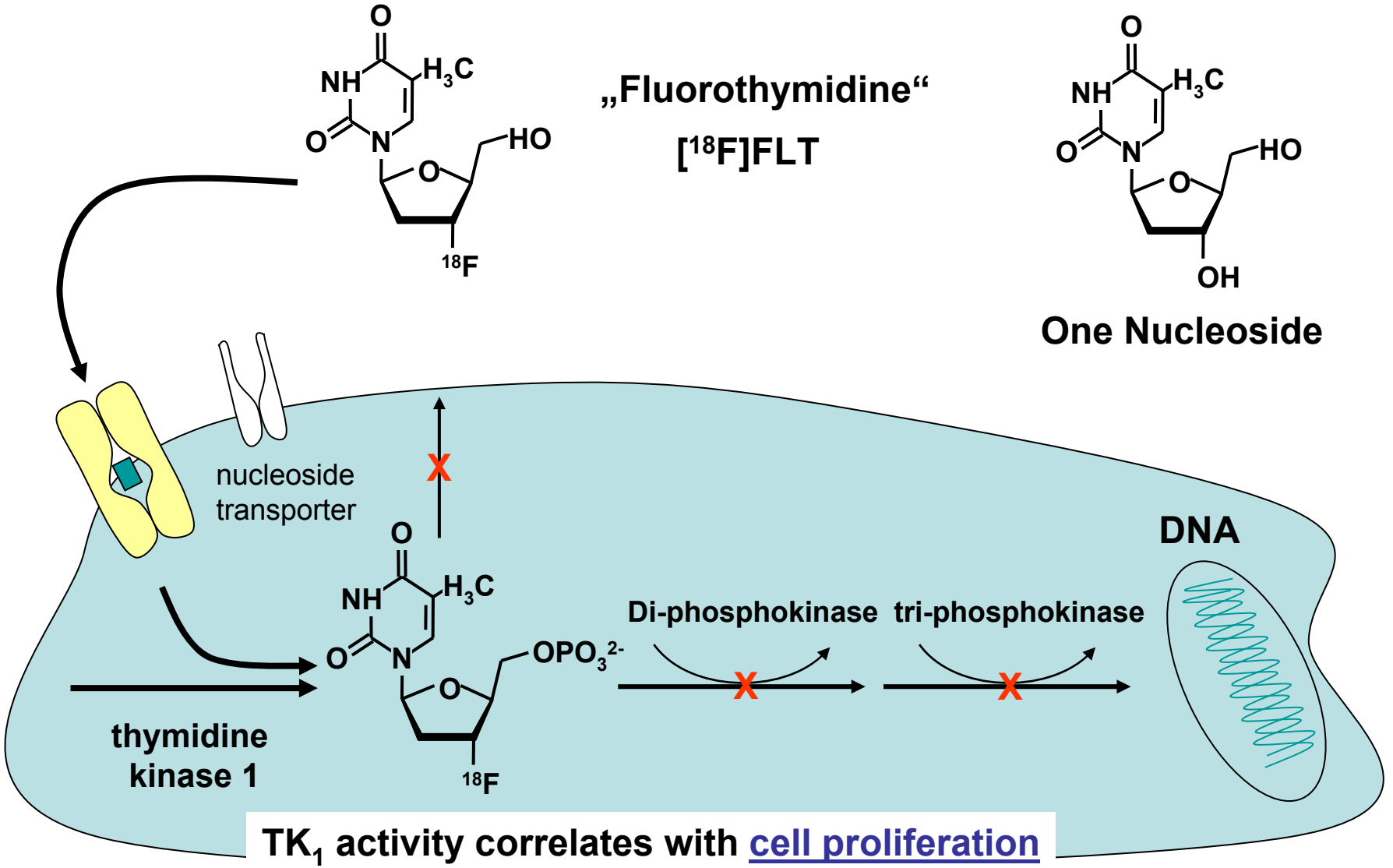

Metabolic Scheme for [^{11}C]Thymidine and FLT

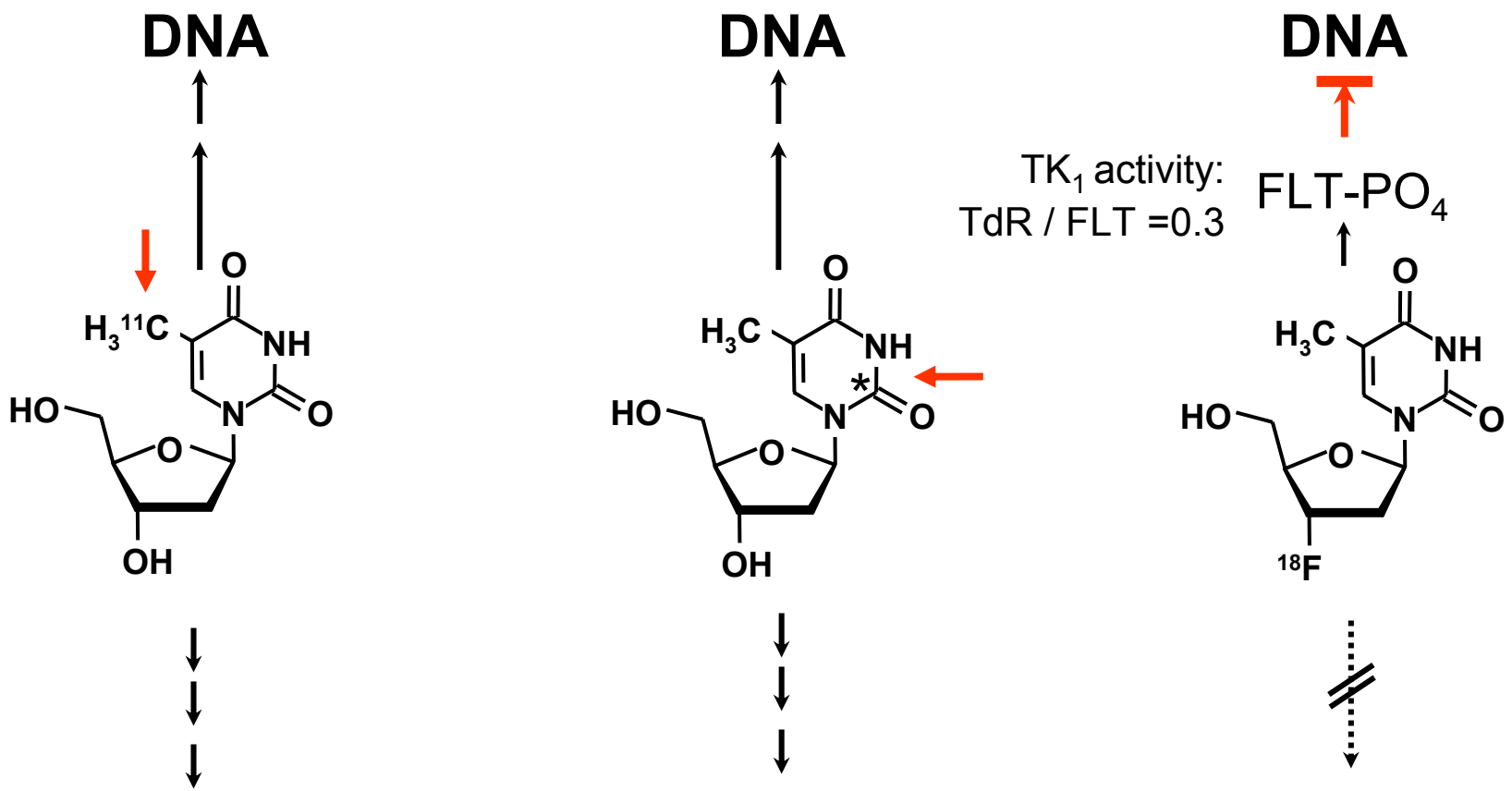

Visualization of Cell Proliferation with ^{18}F-thymidine (FLT) in Esophageal Cancer

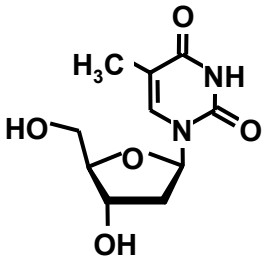

thymidine

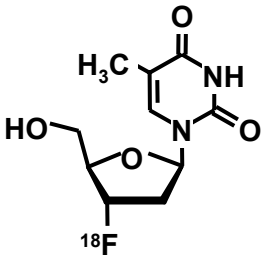

[^{18}F]FLT

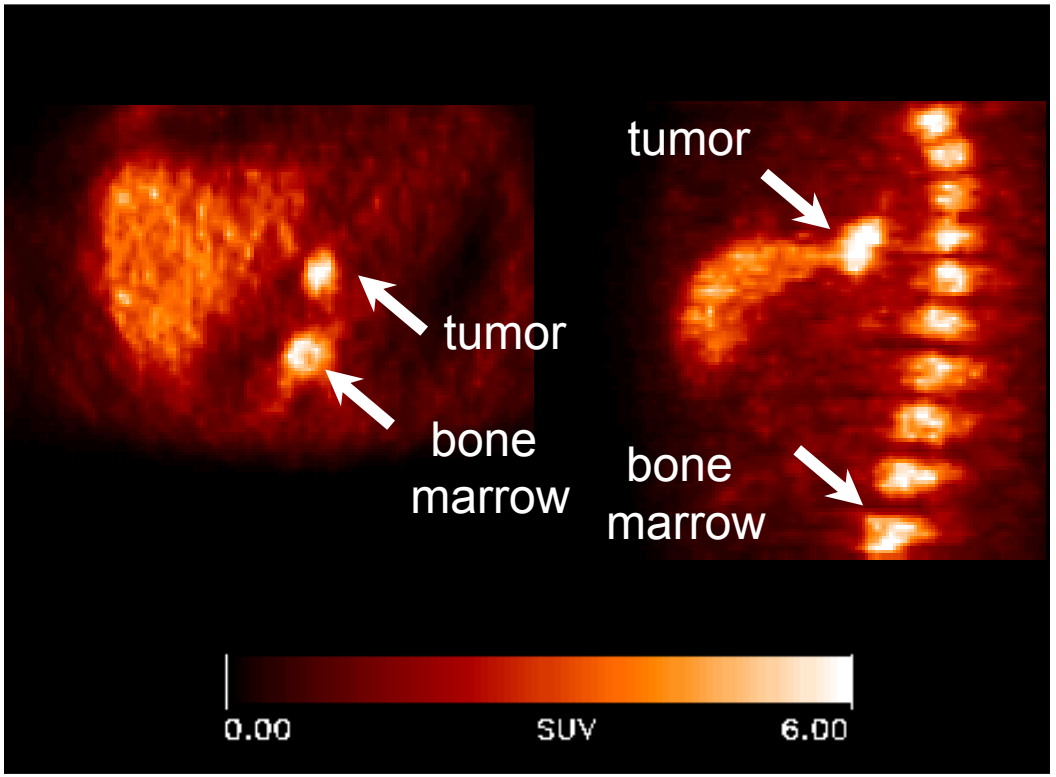

Critical O_2 Levels

Aggressiveness ↑
Tumor Progression

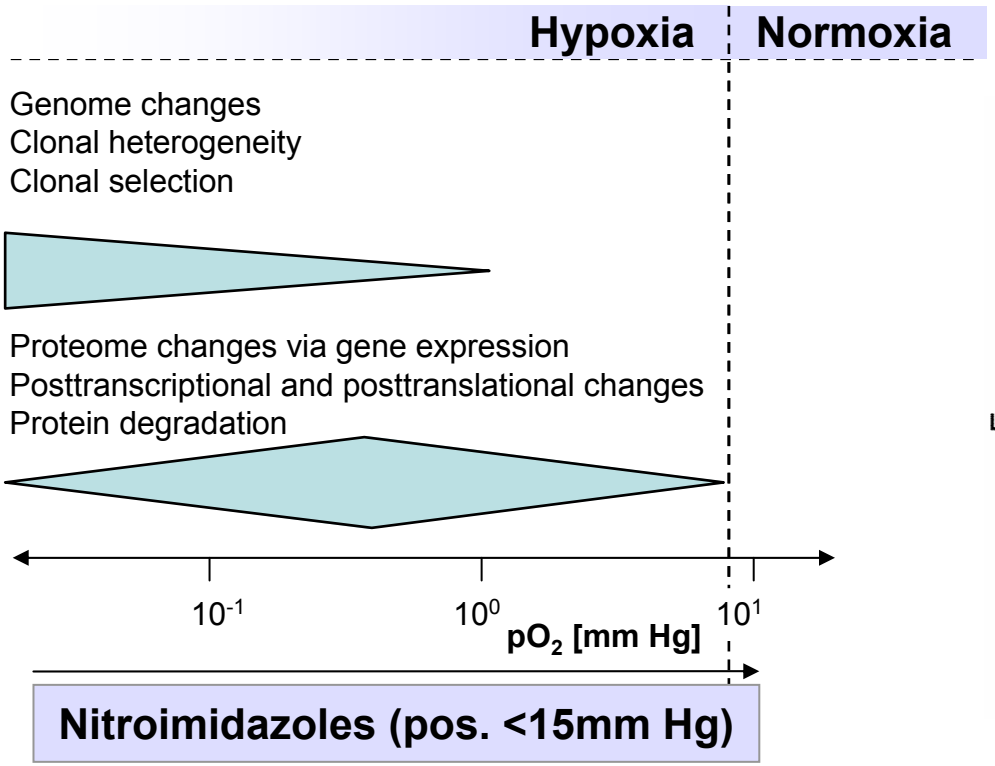

Distribution of medium pO_2 levels for prostatic tumor tissue versus muscle

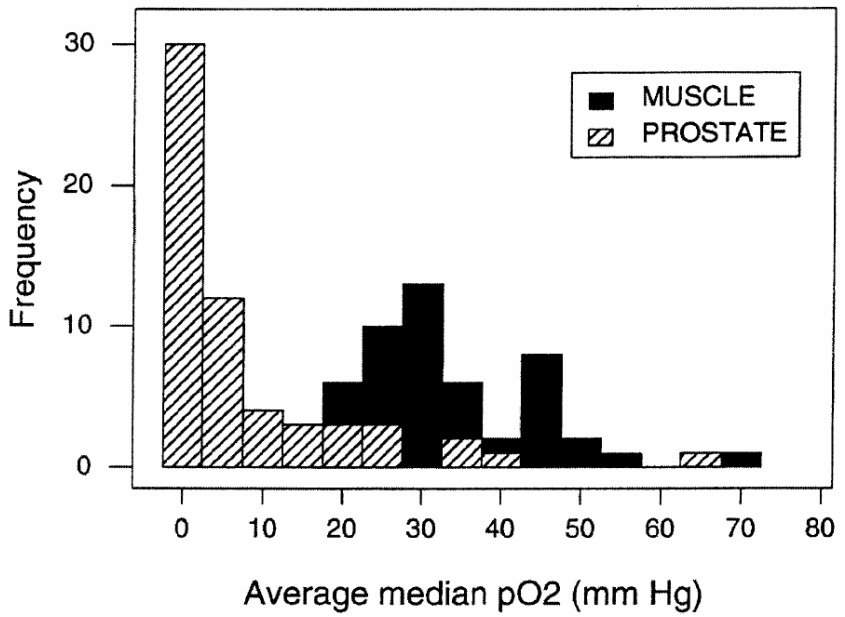

Vaupel P. et al.

The Mechanism of Non-Invasive Detection of Tumor Hypoxia

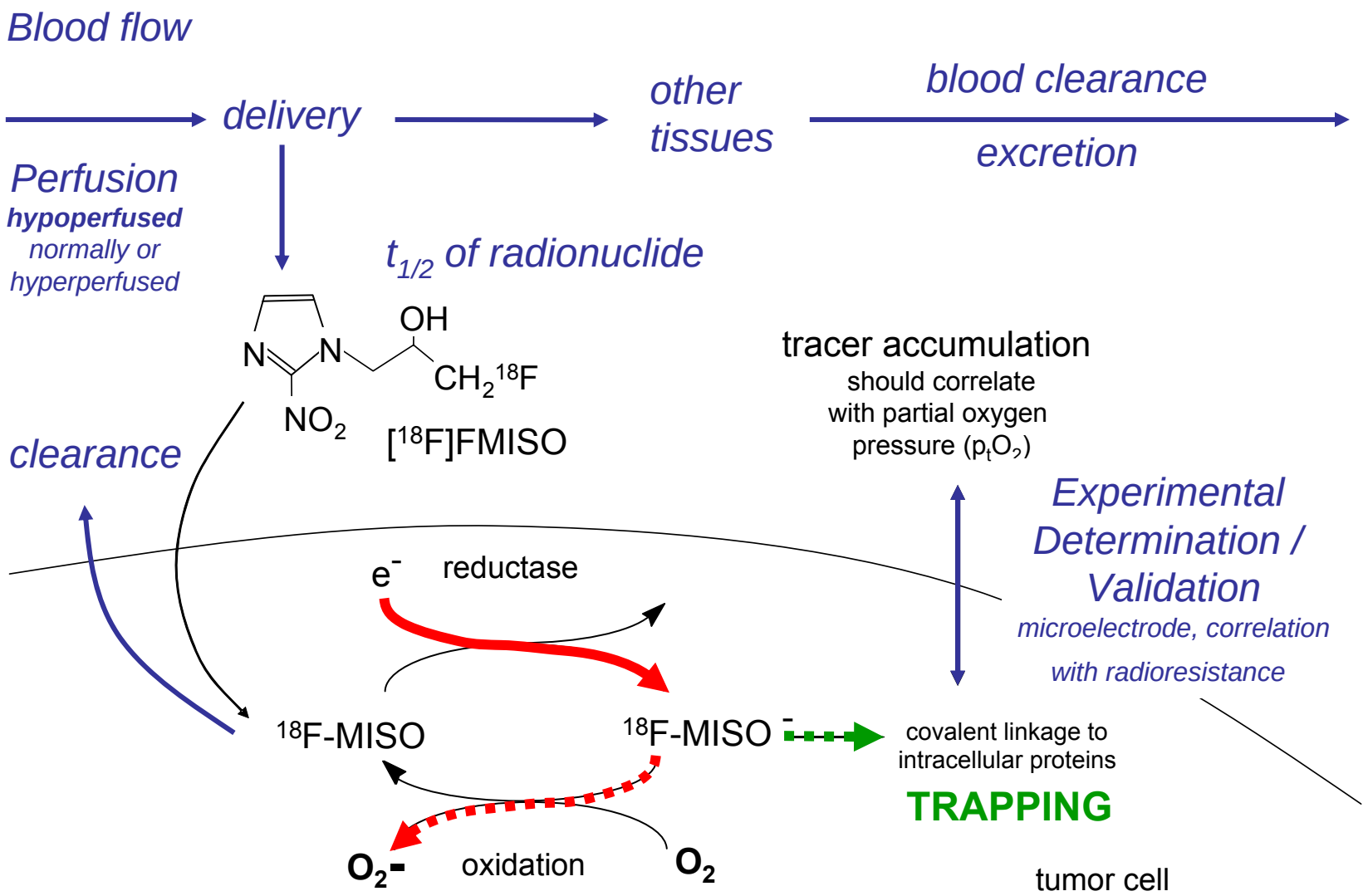

Evaluation of [^{18}F]FAZA

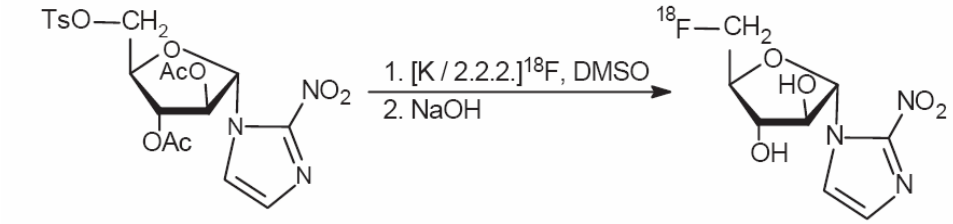

Synthesis of [^{18}F]FAZA:
Radiochemical Yield: 20 ± 4%, 50 min
(Reischl et al., 2005)

Serial, transaxiale PET images -nude mice- with A431 tumors.

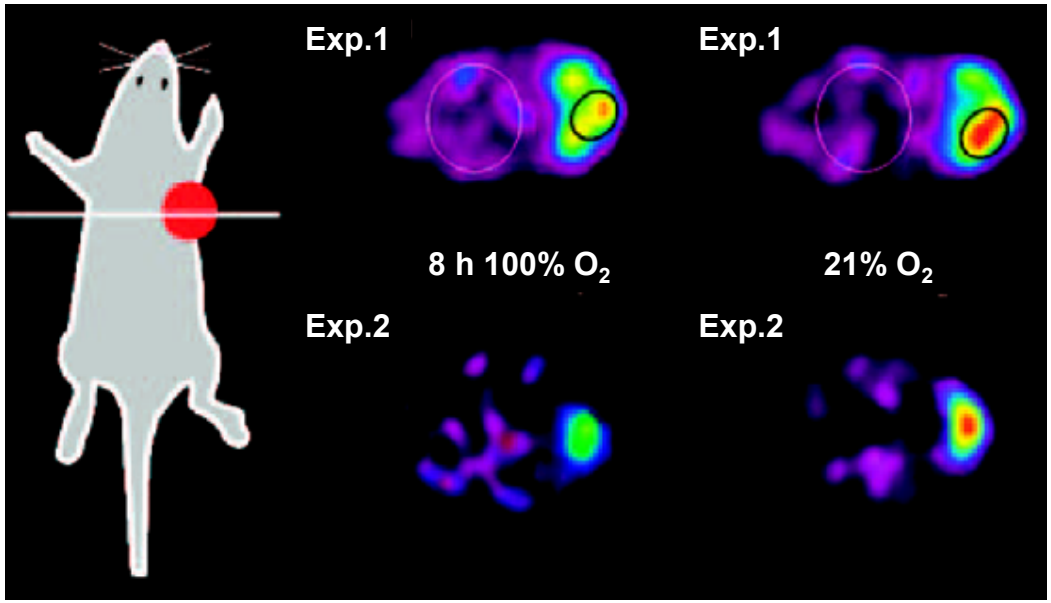

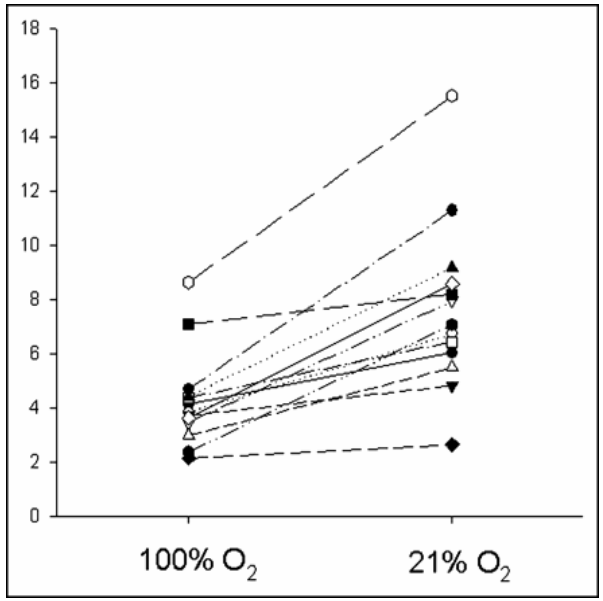

Exp.1	**T/Bk**	**3.7 / 1**	**4.7 / 1**
Exp.2	**T/Bk**	**5.4 / 1**	**11.3 / 1**

Peptide Receptor Imaging: PRI

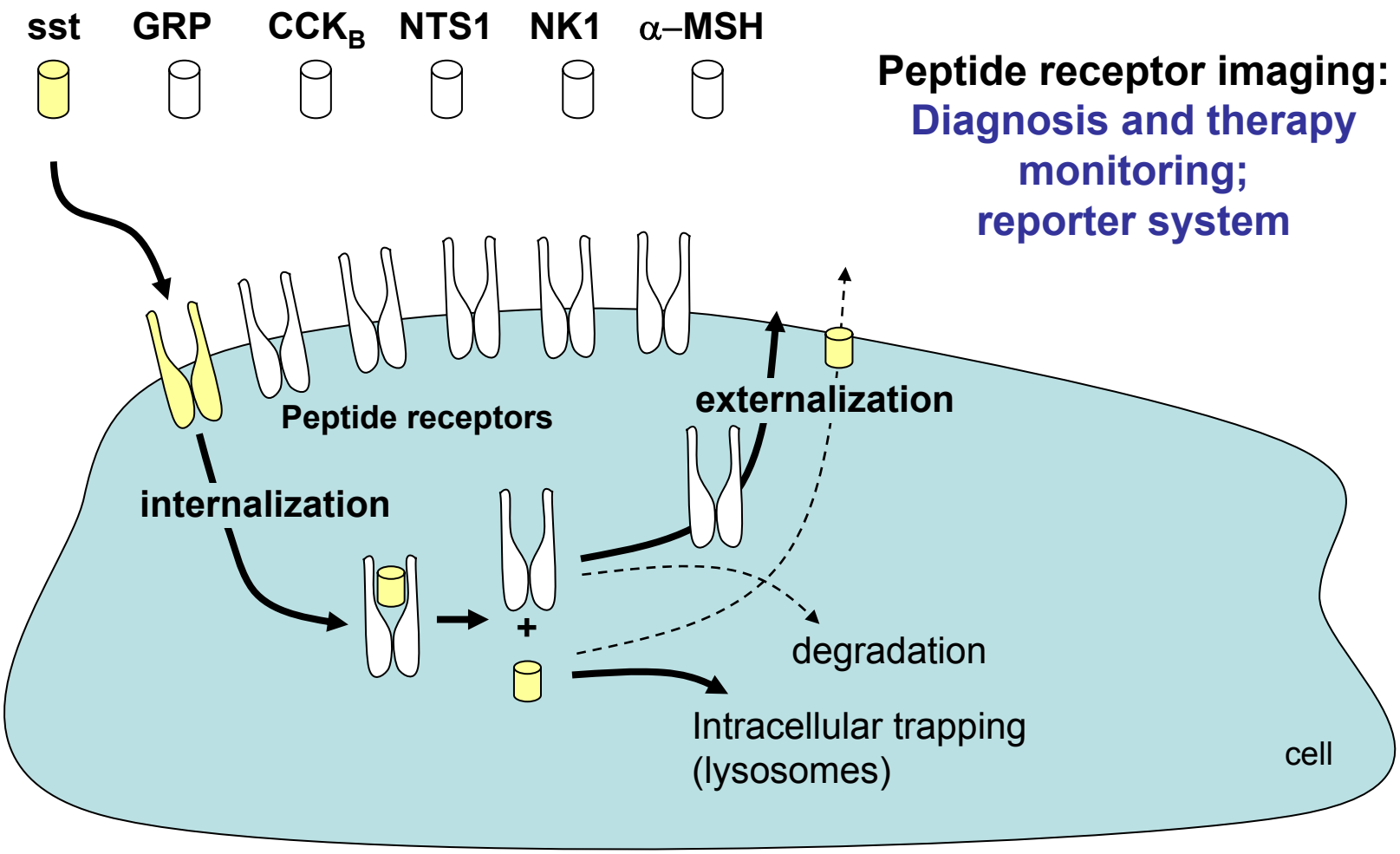

Peptide receptor imaging:
Diagnosis and therapy monitoring;
reporter system

Targets for Radiolabeled Peptides in Human Tumor Tissue

Somatostatin-R	neuroendocrine tumors, small cell lung cancer, medullary thyroid carcinoma, lymphoma (NHL)
Integrins	melanoma, breast tumor, osteosarcoma, glioblastoma
VIP-R	adenocarcinomas, small cell lung cancer, neuroendocrine tumors, lymphoma
CCK-B-R	medullary thyroid carcinoma, small cell lung cancer, stromal ovarian cancer, astrocytoma
Substance P-R	medullary thyroid cancer, small cell lung cancer, breast tumors
Bombesin/ GRP-R	colon cancer, small cell lung cancer, glioblastoma
Neurotensin-R	pancreatic cancer, prostate cancer,small cell lung cancer

Influence of the Carbohydrate on the Biodistribution of Octreotides/-tates

(Mice, AR42J, n=3-5, 60 min p.i.)

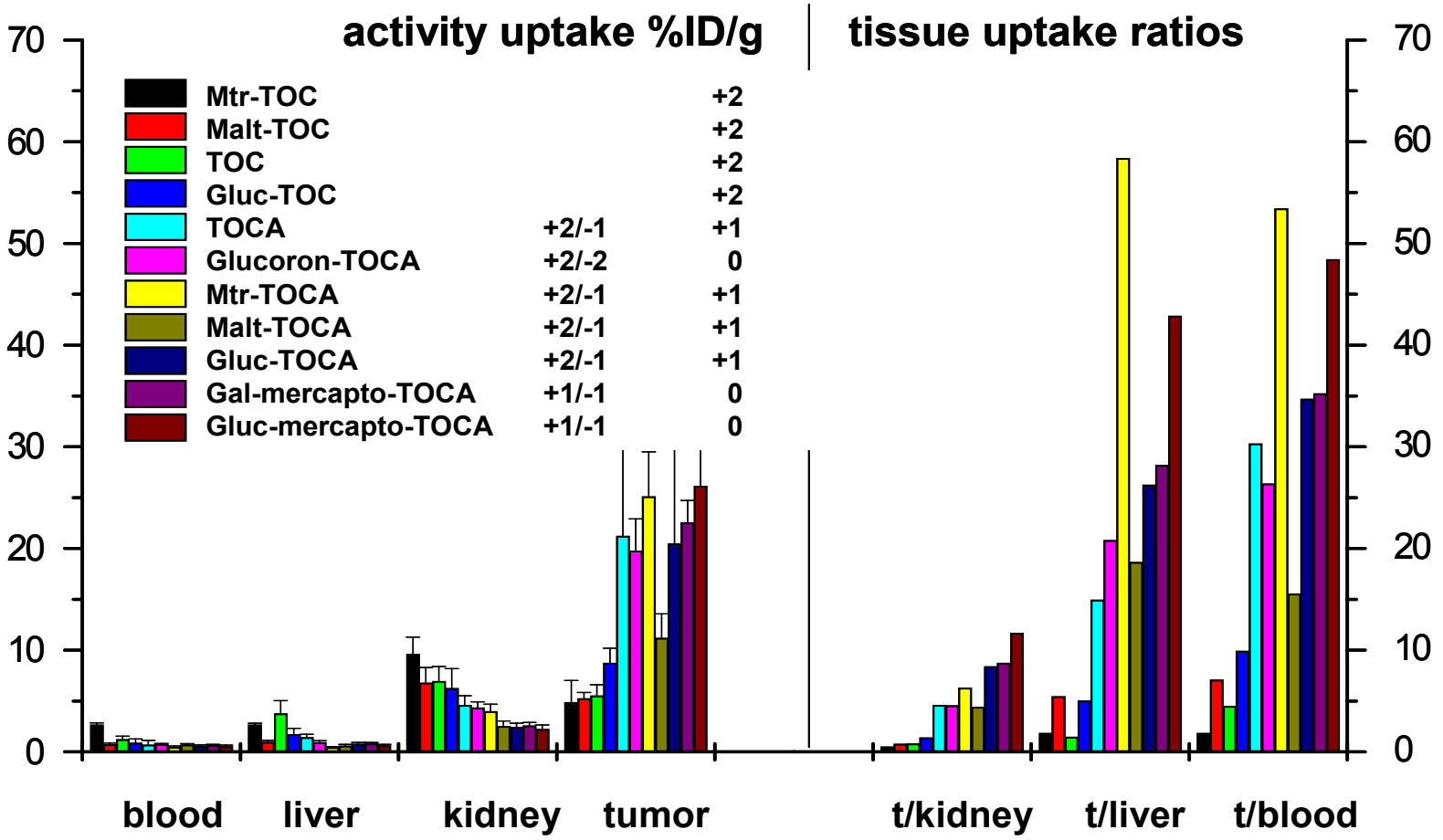

Schottelius, Wester et al. Clin Cancer Res. (2004)

Chemical Structure of Gluc-FP[^{18}F]-TOCA

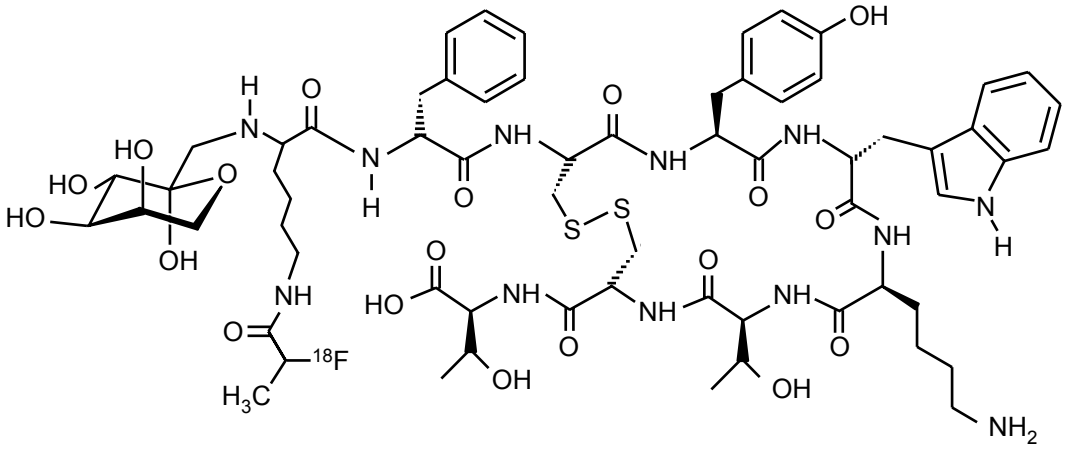

Gluc-Lys([^{18}F]FP)-TOCA

[^{18}F]FP = 2-[^{18}F]Fluoropropionic acid
TOCA = Tyr$_3$-octreotate, -DPhe-Cys-Tyr-DTrp-Lys-Thr-Cys-Thr-OH

Gluc-FP[^{18}F]-TOCA

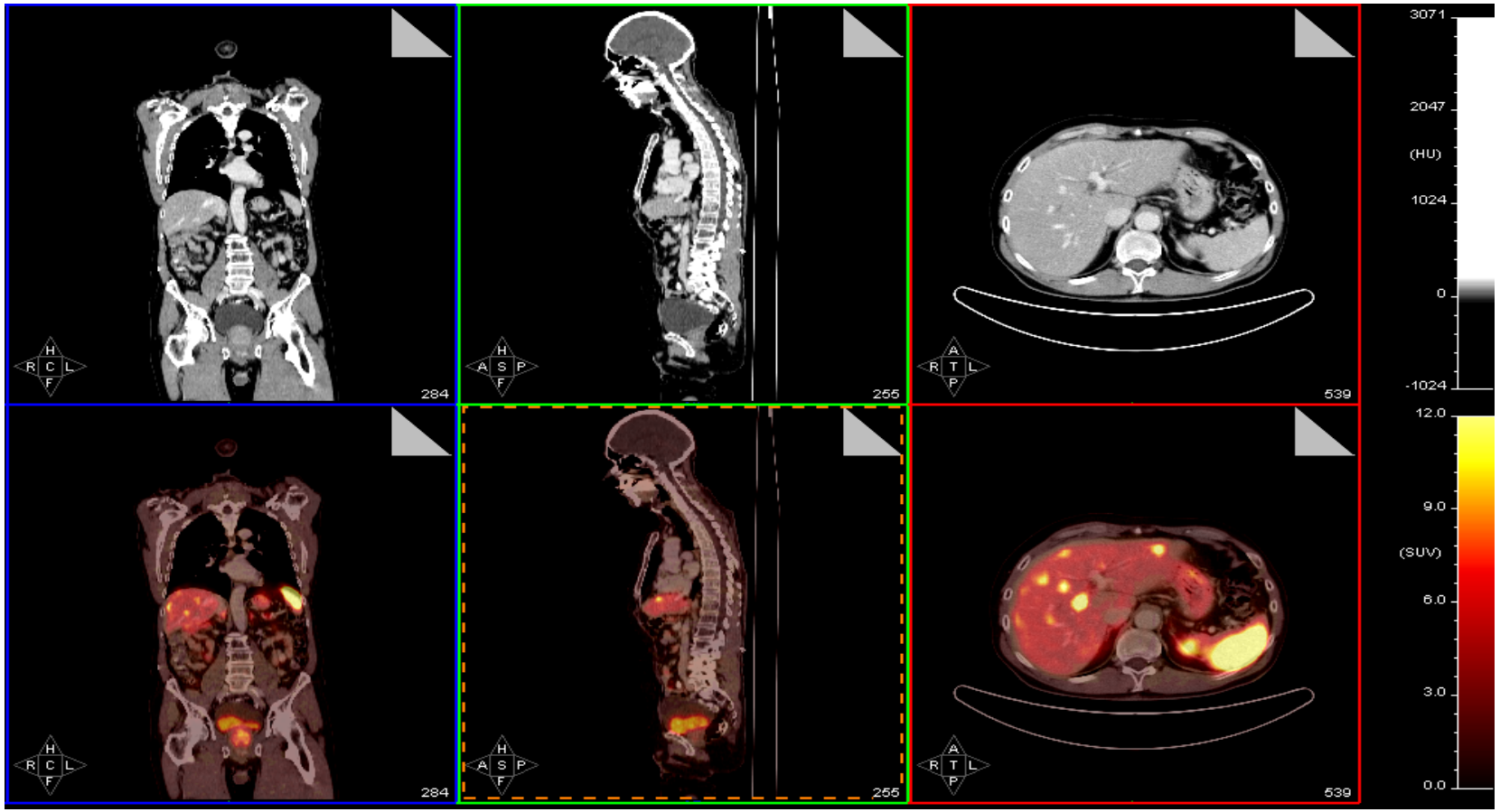

Male patient, 50 yrs, carcinoid with multiple metastases

Imaging of Neoangiogenesis

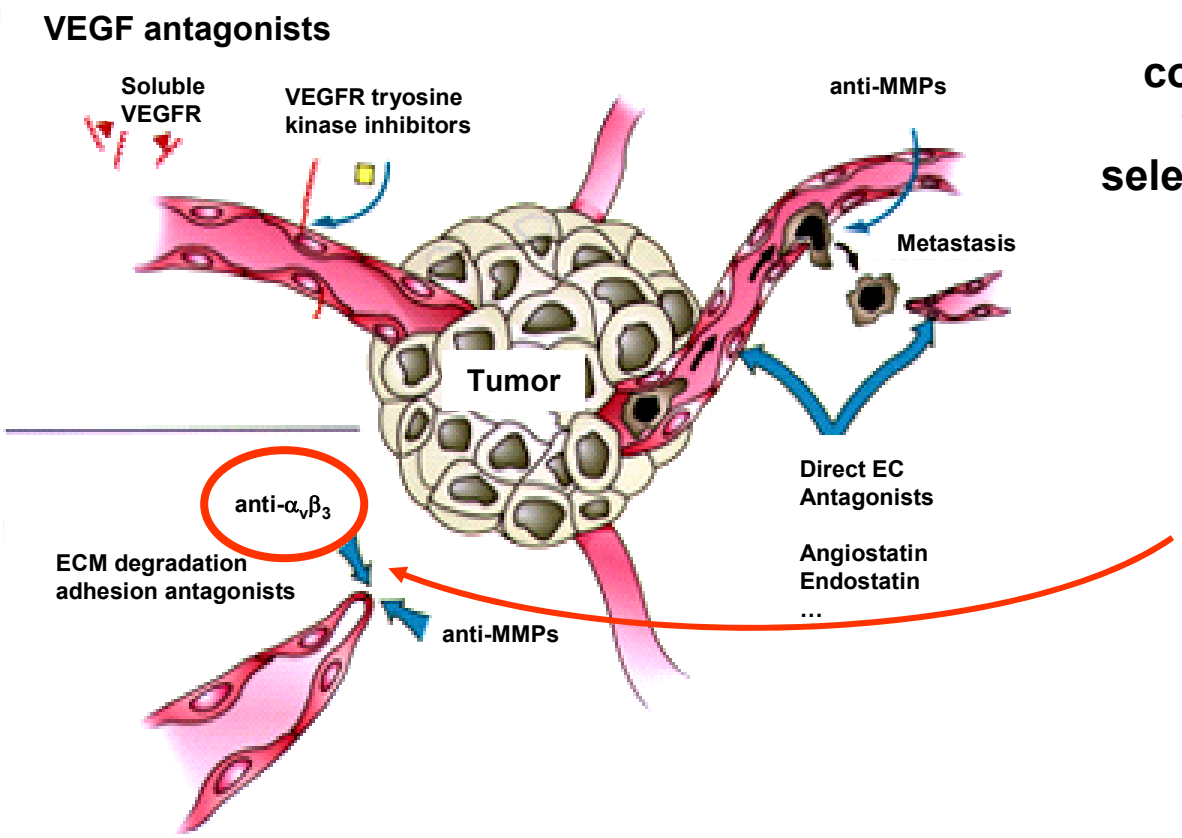

Arg-Gly-Asp (RGD)-containing pentapeptides with high affinity and selectivity to the $\alpha_v\beta_3$-integrin

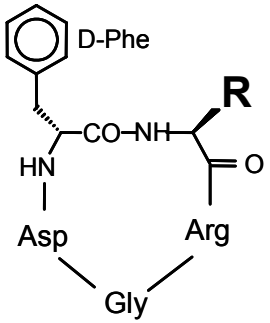

Carbohydrated RGD-Peptide : [^{18}F]Galacto-RGD

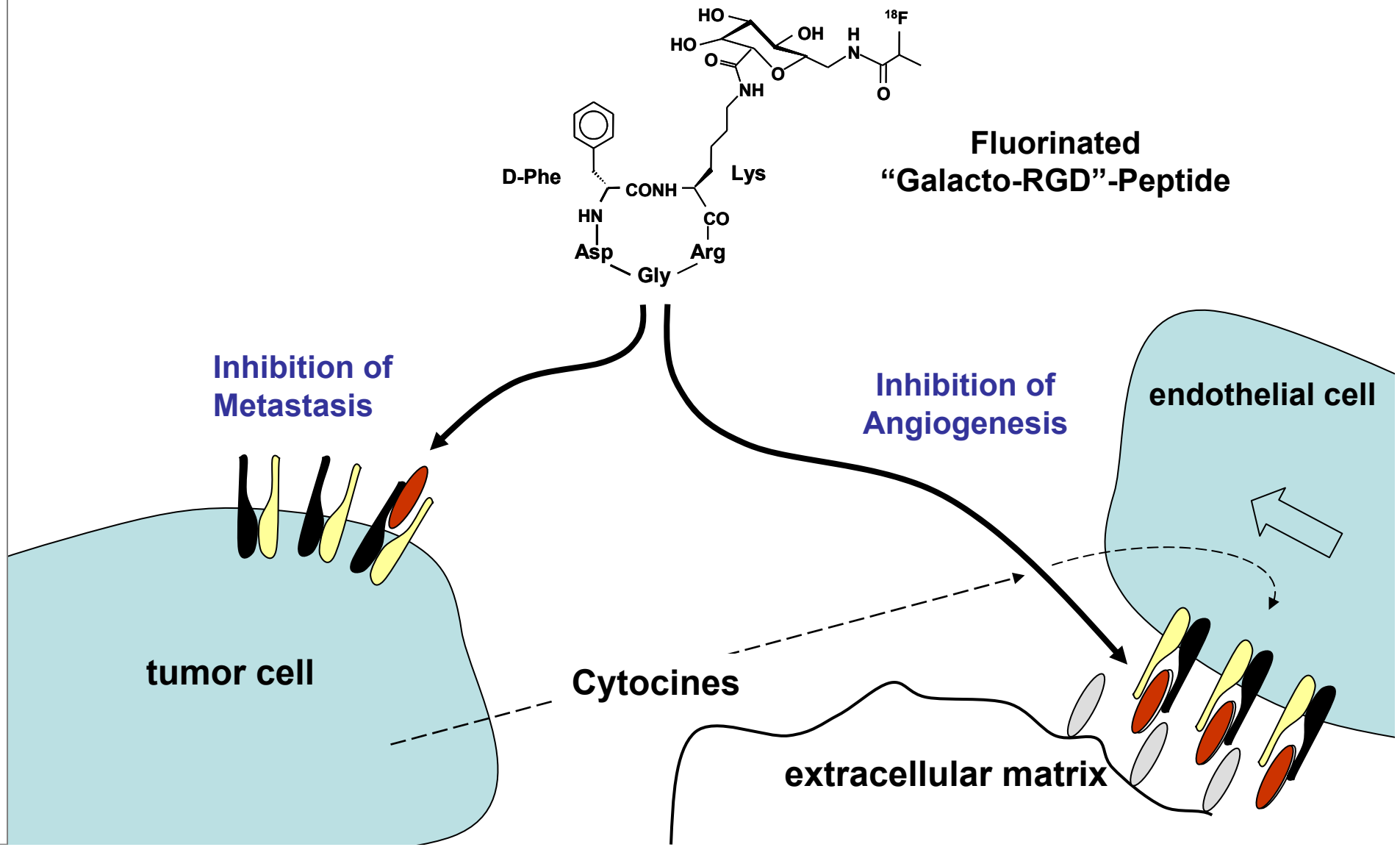

Carbohydrated RGD-Peptides with Improved Pharmacokinetics

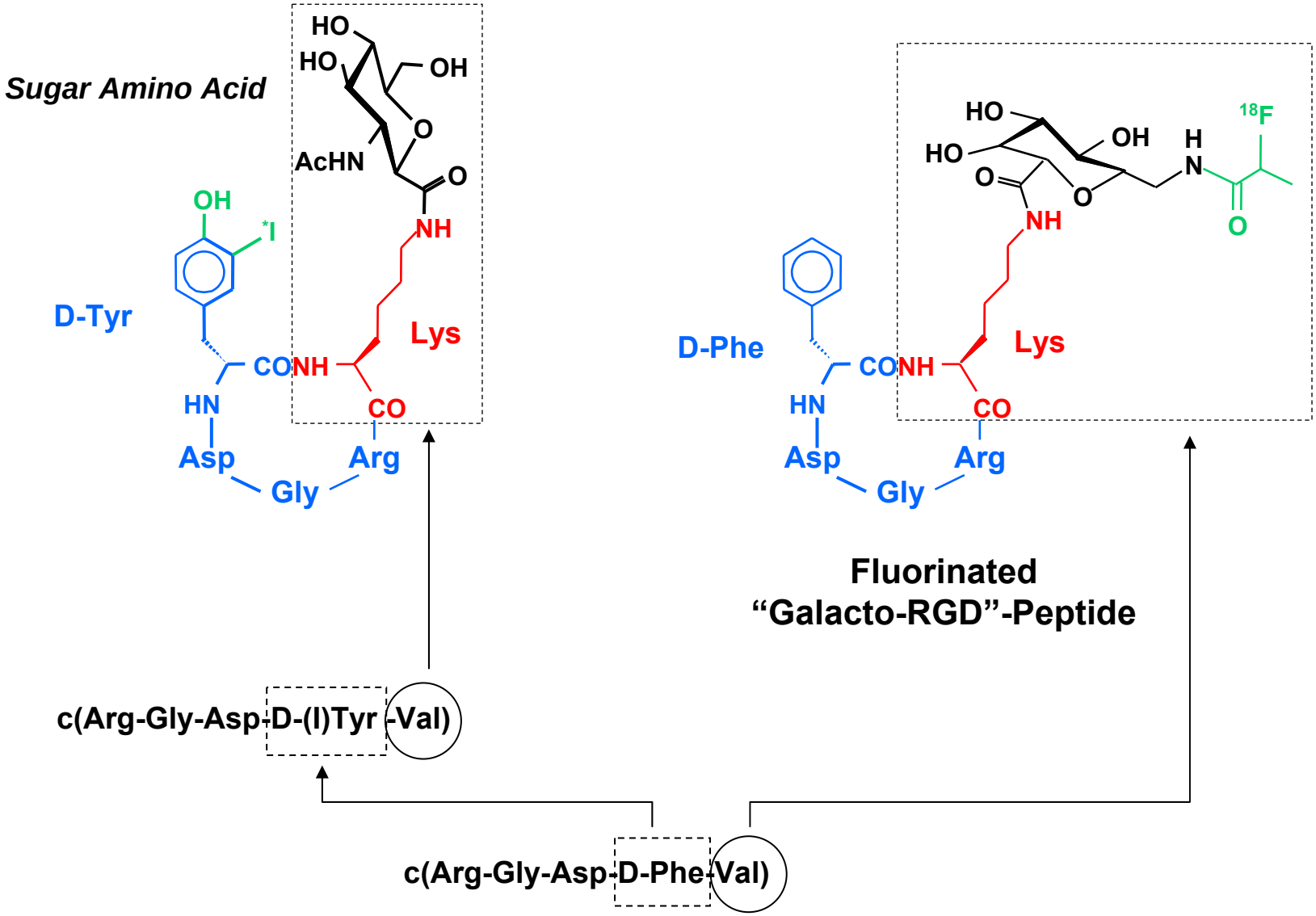

Comparison of the Pharmacokinetics in Selected Tissues

- *c(Arg-Gly-Asp-D-(l)Tyr -Val*): **Log P = -1.89**
- l-Gluco-RGD: **Log P = -2.45**

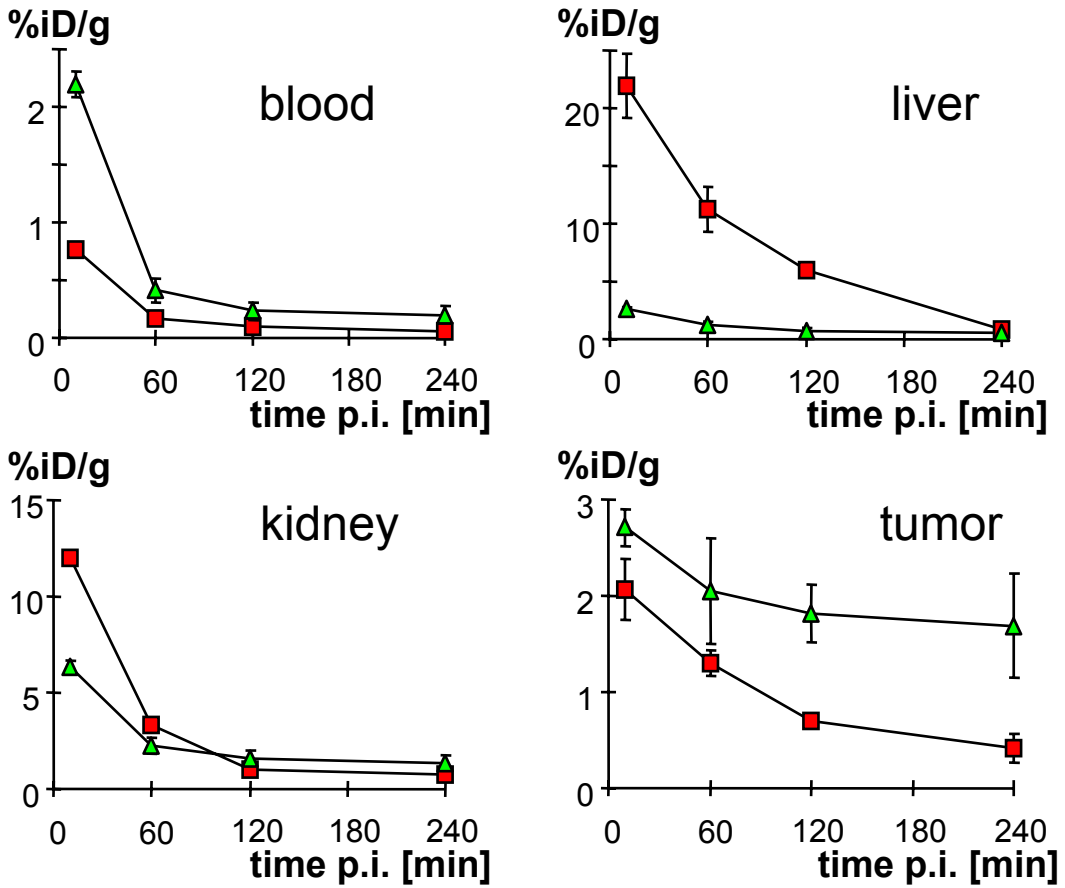

BALB/c mice, osteosarcoma model; comparable data obtained with M21melanoma bearing mice

Non-invasive Monitoring of $\alpha_v\beta_3$ Expression on the Tumor Vasculature

nude mouse bearing a *human* squamous cell carcinoma at the right shoulder

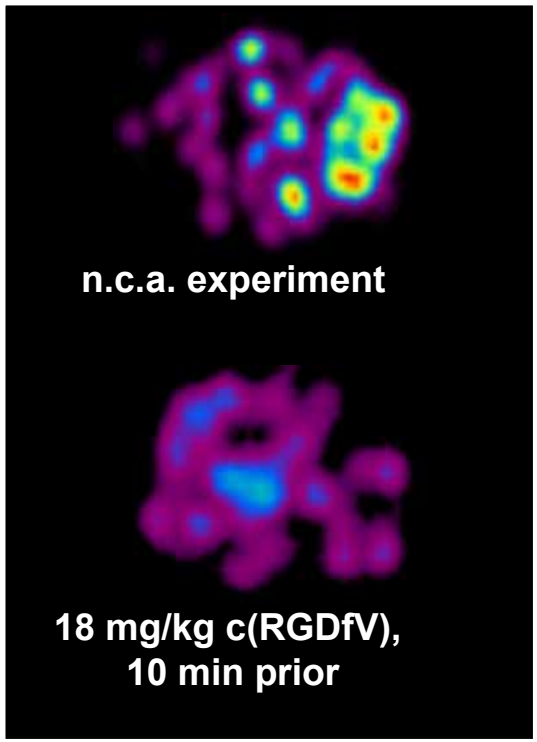

1.5h p.i

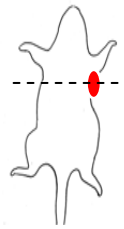

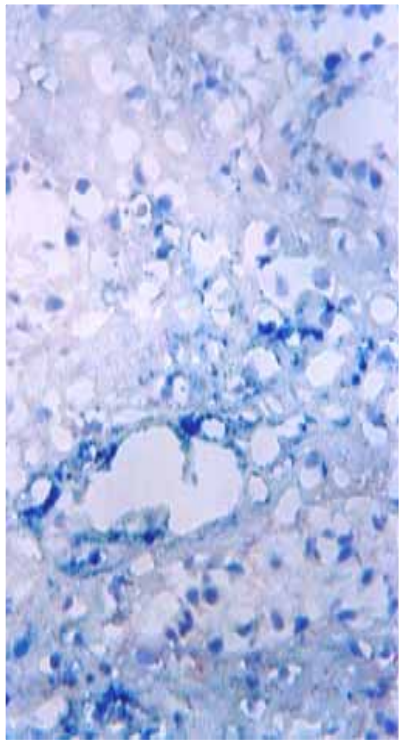

anti human αvβ3
MAb LM609

no expression of αvβ3 on cells

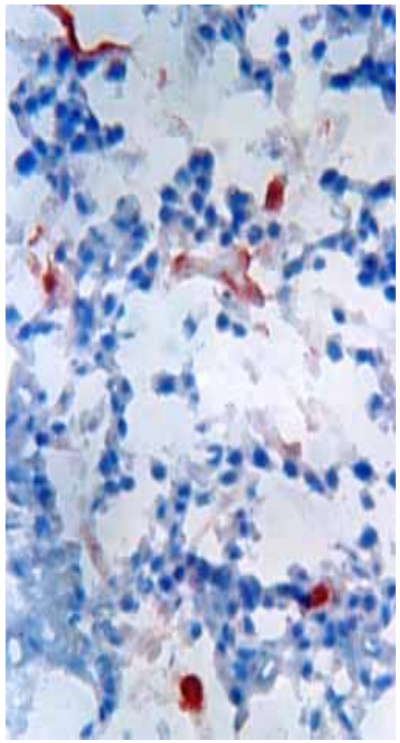

anti murine β3
MAb 2C9.G2

expression of murine β3 on vasculature

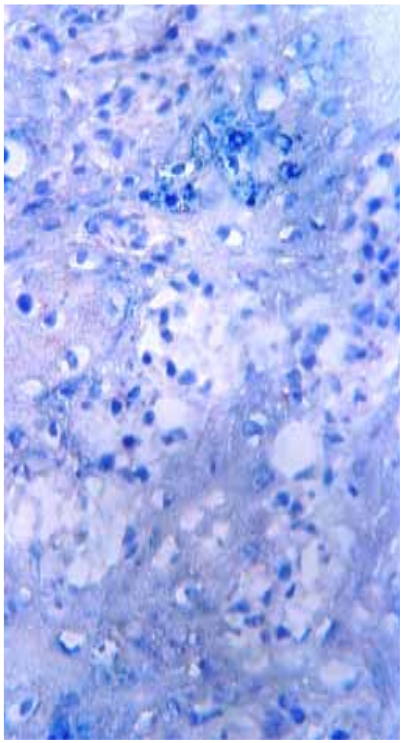

control
(**unspecific** MAb)

Determination of $\alpha_v\beta_3$-Expression in vivo

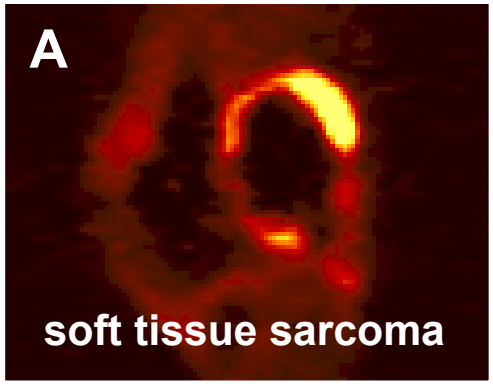

sagittal section, 170 min p.i. ,
circular tracer uptake,
max. SUV=10

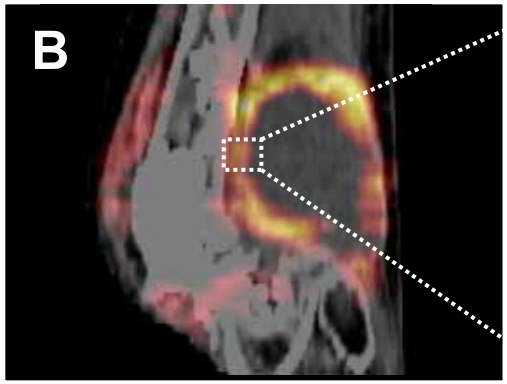

PET/CT image fusion;
uptake corresponds with
the tumor-wall

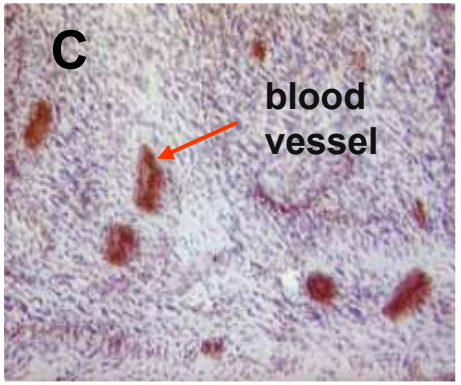

Immunohistochemistry,
MAb LM609, staining of
blood vessels

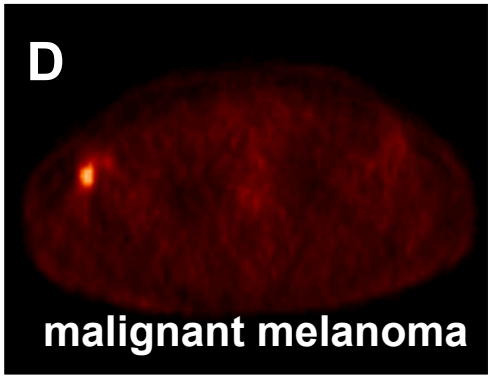

axial section, 140 min p,i,
uptake in the lymph node

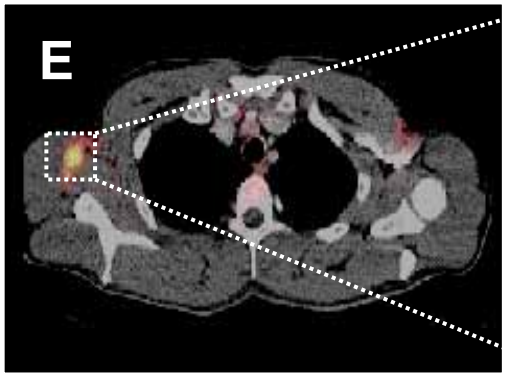

PET/CT image fusion

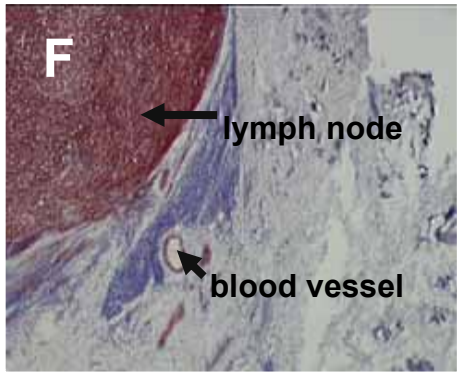

Immunohistochemistry, focal
MAB LM609, staining of
tumor cells and blood vessels

Multiple-Ligand-Tumortargeting (MLT)

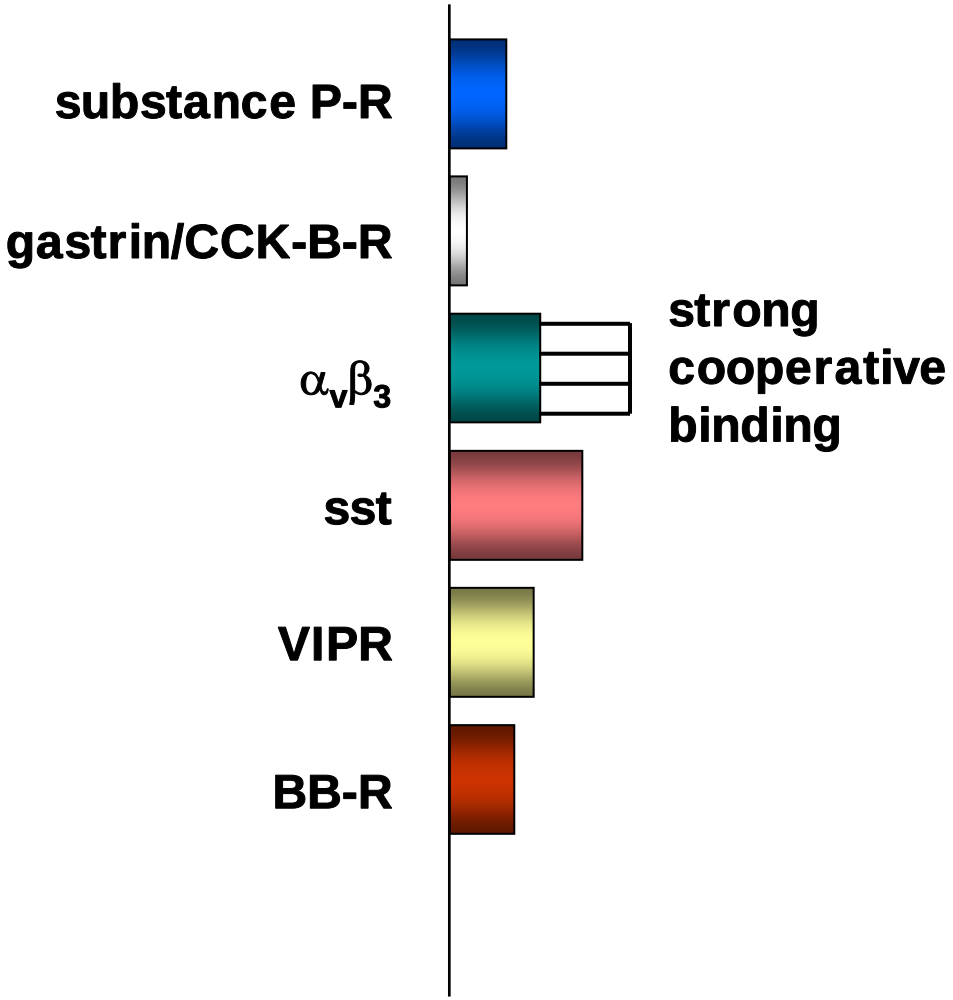

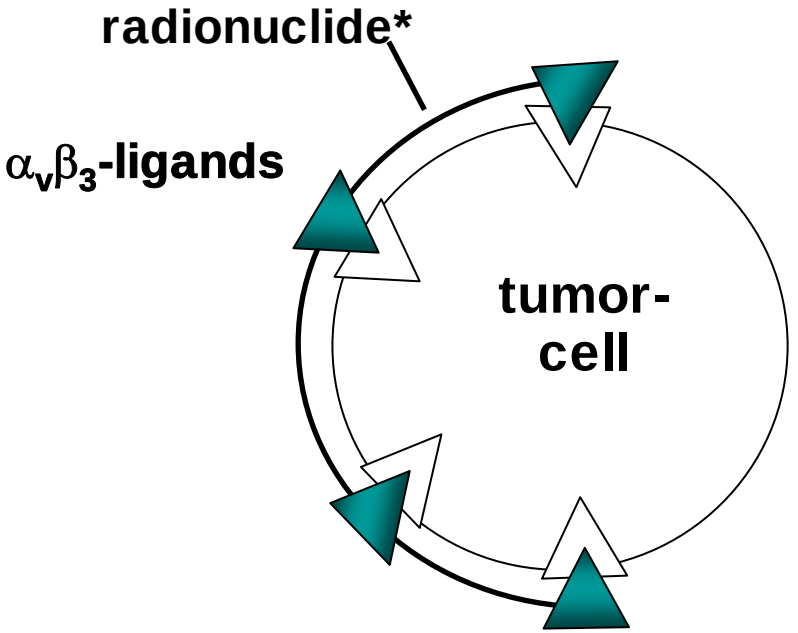

Structure of the Extracellular Domain of $\alpha_v\beta_3$

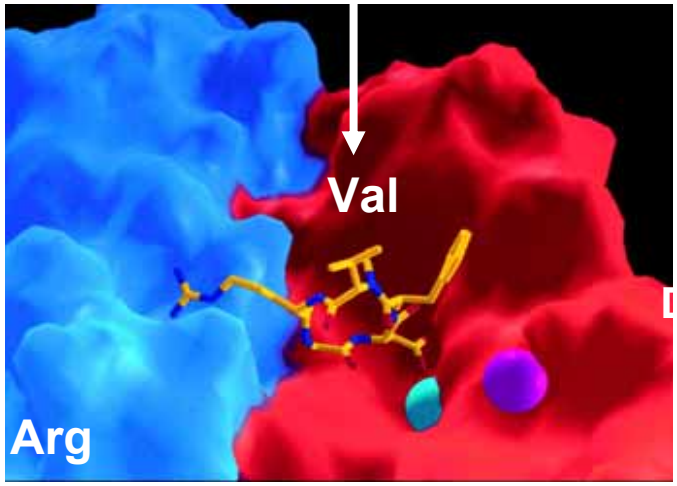

J.-P. Xiong, et. al, Science **2001**.

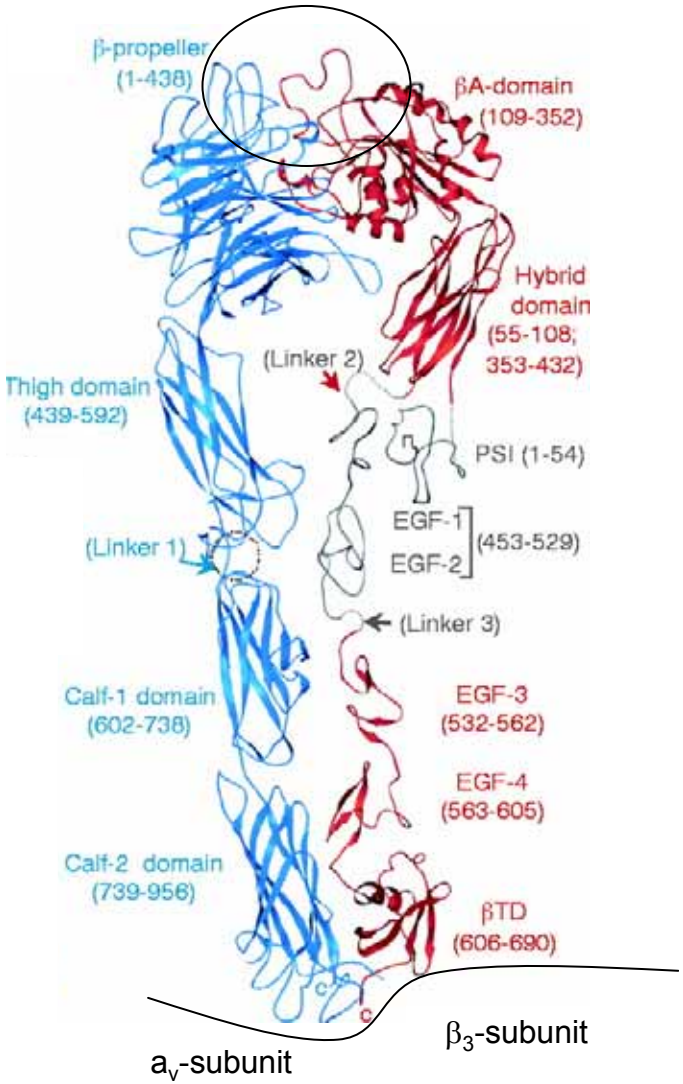

Multimeric [^{18}F]c(RGDfE)-Peptides

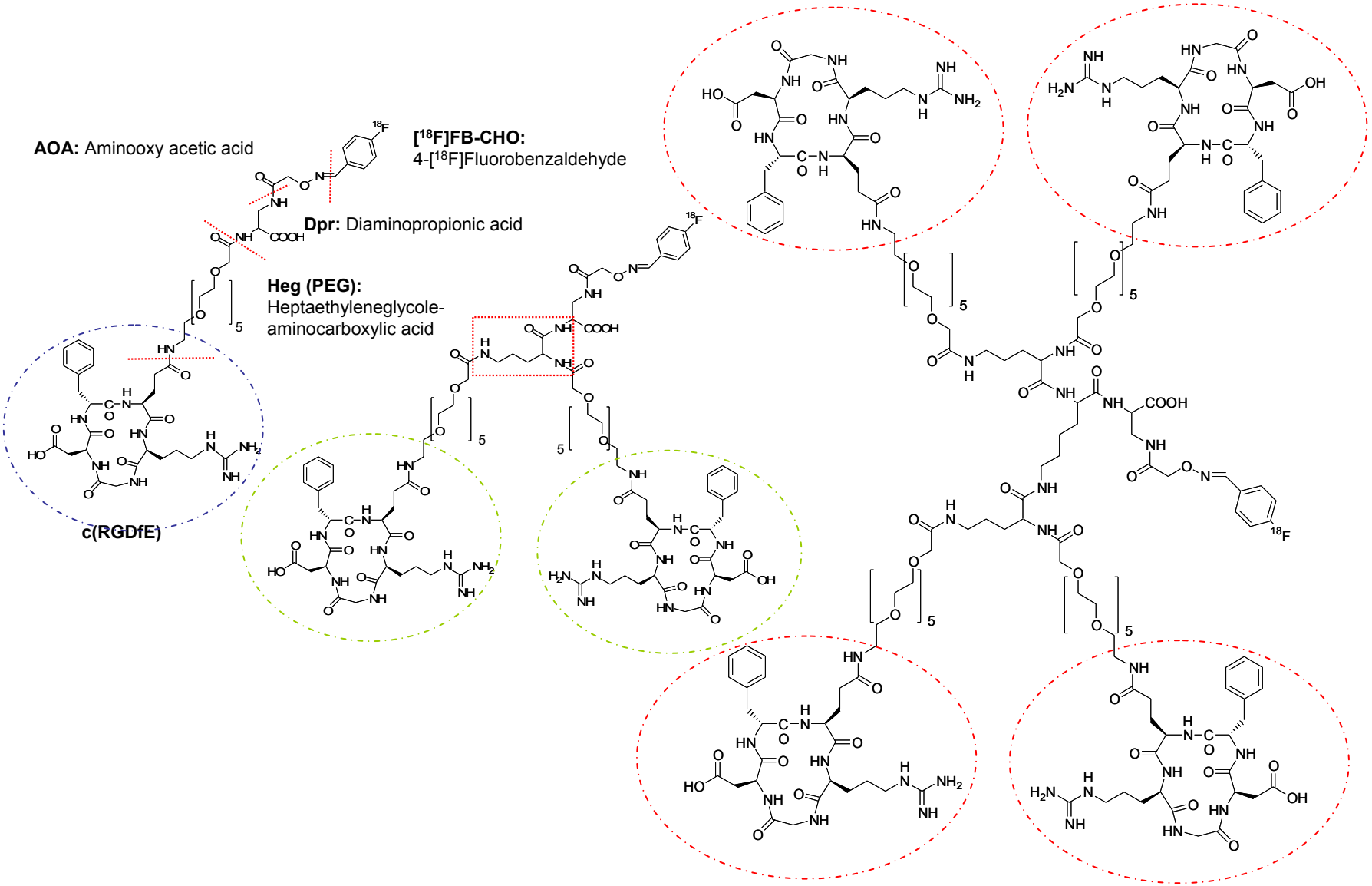

^{18}F-Labeling via Oxime Formation

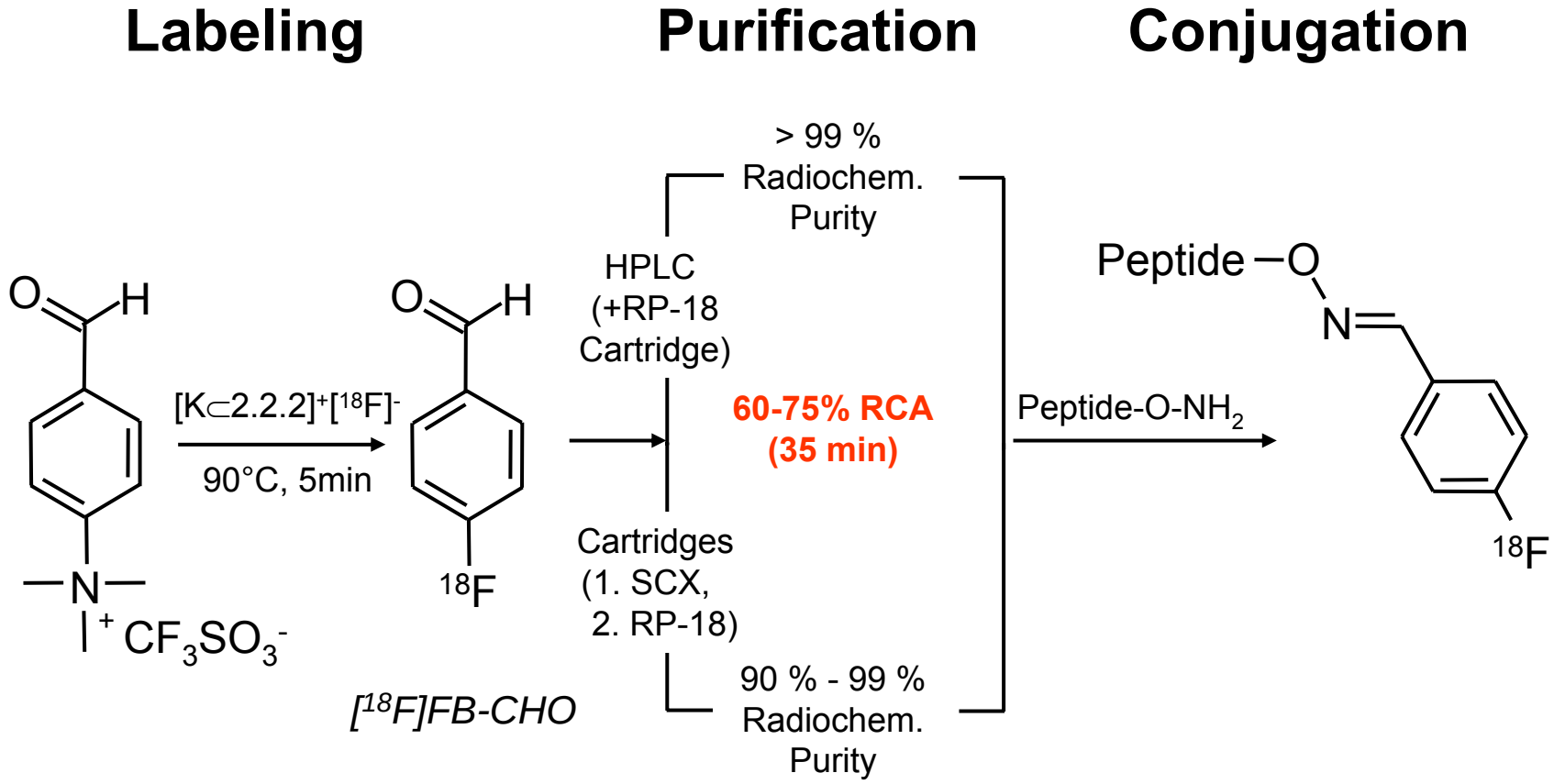

Route suitable for a variety of radiolabeled aldehydes and ketones

Binding Affinities of Multimeric RGD-Peptide Constructs

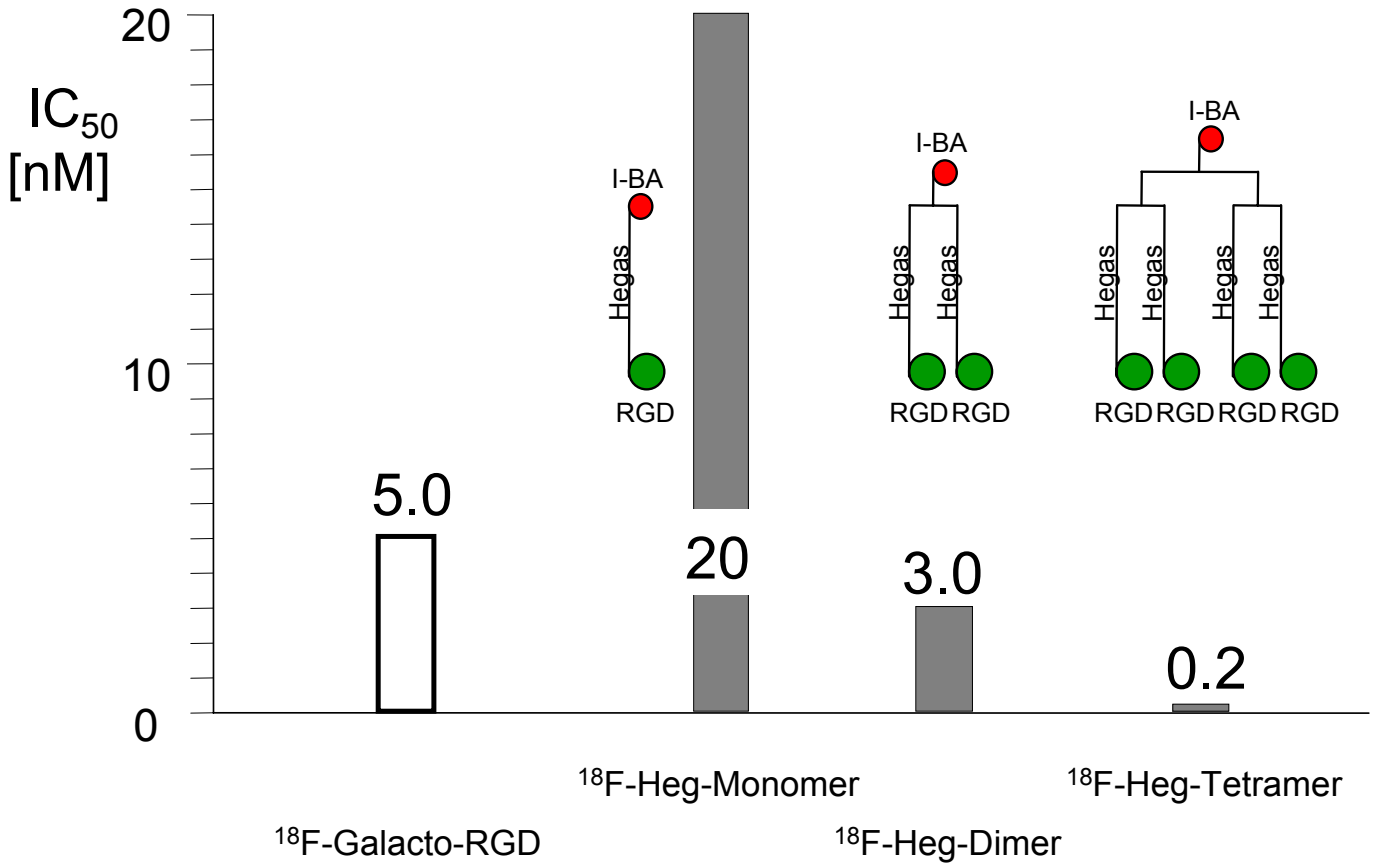

Tumor to Organ Ratios

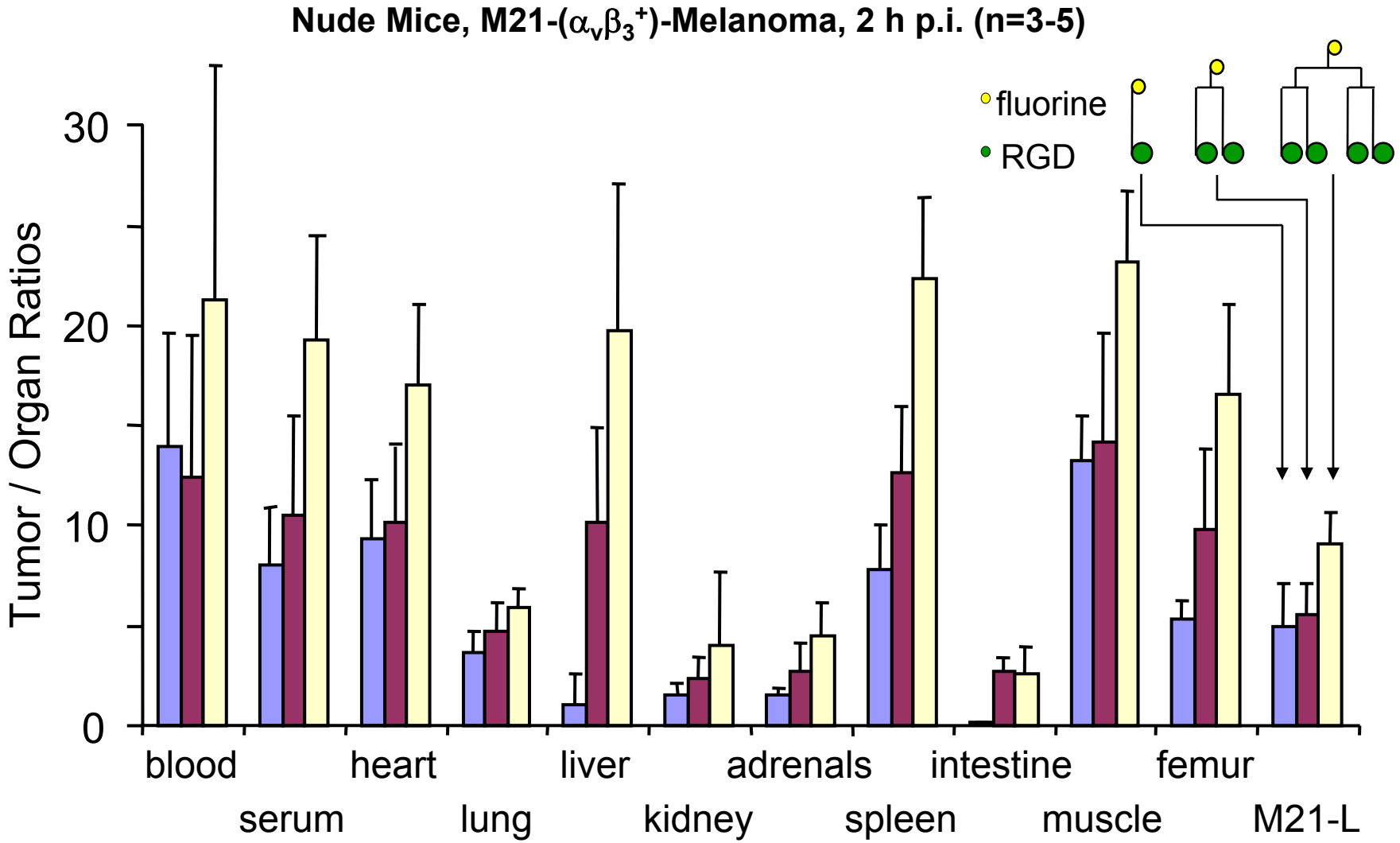

PET Imaging of [^{18}F]RGD-Mono-, Di- and Tetramers

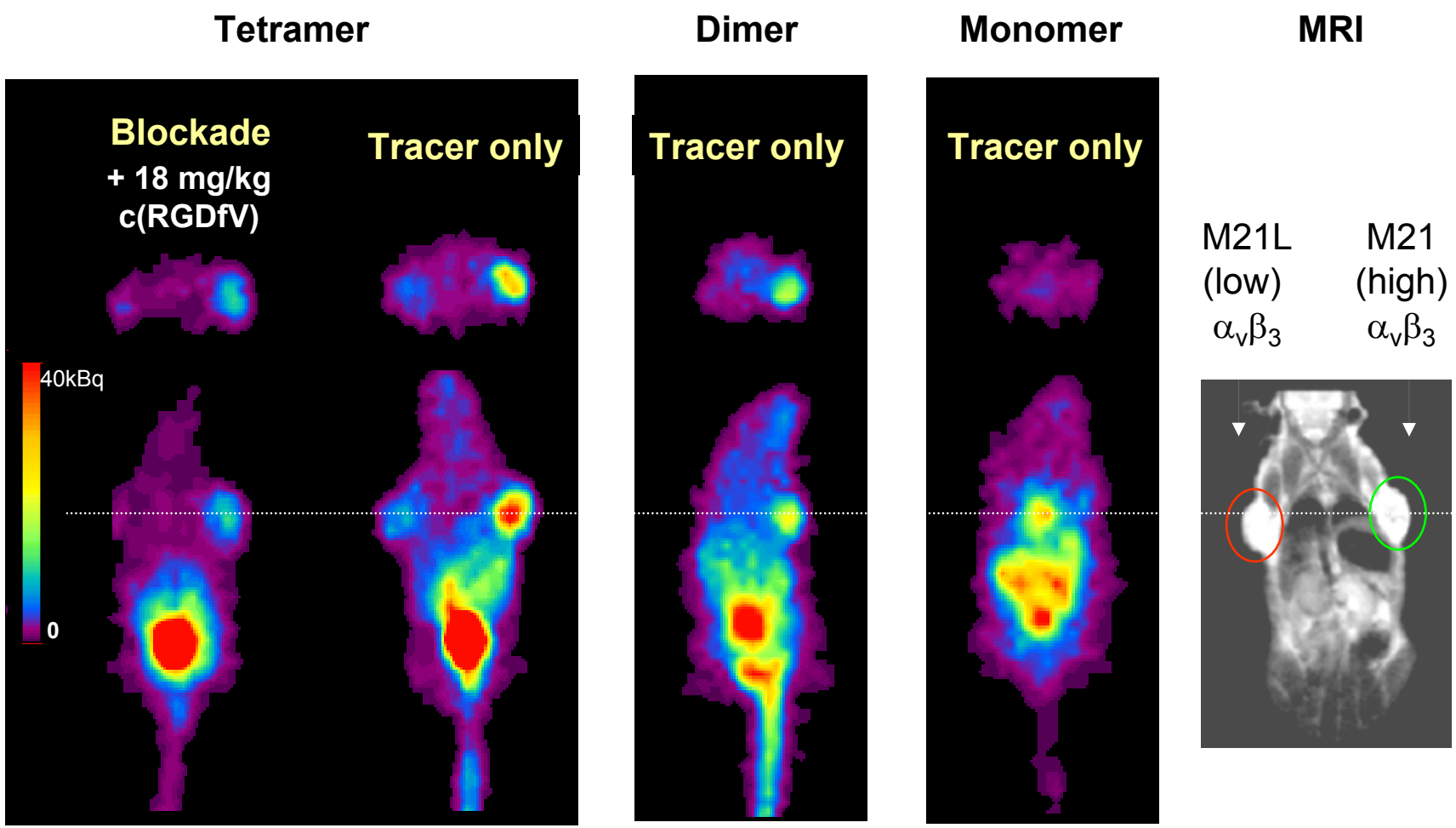

ECAT Exact HR$^+$, 90 min p.i.

Affinities of Multimeric RGD-Peptides with/without RAD-Sequences

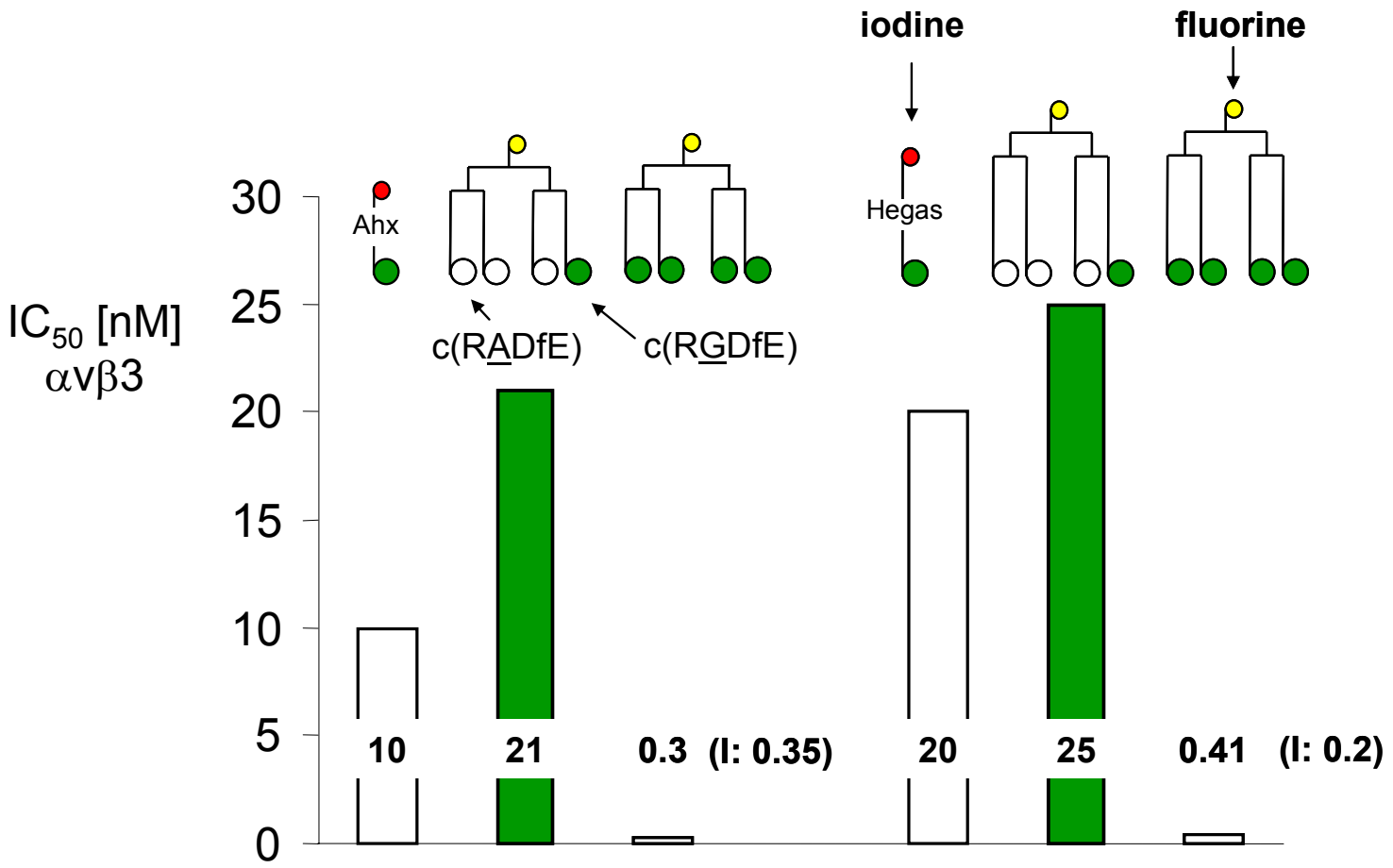

Thumshirn et al. Eur Chem. 2003

PET Imaging of Tetrameric [^{18}F]RGD with and without „Knockout“ Sequences

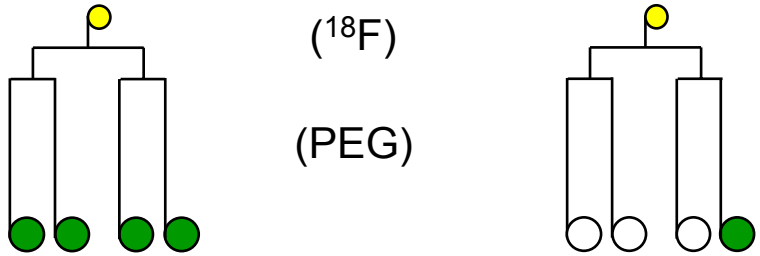

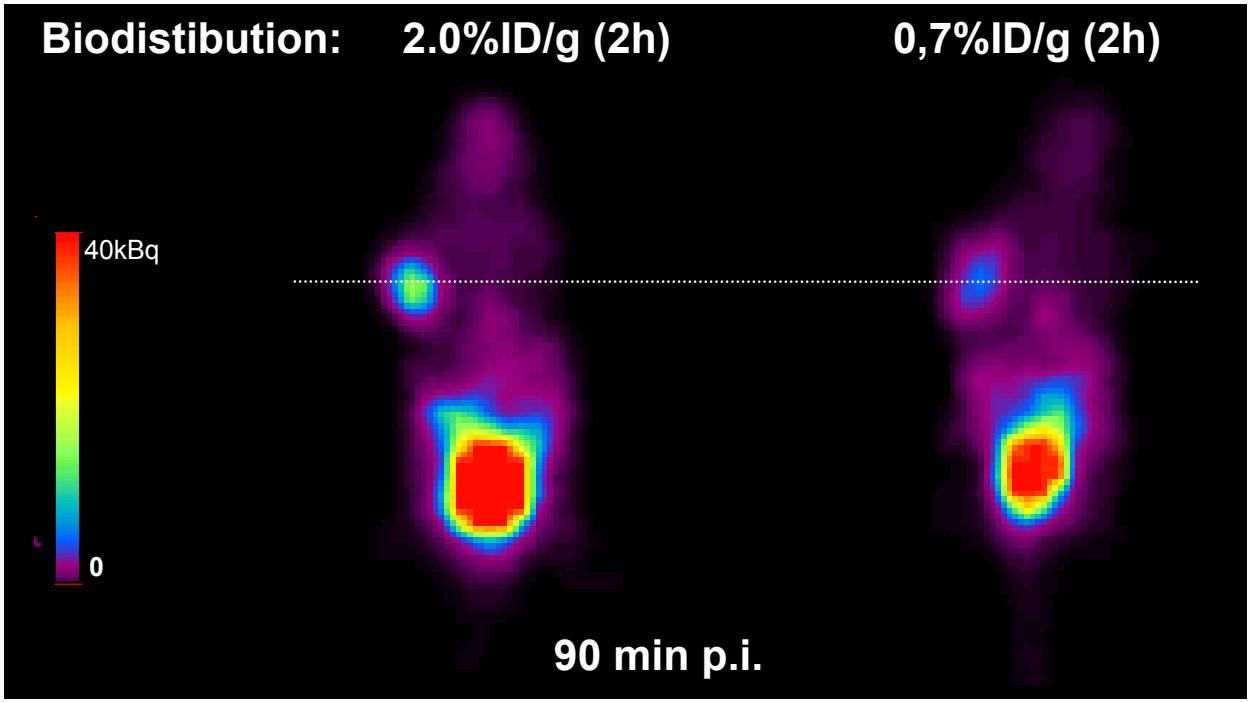

ECAT Exact HR^{+}, 90 min p.i.

Poethko et al. Radiochimica Acta 2004

Radiopharmaceutical Chemistry and Development of Radiopharmaceuticals

Triple T

Target

+ Tracer

+ Technology

= Suitable Radiopharmaceutical and Contrast Agent

Imaging with PET and SPECT

Thorsten Poethko

Nuklearmedizinische Klinik und Poliklinik
und
Institut für Radiochemie
Technische Universität München

Basics of Radionuclide Production

Knowledge of production process

Purification

Recovery of target material

Analytical methods (quality control)

Radionuclide Production

(A) **Cyclotron** **(ca. 250 world-wide)**

(Ion accelerator)

(B) **Reactor** **(ca. 250 Research reactors world-wide)**

(C) **Generators**

General Aspect

Cyclotron-nuclides:
mostly neutron pure

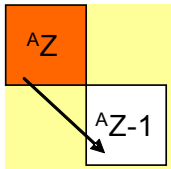

Positron emission: ß+-decay

Electron capture: EC-decay

Reactor-nuclides:
neutron rich

Emission of electron ß⁻-decay

Production of commonly used PET-Nuclides via Compact Cyclotron

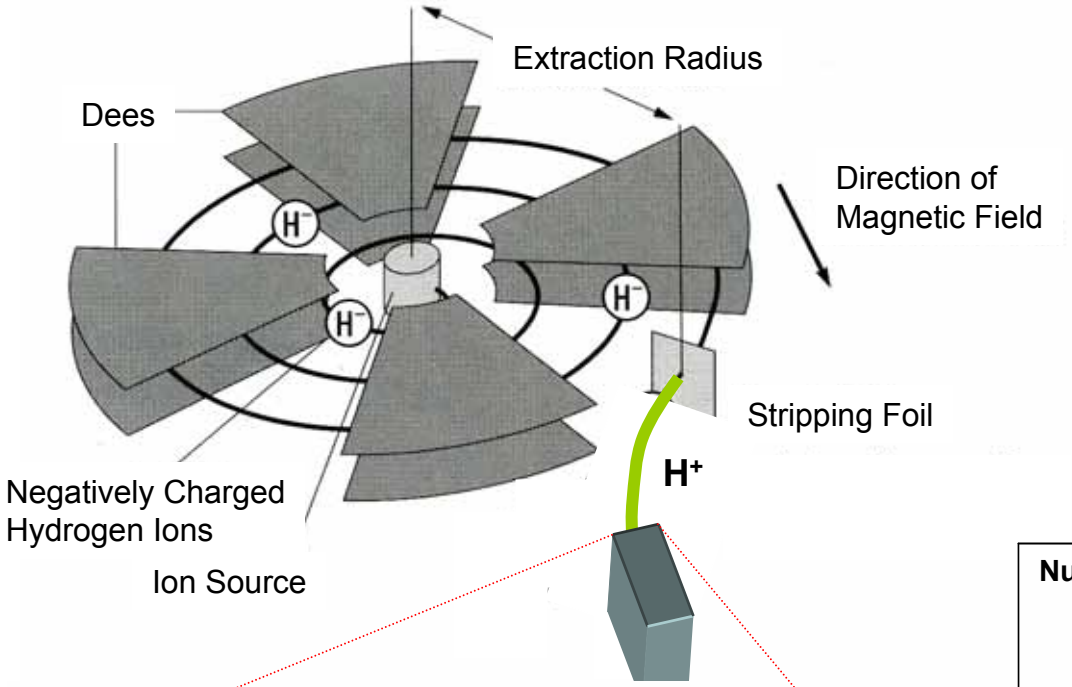

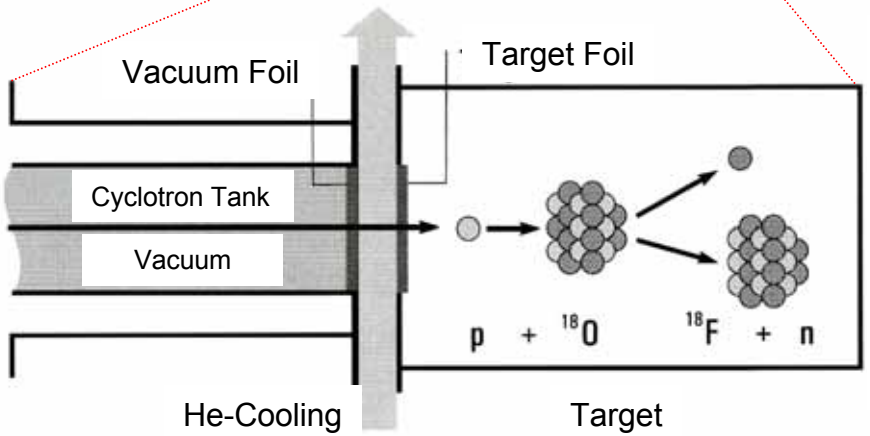

Nuclide	$T_{1/2}$ (min)	Nuclear-Reaction	Energy (MeV)	Mode of decay [%]	Target product
^{11}C	20.4	$^{14}N(p,\alpha)$	13 → 3	β^+ (99.8)	$^{11}CO_2$ ^{11}CO
^{13}N	10.0	$^{16}O(p,\alpha)$	16 → 7	β^+ (100)	$^{13}NO_2^-$ $^{13}NO_3^-$
^{15}O	2.0	$^{15}N(p,n)$	10 → 0	β^+ (99.9)	$^{15}O_2$
^{11}C	109.6	$^{18}O(p,n)$	16 → 3	β^+ (97)	$^{18}F_{aq}^-$ $^{18}F_2$

Selection of Radionuclide

Half-life comparable with kinetics of physiological process ?
(too short, too long)

Do the nuclear and physical properties fulfill the special demands ?
(e.g. pure β^+ - Emitter)

Labeling chemistry compatible with targeting ?
(e.g. metalated CNS-ligands)

Patient dose acceptable ?
(CNS-ligands: C-11 or F-18)

Nuclide availability ?
(Generator, cyclotron, energy range)

PET-Radionuclides

Isotope	Half-life [h]	Positron percentage branching %β^+	Maximum positron energy [MeV] $E\beta^+_{max}$	Intrinsic spacial resolution loss [mm]	Comments
^{18}F	1,8	96,9	0,63	0,7	
^{55}Co	17,5	76	1,50	1,6	$T_{½,D}$ = 2,6 y
^{61}Cu	3,4	61	1,22	1,5	
^{64}Cu	12,7	18	0,65	0,7	
^{66}Ga	9,5	57	4,15	-	
^{68}Ga	1,14	89	1,90	2,4	G: ^{68}Ge / 271d
^{75}Br	1,6	71	1,72	2,2	$T_{½,D}$ = 120 d
^{76}Br	16,2	54	3,94	5,3	
^{86}Y	14,7	33	3,14	1,8	
^{110m}In	1,15	62	2,20	3,0	G: ^{110}Sn / 4,1 h
^{120g}I	1,35	56	4,59	5,4	
^{124}I	100,3	23	2,14	2,3	

Resolution Limitation due to Positron Energy

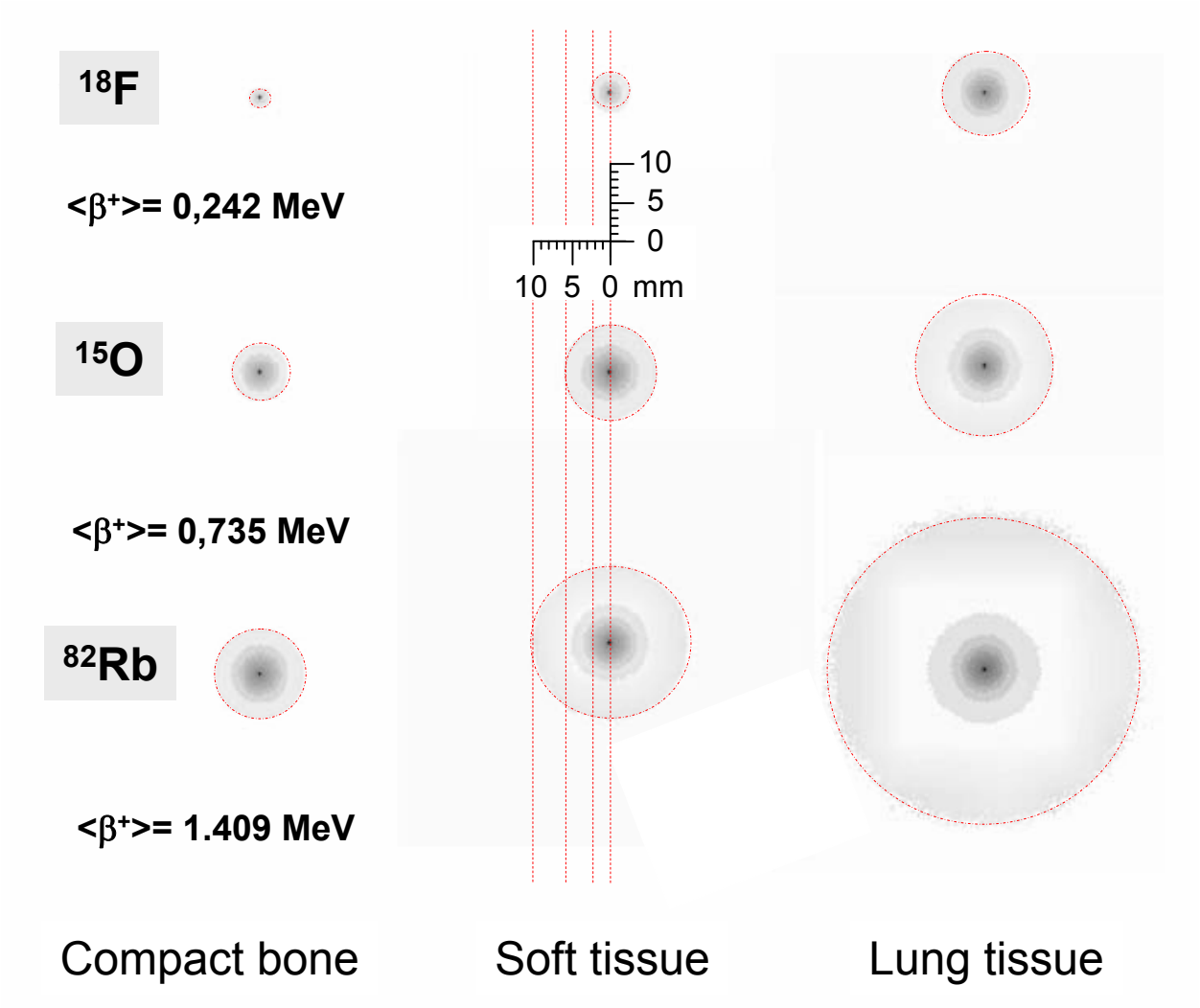

Positron-Emission

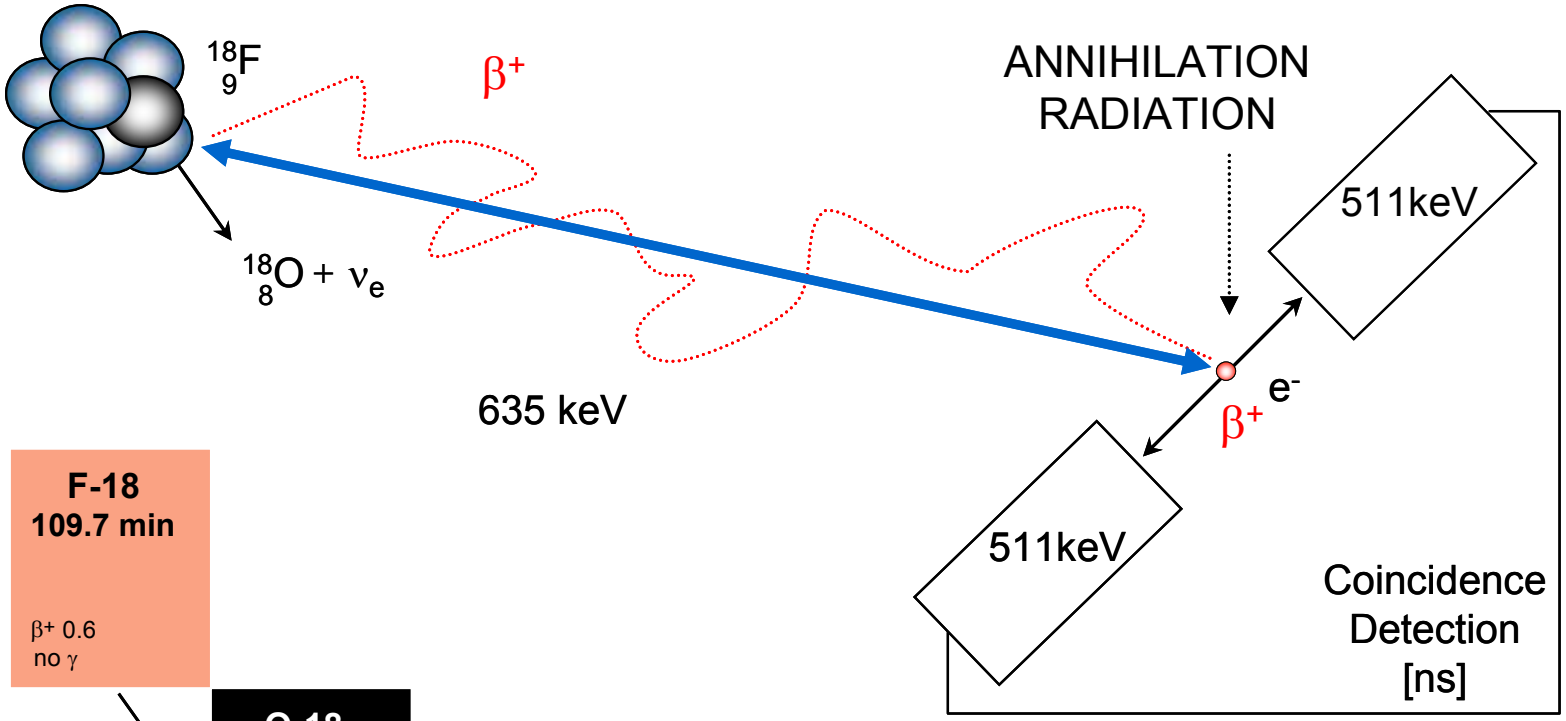

F-18
109.7 min

β^+ 0.6
no γ

O-18
0,200

σ 0.00016

Production of F-18

Nuclear reaction	$^{18}O(p,n)^{18}F$	$^{16}O(^{3}He,n)^{18}F$	$^{20}Ne(d,\alpha)^{18}F$	$^{18}O(p,n)^{18}F$
Target	$H_2{}^{18}O$	H_2O	Ne (0.1-0.2% F_2, 18 bar)	$^{18}O_2$ (20 bar) (2. + 0.1% F_2)
Energy range of bombarding particle [MeV]	16 → 0	36 → 0	11.2 → 0	10 → 0
Chemical form	$[^{18}F]F_{aq}^-$	$[^{18}F]F_{aq}^-$	$[^{18}F]F_2$	$[^{18}F]F_2$
Thick target yield [MBq $\mu A^{-1} h^{-1}$]	2.200	250	350-450	~350
Specific activity [TBq $mmol^{-1}$]	40×10^3	40×10^3	0.04–0.4	0.04-2

- **Mainly produced via $^{18}O(p,n)^{18}F$-reaction**
- **Product:** **$^{18}F_{aq}^-$ with high specific activity and up to 100% radiochemical yield, compared to $[^{18}F]F_2$ with low specific activity and max. 50% radiochemical yield**

^{18}F-Fluoride Chemistry

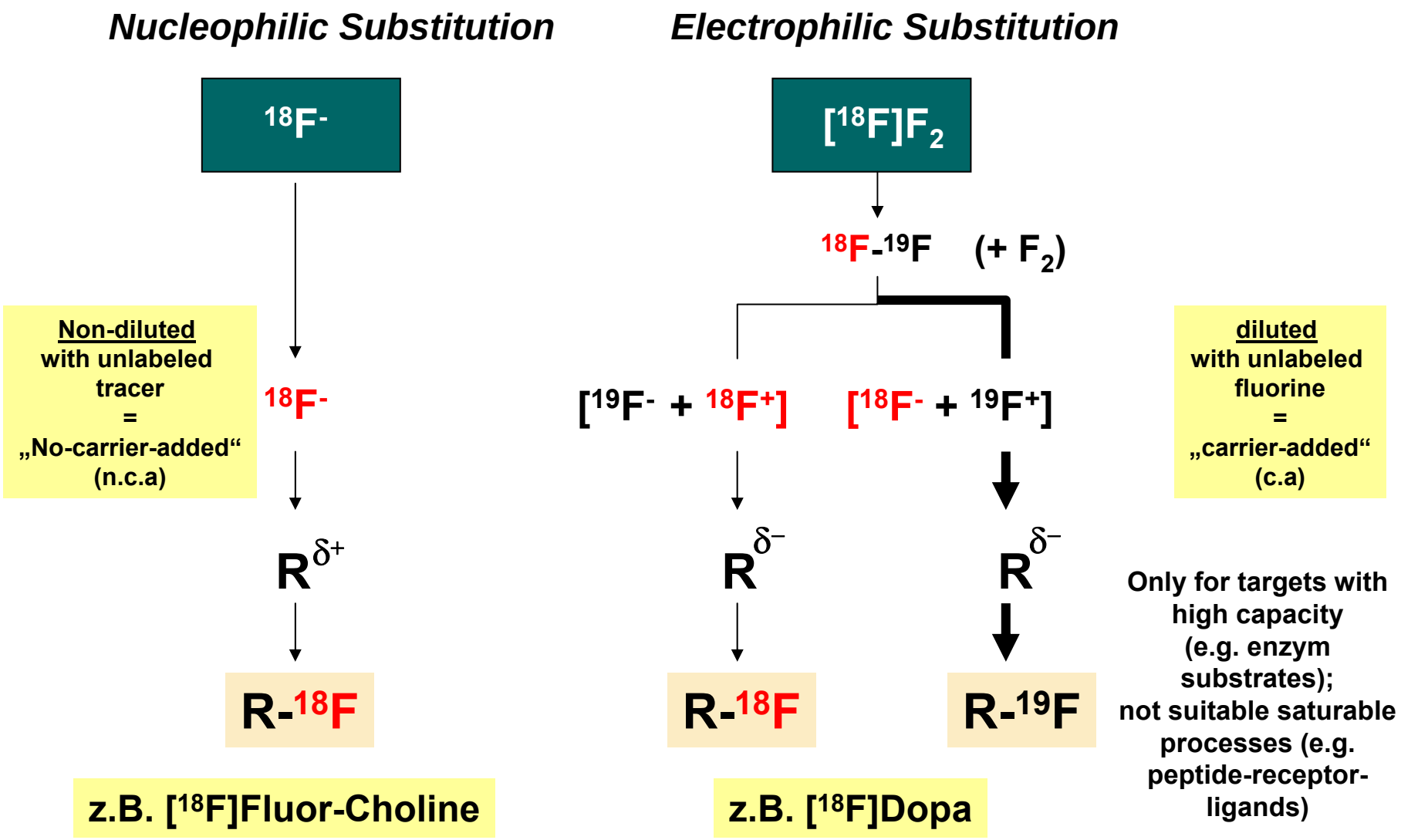

Production Scheme: Radiopharmaceutical Production

Cyclotron und on-line synthesis

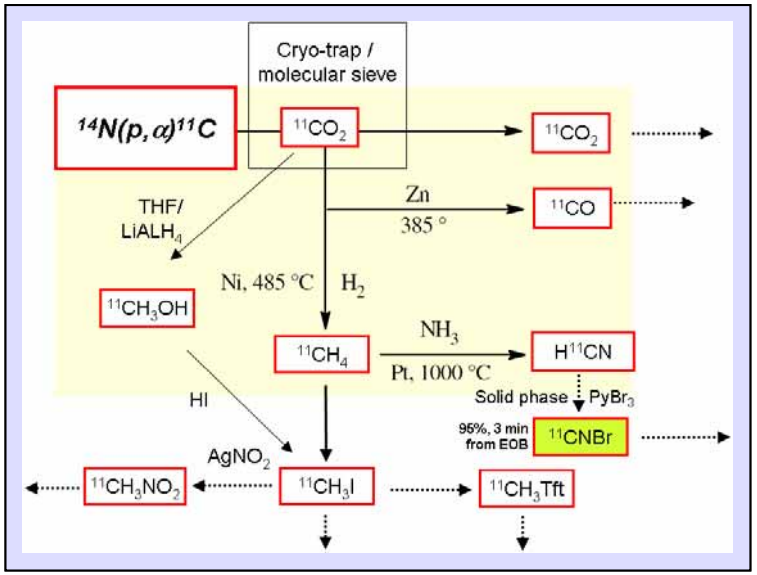

Automatic production

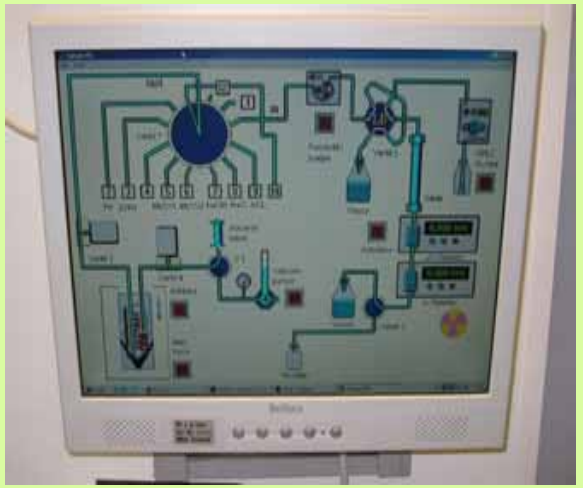

Quality control

Application

Automatic Synthesis

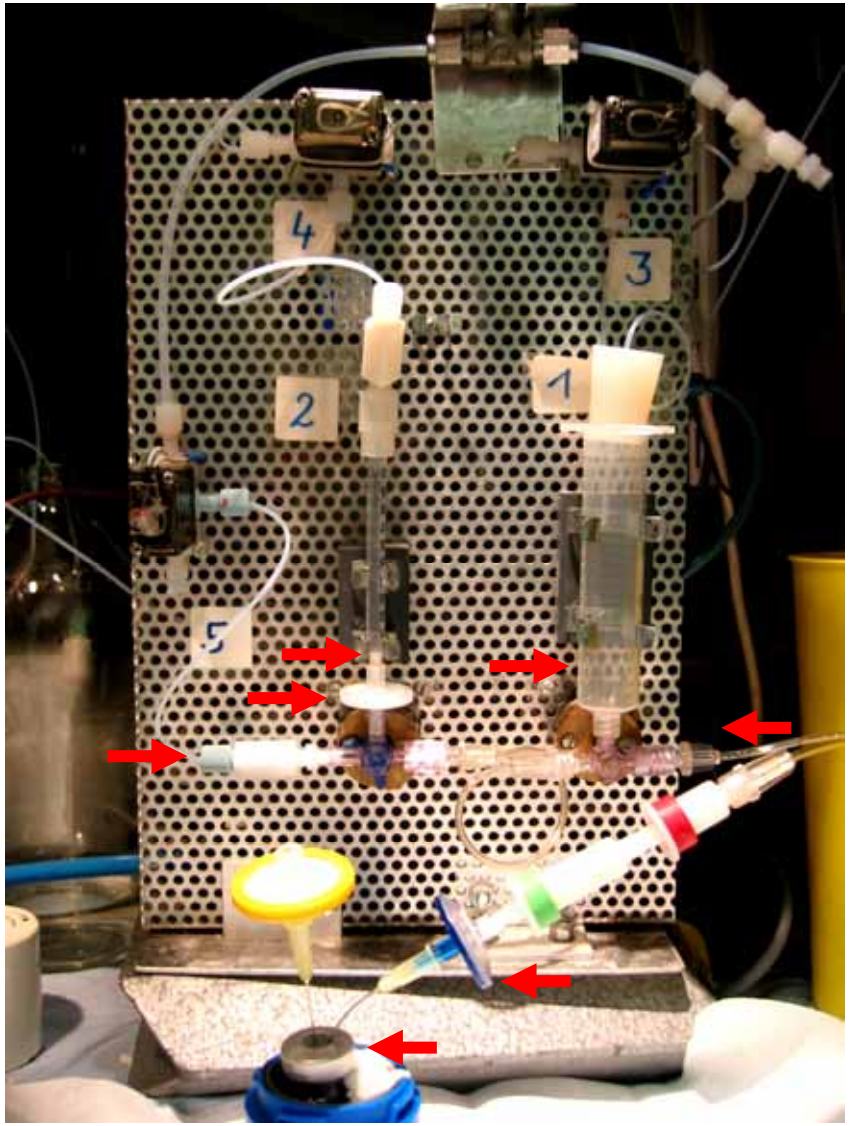

^{11}C-Methionine Production

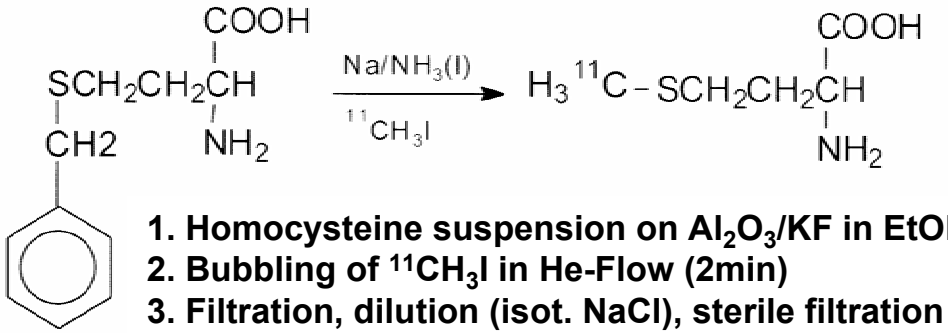

1. Homocysteine suspension on Al_2O_3/KF in EtOH
2. Bubbling of $^{11}CH_3I$ in He-Flow (2min)
3. Filtration, dilution (isot. NaCl), sterile filtration

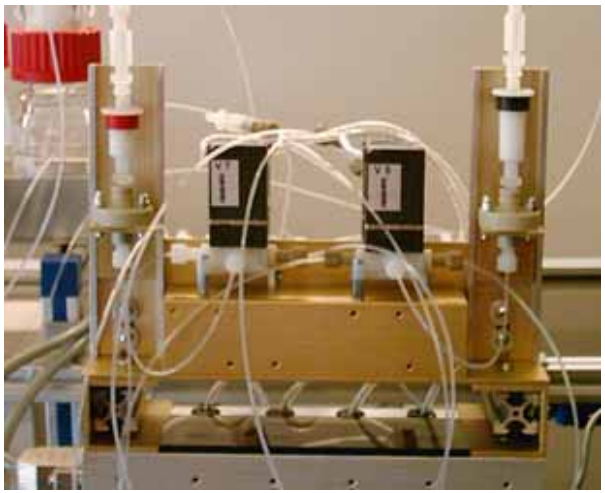

Generators for Positron Emission

Isotope	Half-life	Mode of decay	E_{β^+} [keV]
^{68}Ge	271 d	EC (100%)	
↓			
^{68}Ga	68 min	β^+ (90%), EC (10%)	1900
^{62}Zn	9.2 h	β^+ (93%), EC (7%)	660
↓			
^{62}Cu	9.7 min	β^+ (98%), EC(2%)	2930
^{82}Sr	25 d	EC (100%)	
↓			
^{82}Rb	1.3 min	β^+ (96%), EC (4%)	3350

Structure of „non-isotopic“ Radiopharmaceuticals

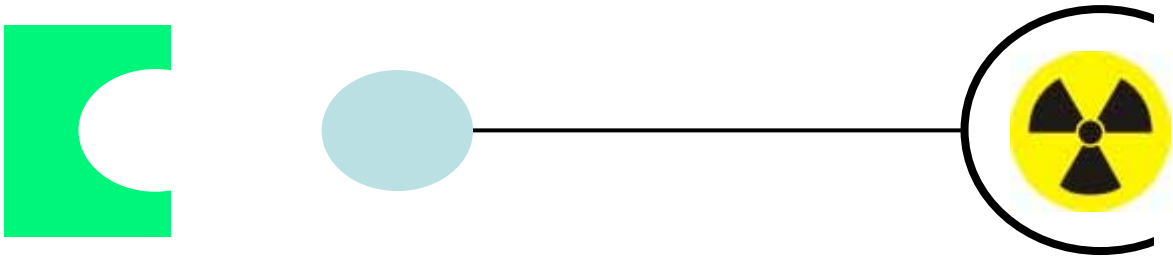

Address, Target	**Pharmacophor, biospecific binding**	**Spacer, Linker**	**Labeling, Label**
Intra-/Extracellular Receptors Transporter Enzyme Antigens RNA …	Small org. Molecules Peptidomimetics Peptide Protein Antibody Complex (Ions)	Metabolic stabile Metabolic labile Enzymatic cleavable Hydrolytic sensitive pH sensitive	Covalent Complex Statically distributed Defined bondage No-carrier-added Carrier-added

Peptide, Protein and Macromolecule Labeling with Radiometals

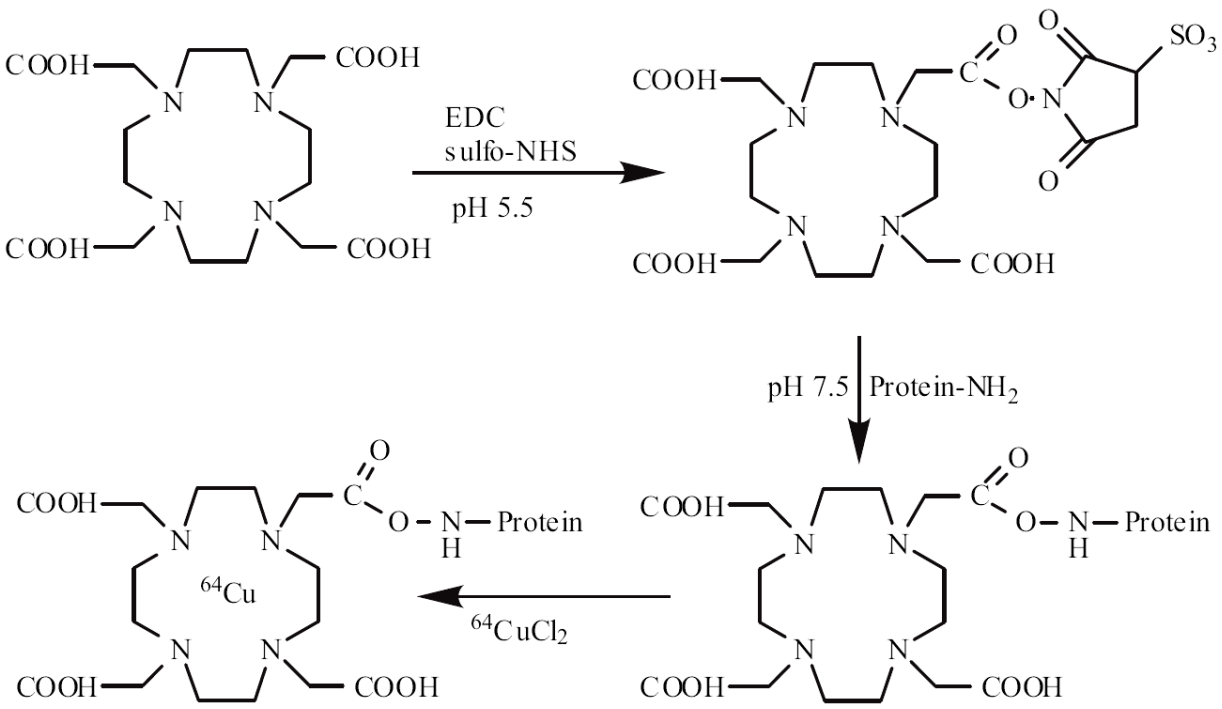

In, Ga, Cu …
Lu, Y, Bi, Ac …
Fe, Gd, …..

Radionuclide Production for SPECT

SPECT = Single-Photon-Emission-Computer Tomography

All these nuclides are commercially produced and sold

as radionuclide,

generators

or readily-prepared radiopharmaceuticals

Most important SPECT-Isotope is Technetium (^{99m}Tc) !

SPECT - Isotopes

Radio nuclide	$T_{1/2}$	Mode of decay	Main-γ-Lines	Productions data		
				Nuclear reaction	Energy range [MeV]	Yield [MBq/µAh]
^{67}Ga	3.26 d	EC (100)	93 (27%)	^{68}Zn(p,2n)	26→18	185
^{99}Mo	2.75 d	b- (100)	181 (6%) 740 (12%)	^{235}U(n,f) ^{98}Mo(n,g)	σ_{th}= 0.14b	
↓						
^{99m}Tc	6.0 h	IT (100)	141 (87%)			
^{111}In	2.8 d	EC (100)	173 (91%) 247 (94%)	^{112}Cd(p,2n)	25→18	166
^{123}I	13.2 h	EC (100)	159 (83%)	^{123}Te(p,n) ^{124}Xe(p,x)^{123}Xe ^{127}I(p,5n)^{123}Xe	14.5→10 29→23 65→45	137 414 777
^{201}Tl	3.06 d	EC (100)	68-82 (RL) 166 (10.2%)	^{210}Tl(p,3n)^{201}Pb	28→20	

^{99m}Tc-Generator (1)

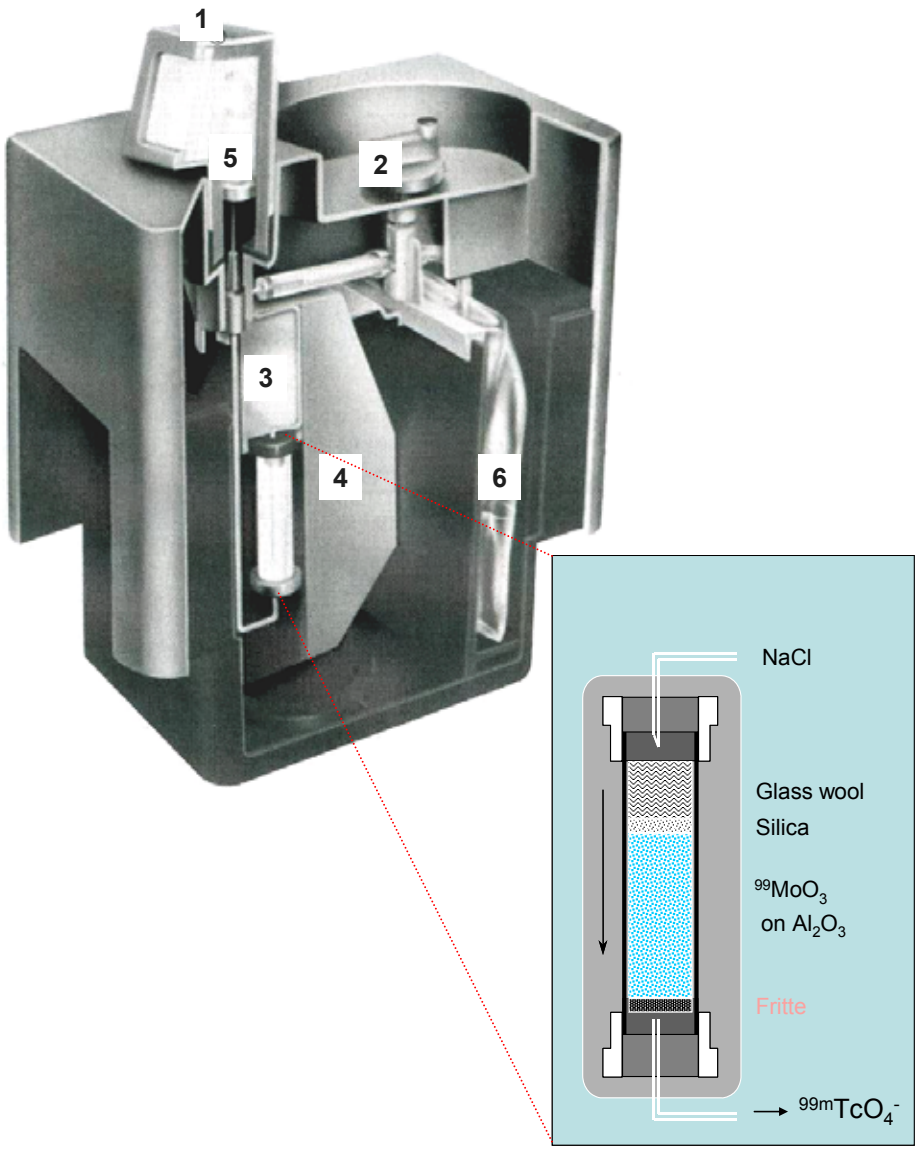

(1) Simple Handling

Insert vacuum flask and elute desired volume.

(2) Transport-Security-valve

Prevent an elution after production and during transport

(3) Shifted needle

Reduction of energy rich Mo-radiation

(4) Max. protection against radiation

Protection from all side.
^{99}Mo-column is covered at least with 52 mm Pb.
Supplementary shielding with overall 98 mm Pb.

(5) High concentrated activity

Total ^{99m}Tc-activity is less than 5 mL volume.

(6) Ready for use

Sterile, closed system.

Labeling of Tc-Radiopharmaceuticals

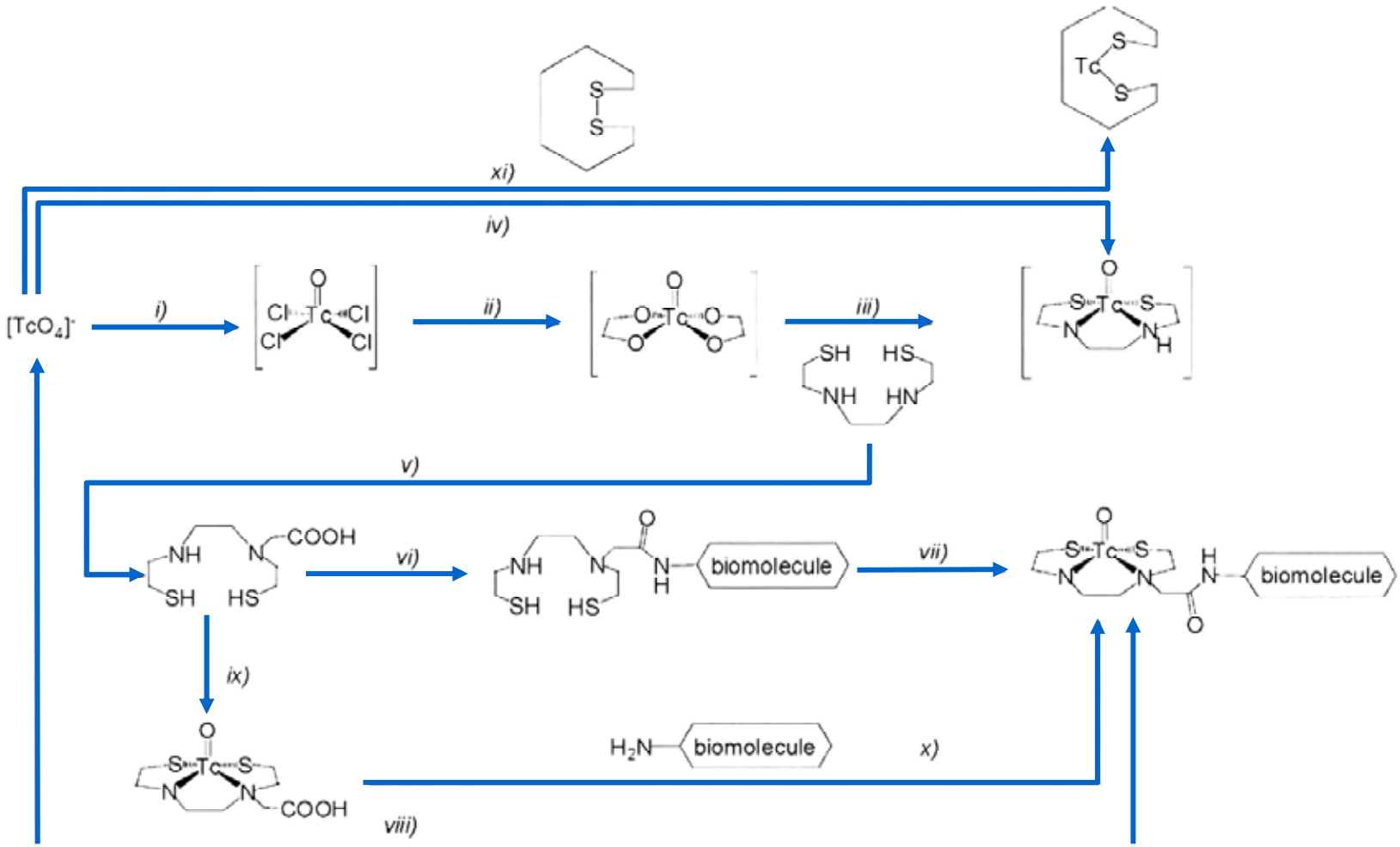

Tracer Properties: Influence of the Nuclide

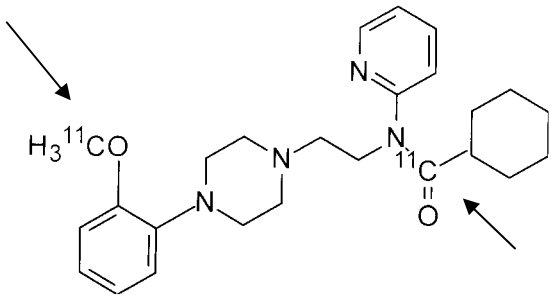

WAY 100638 (5-HT_{1A}-receptor ligand)

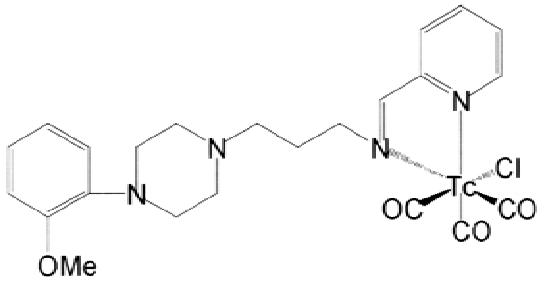

^{99m}Tc-WAY 100638-analog
(as 5-HT_{1A}-receptor ligand)

^{11}C **^{18}F** **^{123}I** **^{99m}Tc** **^{68}Ga / ^{111}In**

Change in structure

Predictability of biological integrity

Complexity of radiopharmaceutical development

Molecular Imaging by Radiotracer

Targeting biochemical processes in living organism
on basis of molecular interaction between tracer und target

by **radiolabeled, „molecular probes**“, changing their concentration at the target in a specific way

and suitable **detection systems** for non-invasive, quantitative and repetitive measurement

with the aim of **exploring** physiological processes,
diagnostics und therapy as well as **therapy monitoring**

Target Structures in Oncology

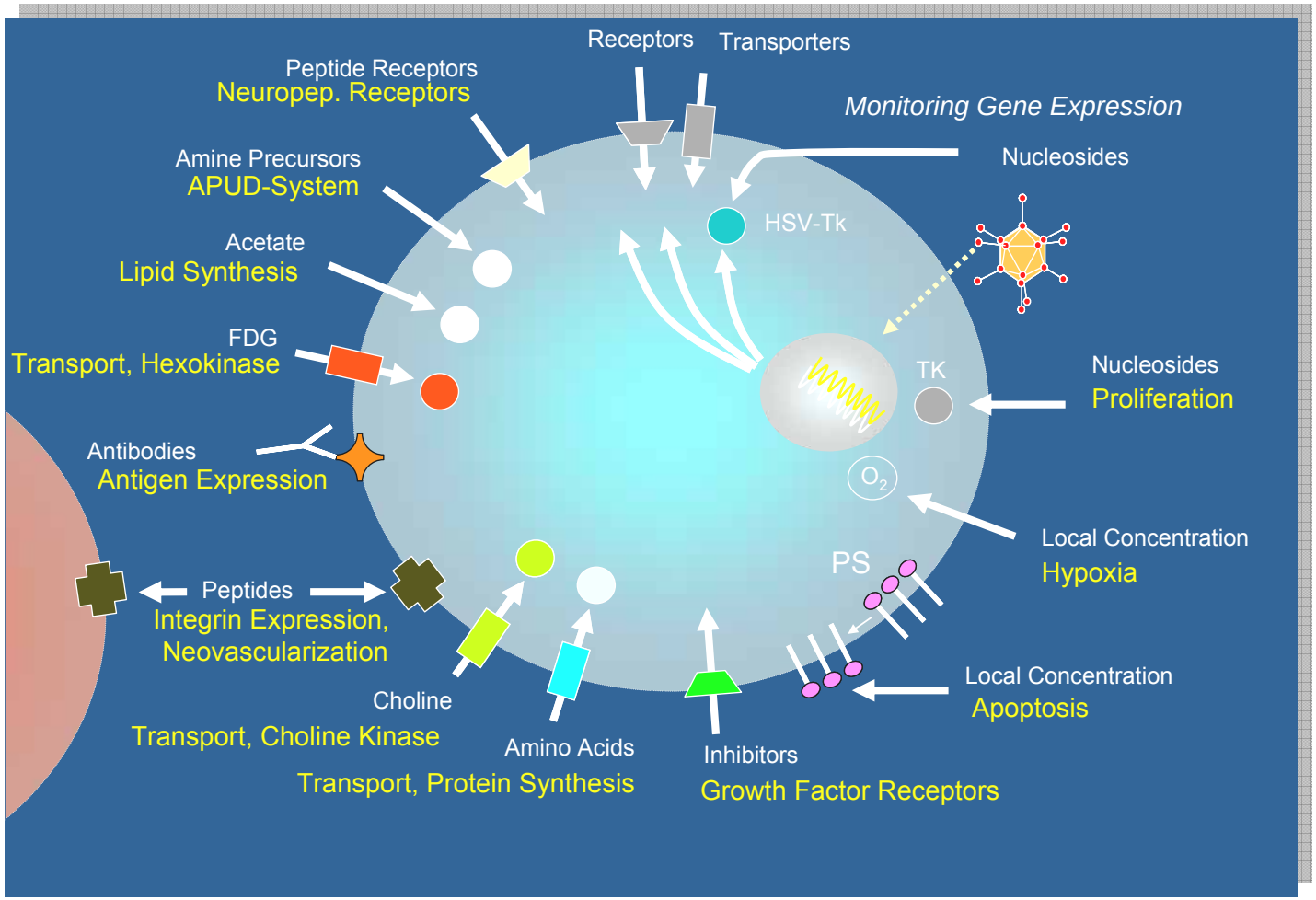

Characterization of the tumor biology by molecular imaging

2-[^{18}F]Fluoro-2-Deoxy-Glucose-Synthesis ([^{18}F]FDG)

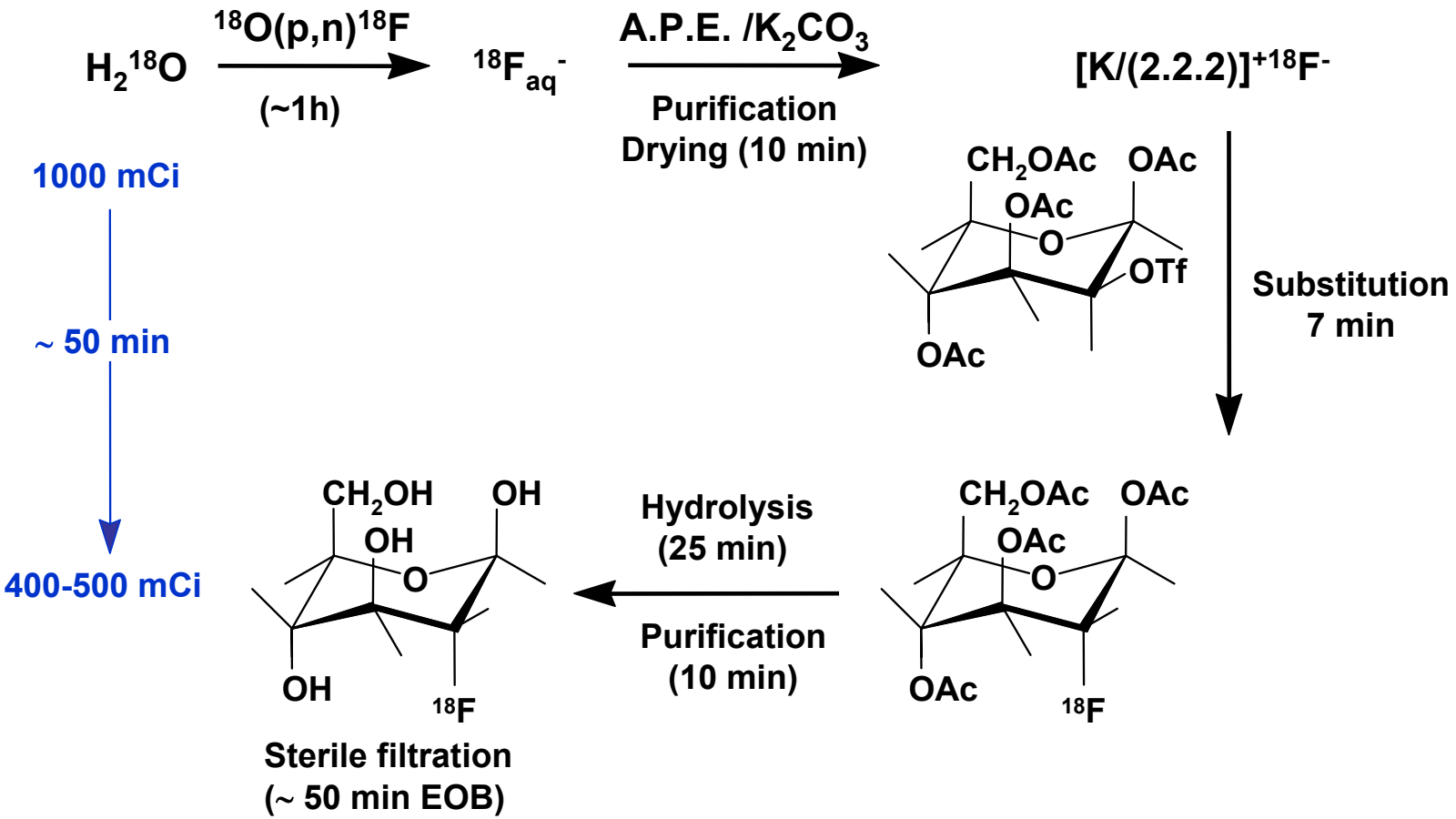

GMP Production of FDG
2-[^{18}F]Fluor-2-deoxy-D-Glucose, TU Munich

Scheme of [^{18}F]FDG Uptake

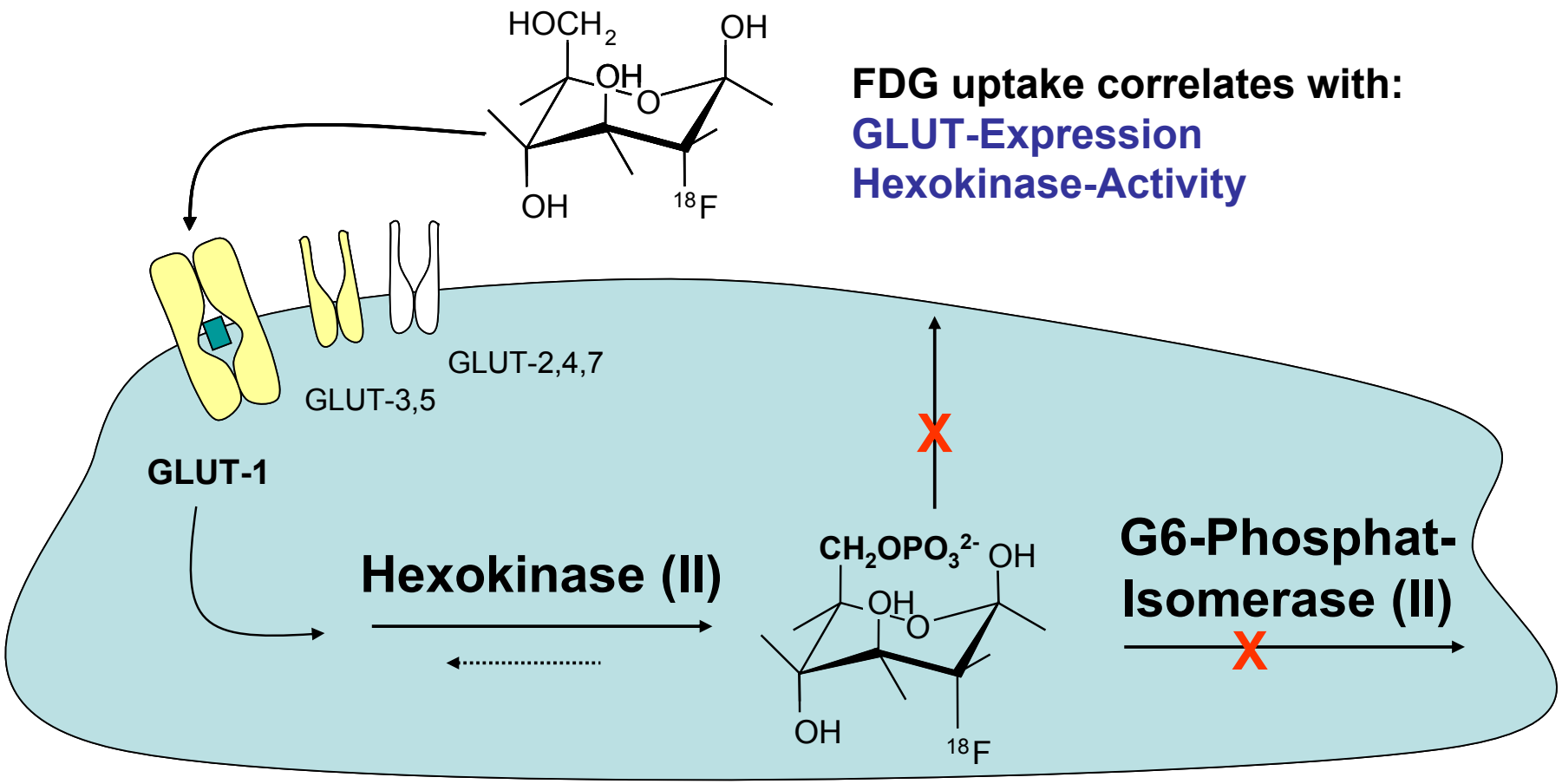

[^{18}F]FDG:
Therapy control –gastric carcinoma-

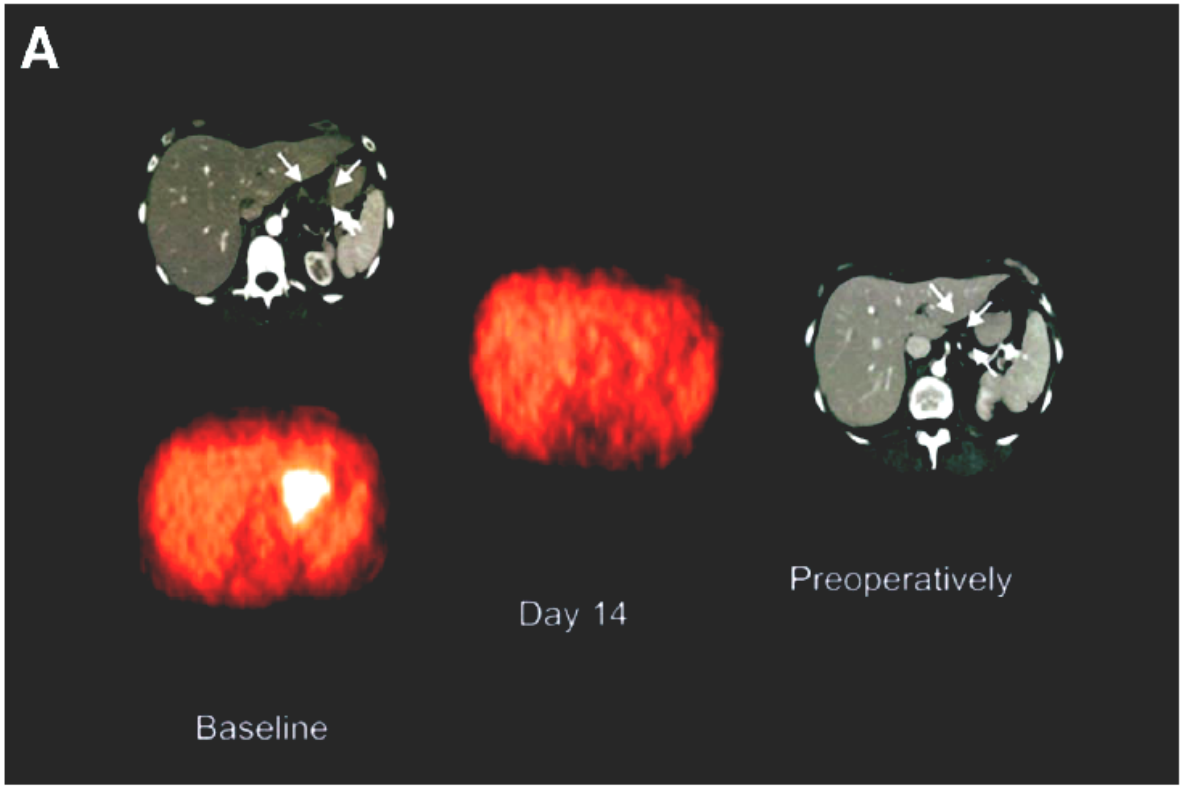

Amino Acid Transport

Primary target: Rate measurement of regional protein synthesis
But: During the short time period after injection the accumulation of tracer represent only the accumulation of amino acid by special transport systems

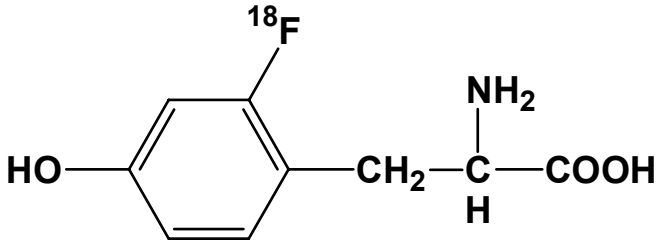

2-Fluoro-L-Tyrosin **2-[^{18}F]Tyr**

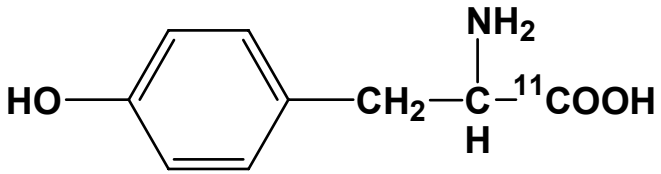

L-Tyrosin **1-[^{11}C]Tyr**

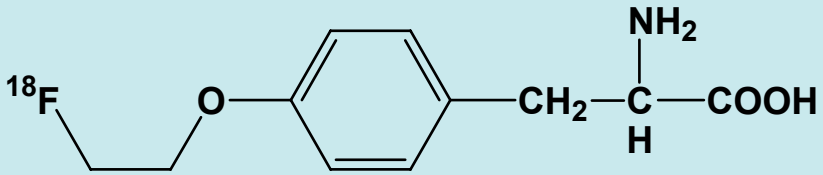

O-(2-Fluoroethyl)-L-Tyrosin **[^{18}F]FET**

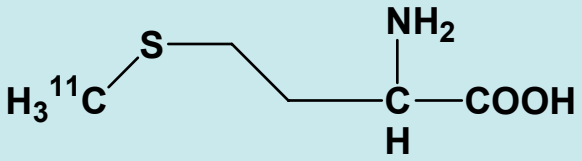

L-Methionine **[^{11}C]MET**

[^{18}F]FDG-PET versus [^{11}C]MET-PET
-Brain Tumor-

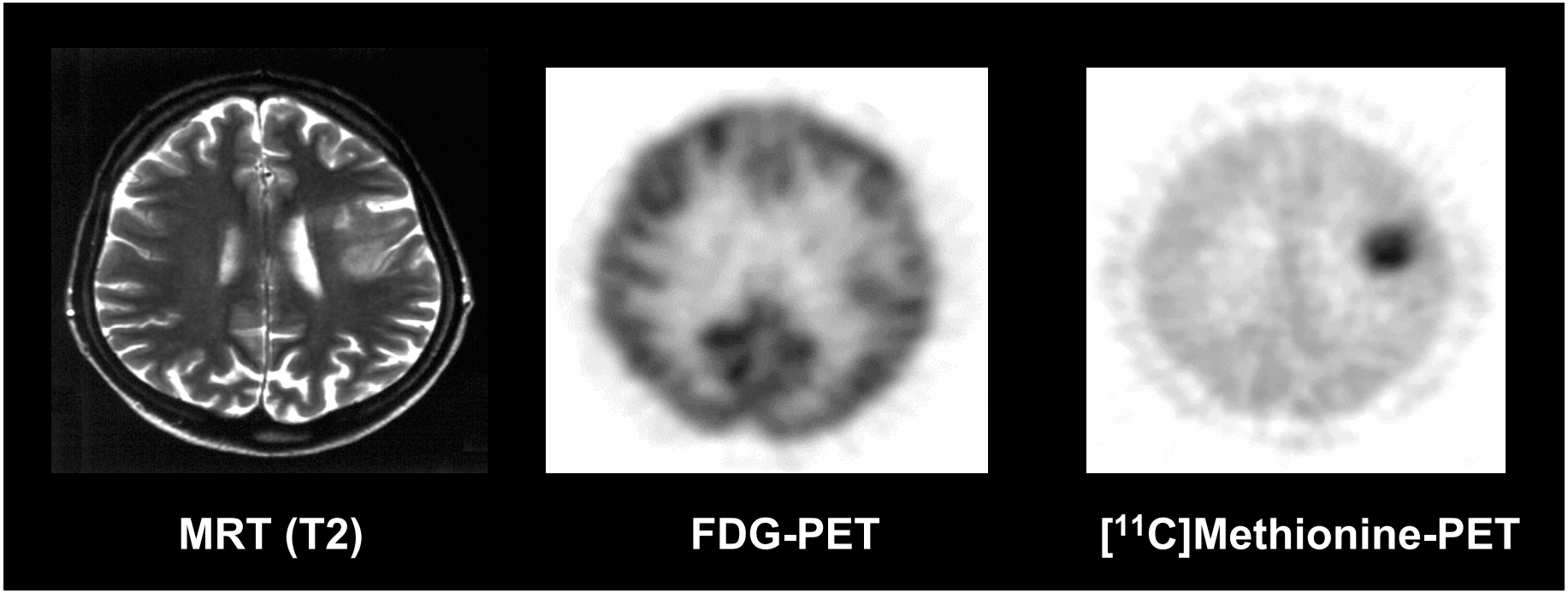

O-(2-[^{18}F]Fluoroethyl)-L-Tyrosin: [^{18}F]FET (2)

FDG also accumulates in inflammation,
amino acids and especially FET does not accumulate in inflammation.

Squamous cell carcinoma

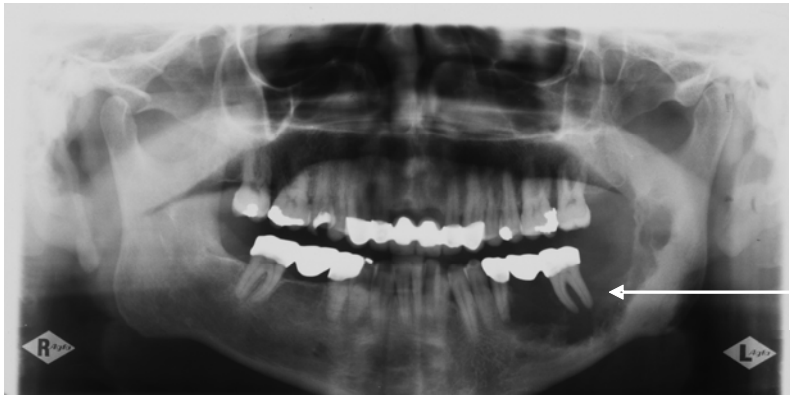

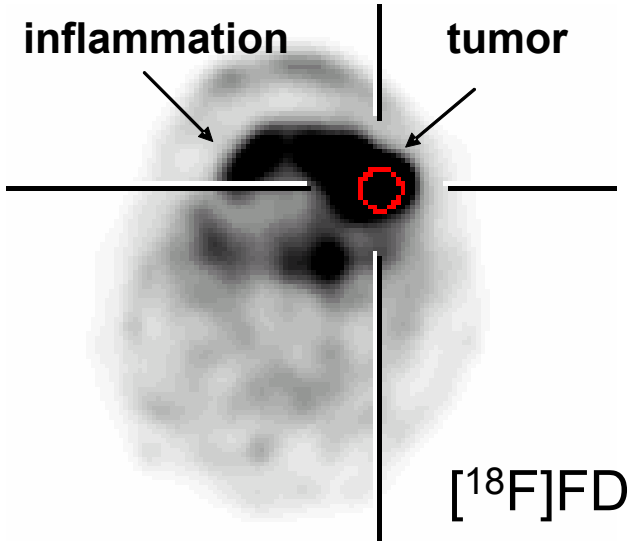

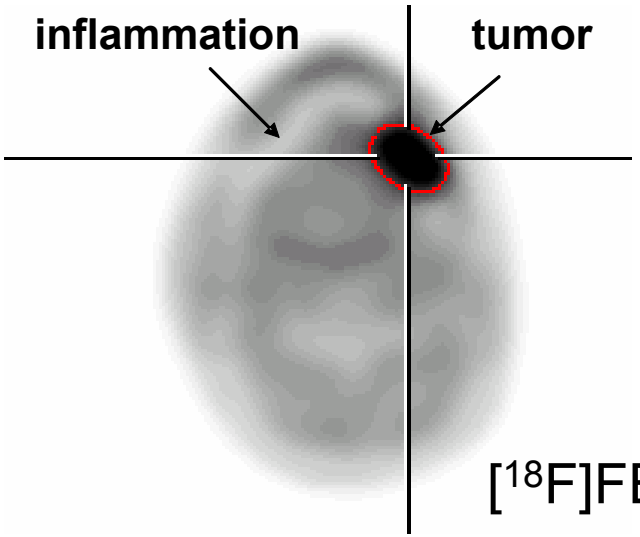

Imaging of Metastatic Prostate Cancer

^{11}C-Acetate:	**Prostate cells undergo metabolic transformation from citrate producing normal cells to citrate oxidizing malignant cells (Costello LC et al. *Urology* 1997)**
^{18}F/^{11}C-Cholines:	**malignant transformation is associated with induction of choline kinase activity (e.g. Kotzerke et al. and refs herein; J Nucl Med. 2002)**
(^{18}F-Fluoide):	**(for bone metastasis)**

Biochemical Model: Choline

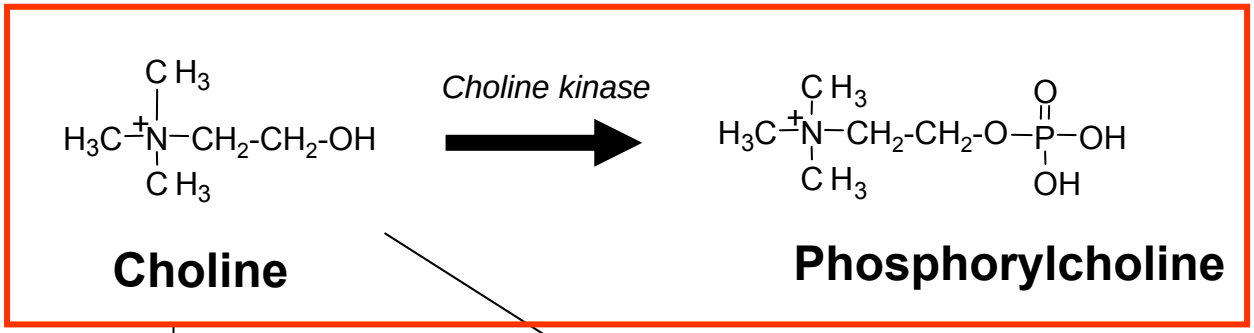

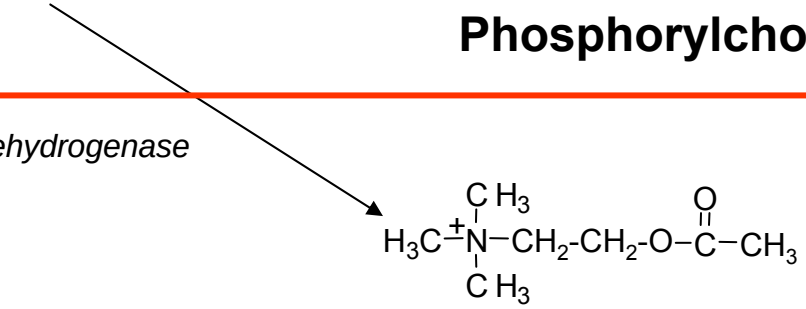

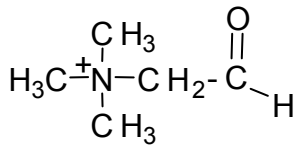

Betain-aldehyde

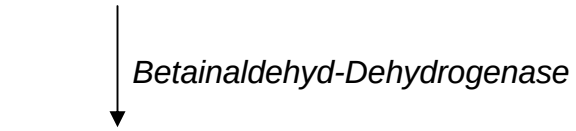

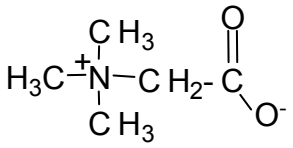

Betain

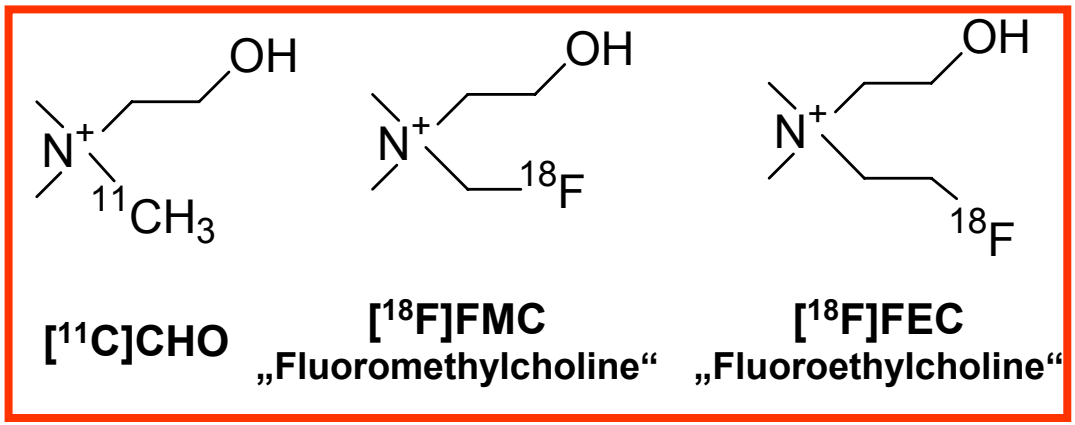

^{11}C-Choline-PET

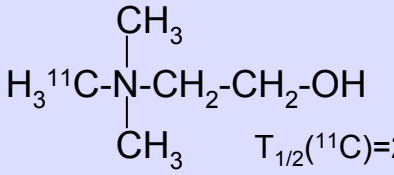

$T_{1/2}(^{11}C)$=20 min

^{18}F-Choline-PET

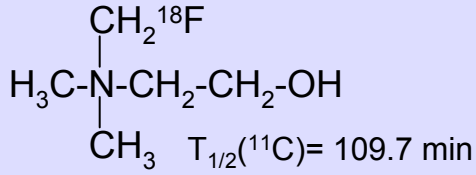

$T_{1/2}(^{11}C)$= 109.7 min

Bladder cancer metastasis

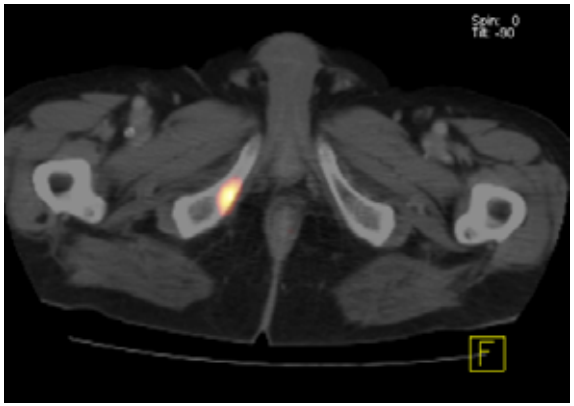

PET/CT

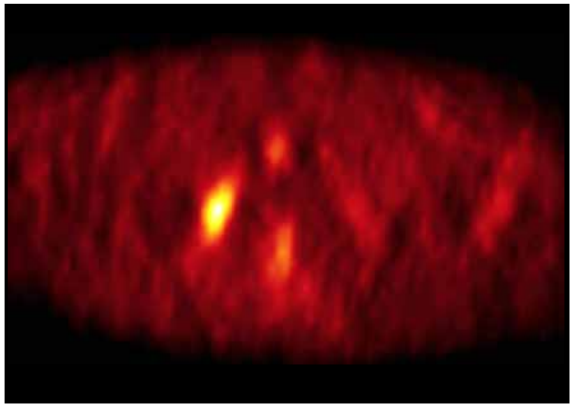

PET

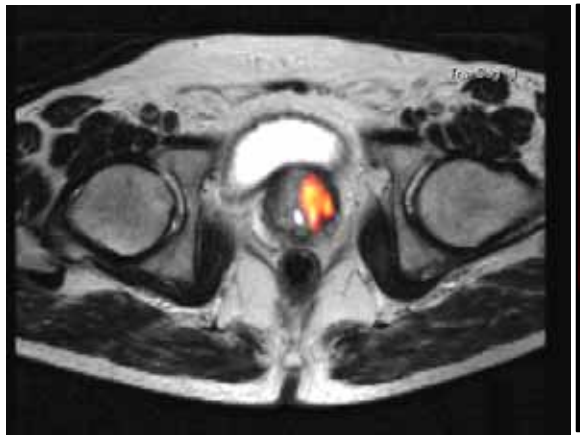

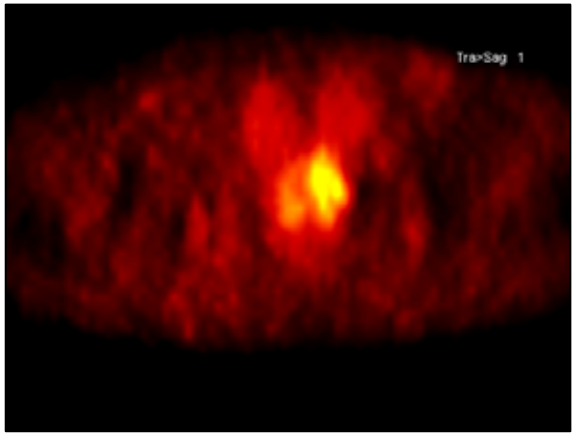

Prostate carcinoma

Tracer accumulation with:

1. Cellular accumulation by choline transporter;
(Signal in the first minutes after injection)

2. and followed by phosphorylation by choline kinase.
(Signal by late imaging)

3´-[^{18}F]Fluoro-3´-Deoxy-Thymidine: [^{18}F]FLT

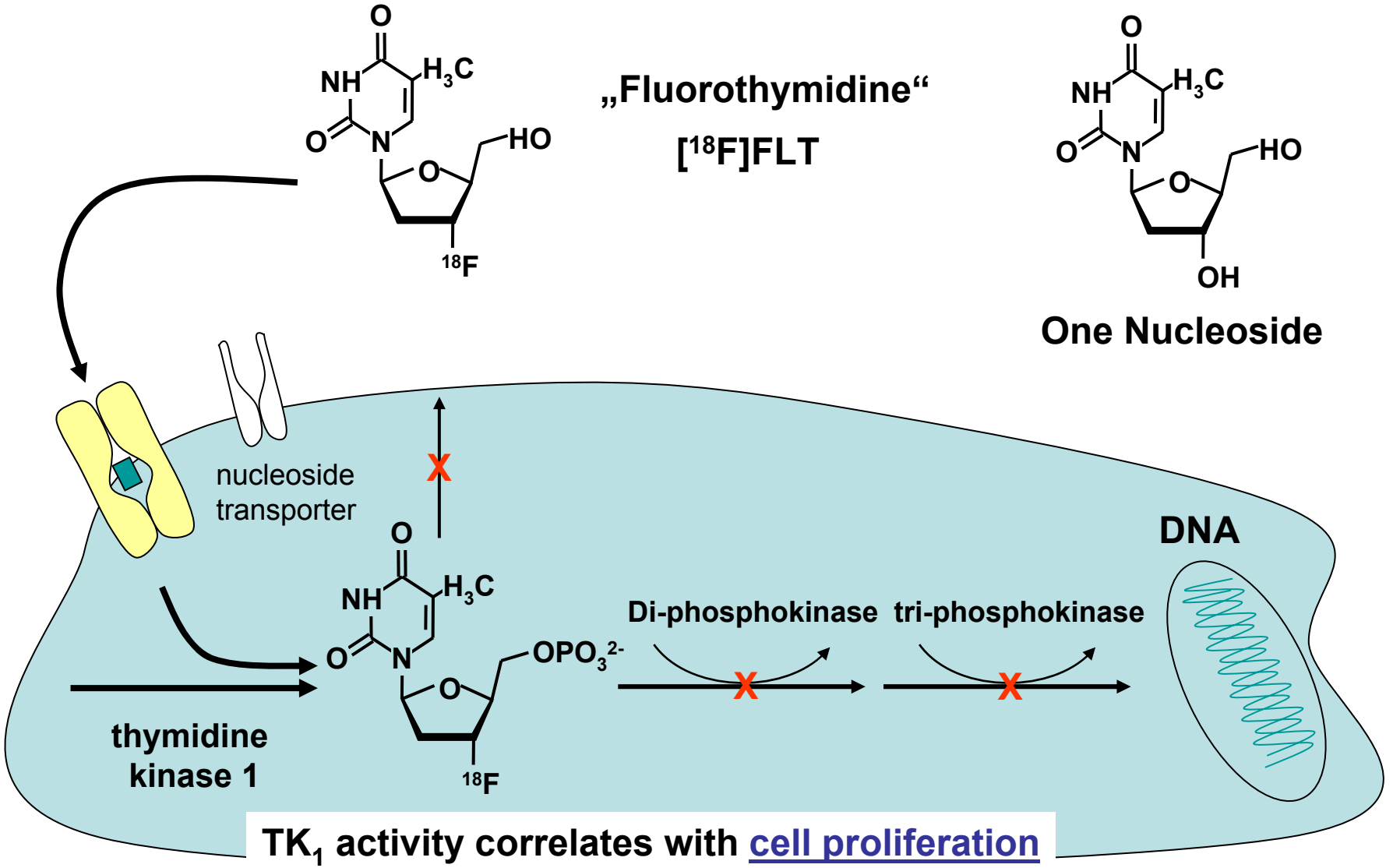

Metabolic Scheme for [^{11}C]Thymidine and FLT

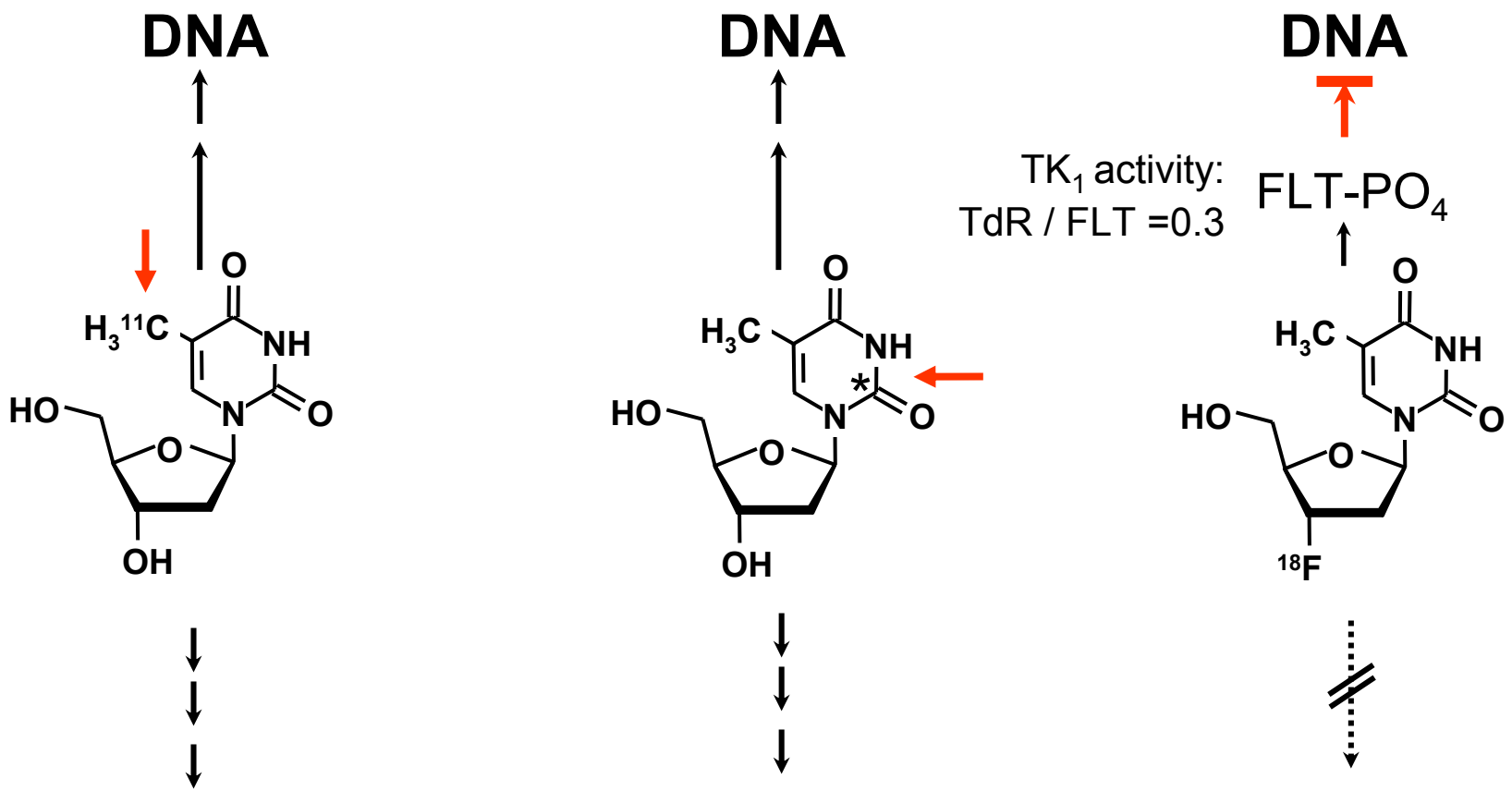

Visualization of Cell Proliferation with ^{18}F-thymidine (FLT) in Esophageal Cancer

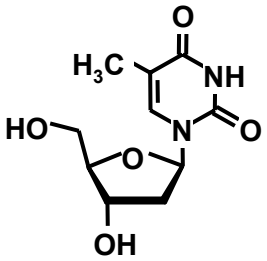

thymidine

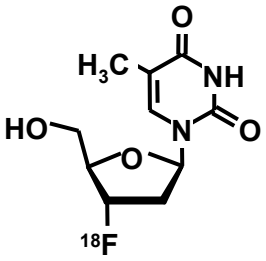

[^{18}F]FLT

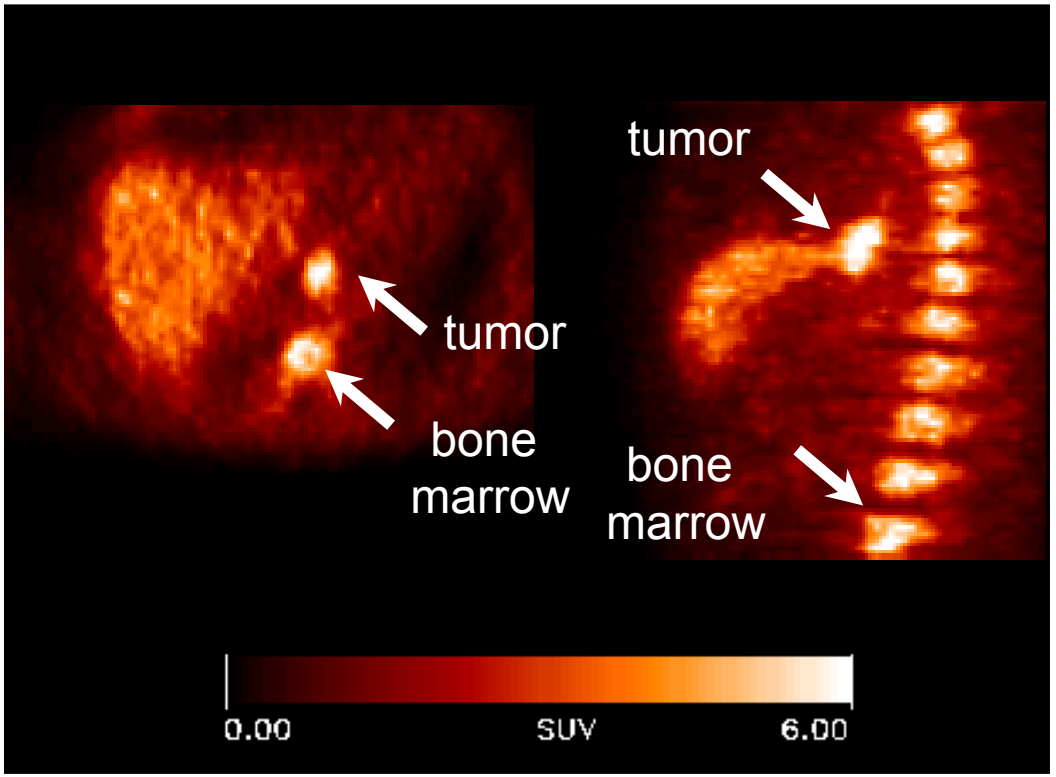

Critical O_2 Levels

Aggressiveness ↑
Tumor Progression

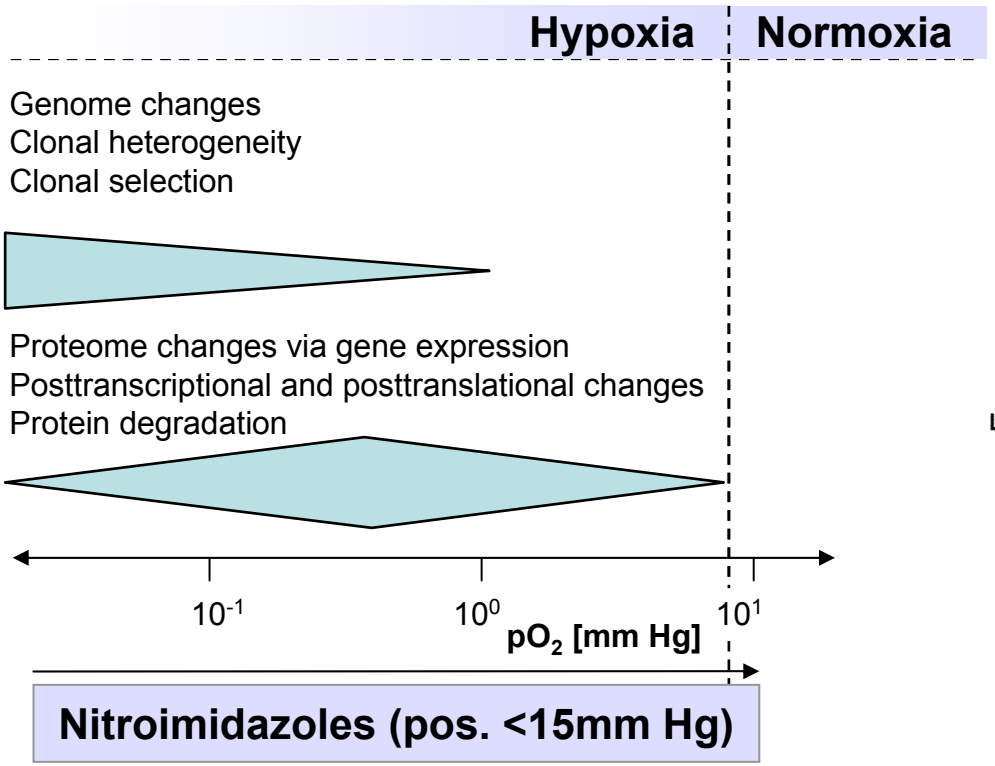

Distribution of medium pO_2 levels for prostatic tumor tissue versus muscle

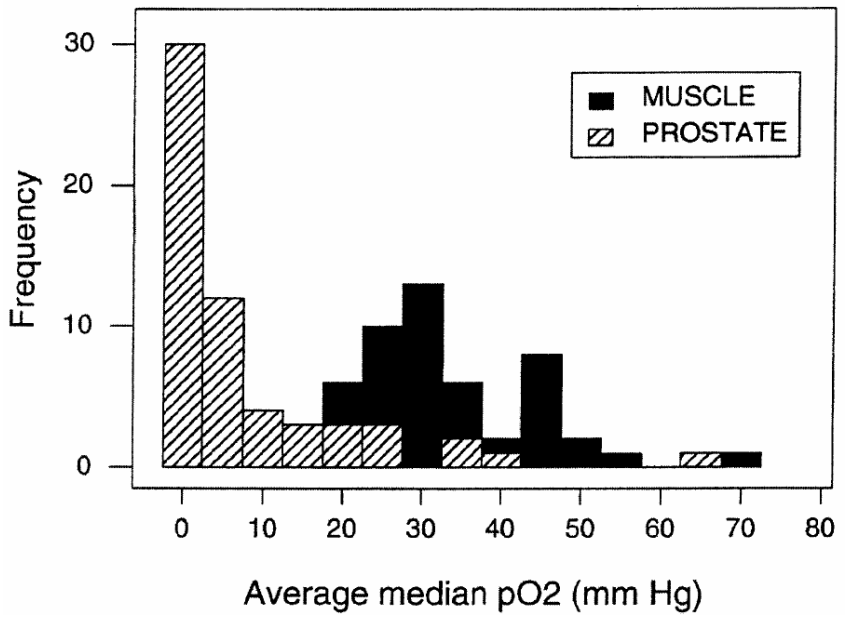

Vaupel P. et al.

The Mechanism of Non-Invasive Detection of Tumor Hypoxia

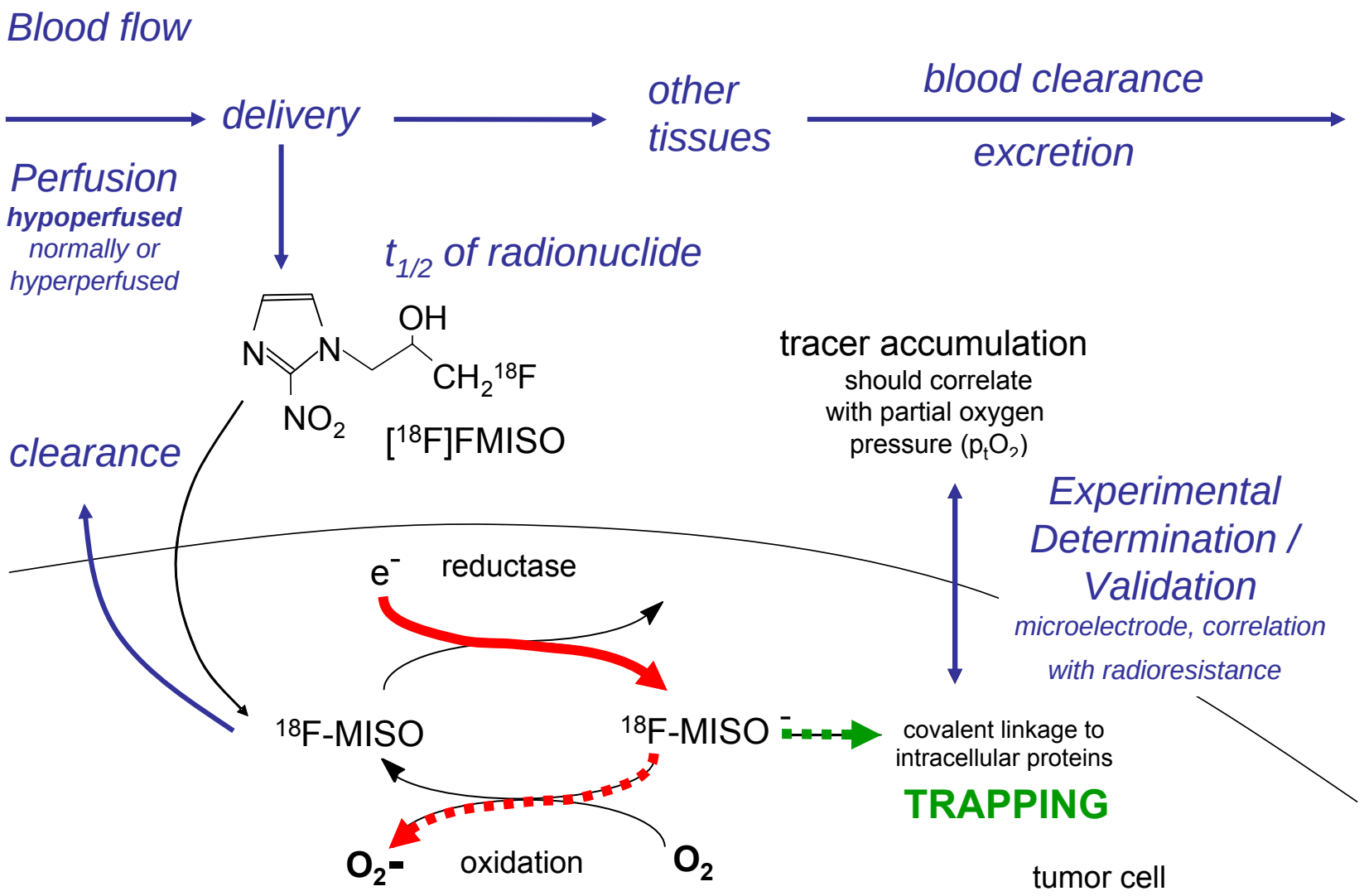

Evaluation of [^{18}F]FAZA

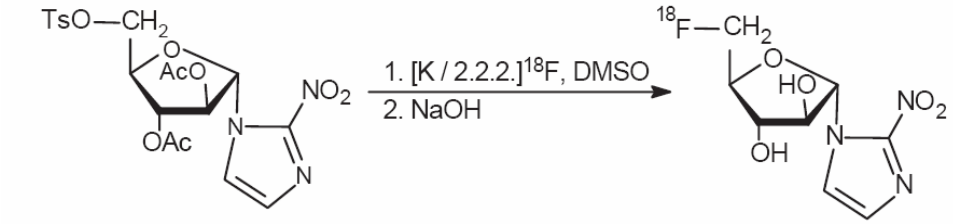

Synthesis of [^{18}F]FAZA:
Radiochemical Yield: 20 ± 4%, 50 min
(Reischl et al., 2005)

Serial, transaxiale PET images -nude mice- with A431 tumors.

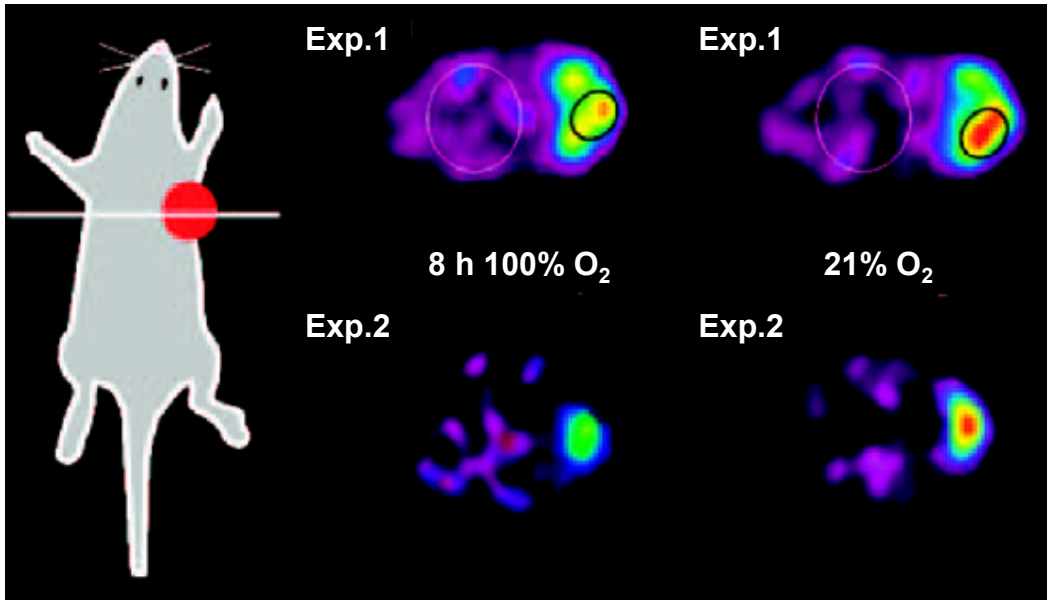

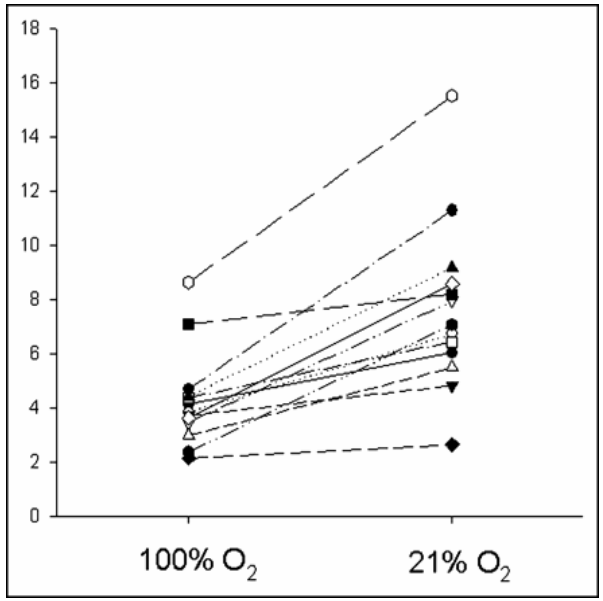

Exp.1	**T/Bk**	**3.7 / 1**	**4.7 / 1**
Exp.2	**T/Bk**	**5.4 / 1**	**11.3 / 1**

Peptide Receptor Imaging: PRI

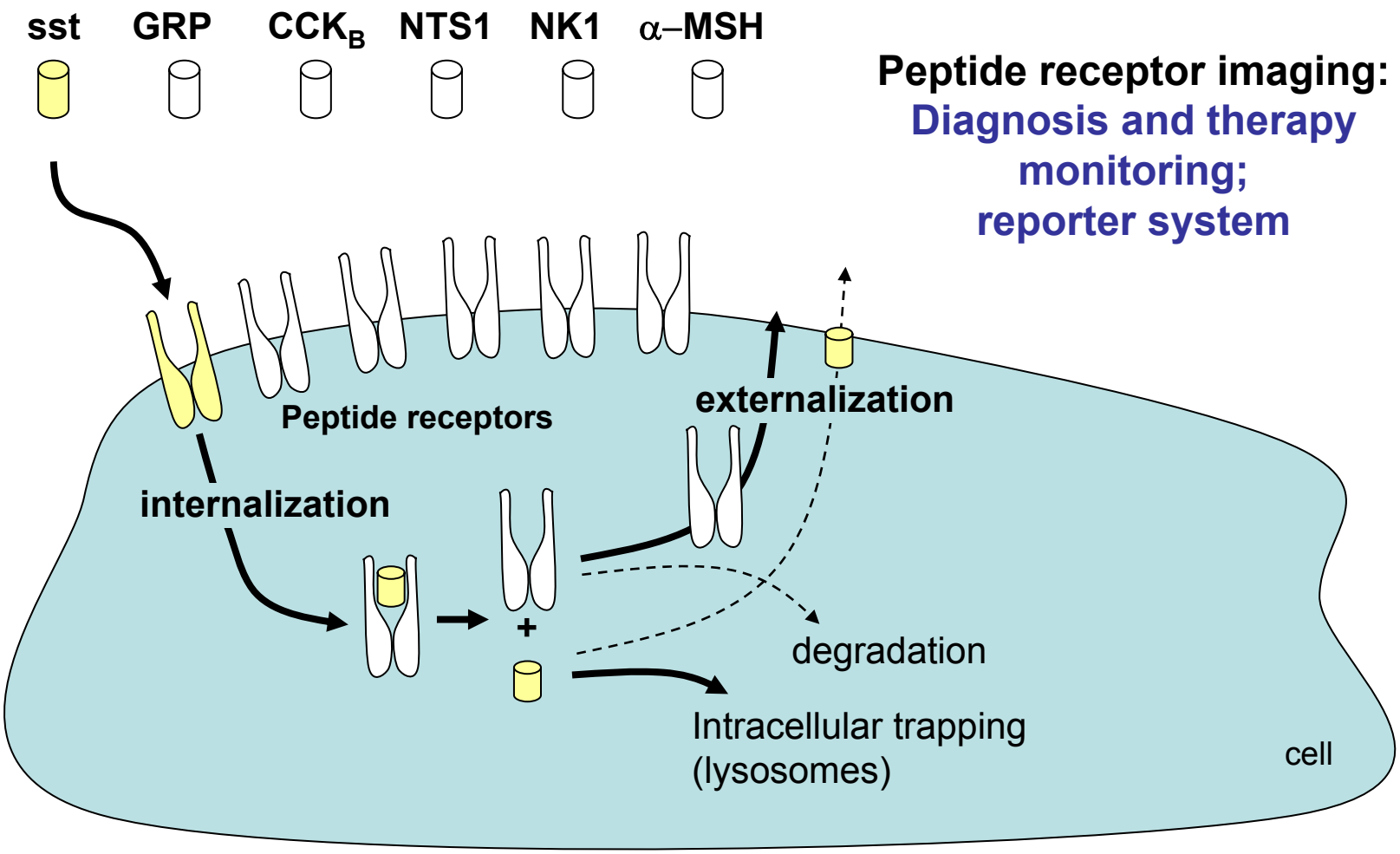

Peptide receptor imaging:
Diagnosis and therapy monitoring;
reporter system

Targets for Radiolabeled Peptides in Human Tumor Tissue

Somatostatin-R	neuroendocrine tumors, small cell lung cancer, medullary thyroid carcinoma, lymphoma (NHL)
Integrins	melanoma, breast tumor, osteosarcoma, glioblastoma
VIP-R	adenocarcinomas, small cell lung cancer, neuroendocrine tumors, lymphoma
CCK-B-R	medullary thyroid carcinoma, small cell lung cancer, stromal ovarian cancer, astrocytoma
Substance P-R	medullary thyroid cancer, small cell lung cancer, breast tumors
Bombesin/ GRP-R	colon cancer, small cell lung cancer, glioblastoma
Neurotensin-R	pancreatic cancer, prostate cancer,small cell lung cancer

Influence of the Carbohydrate on the Biodistribution of Octreotides/-tates

(Mice, AR42J, n=3-5, 60 min p.i.)

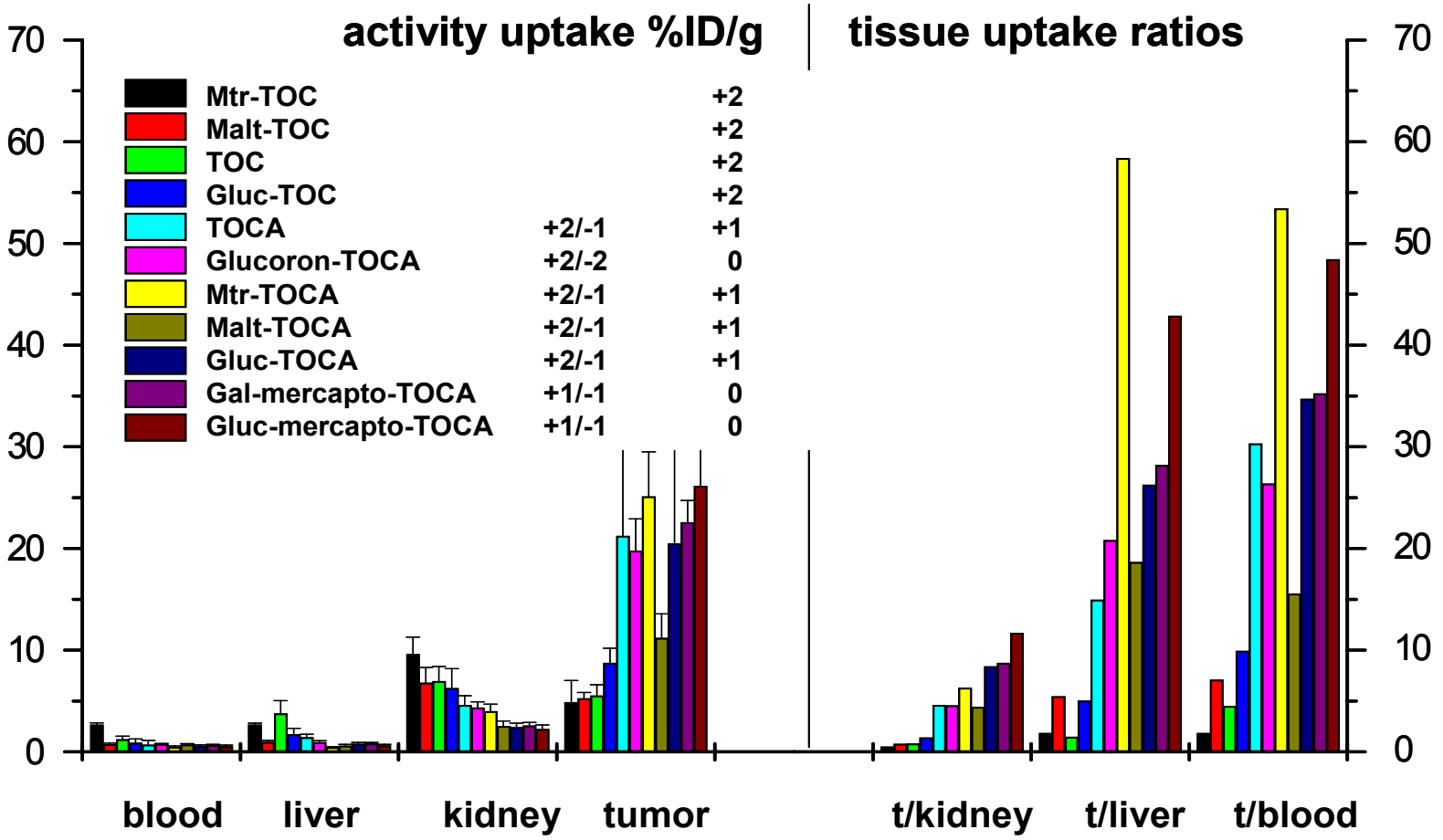

Schottelius, Wester et al. Clin Cancer Res. (2004)

Chemical Structure of Gluc-FP[^{18}F]-TOCA

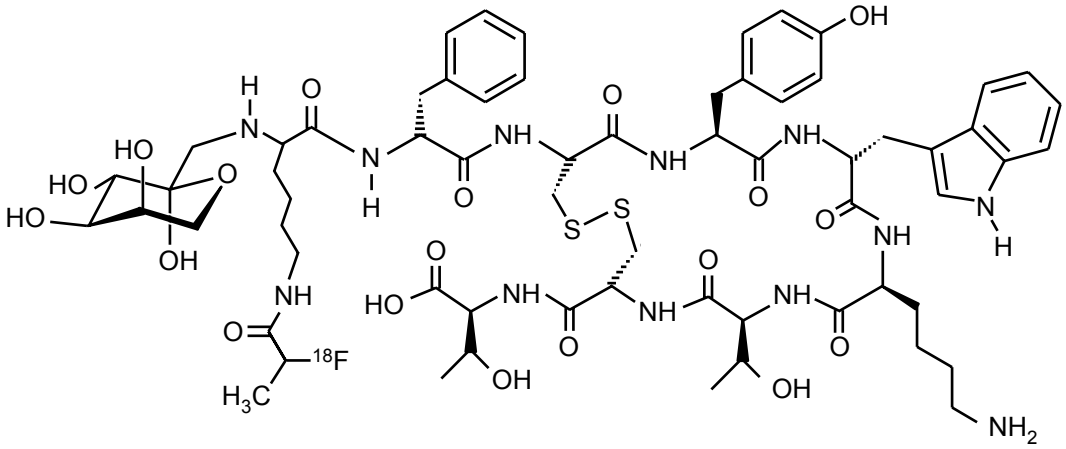

Gluc-Lys([^{18}F]FP)-TOCA

[^{18}F]FP = 2-[^{18}F]Fluoropropionic acid
TOCA = Tyr$_3$-octreotate, -DPhe-Cys-Tyr-DTrp-Lys-Thr-Cys-Thr-OH

Gluc-FP[^{18}F]-TOCA

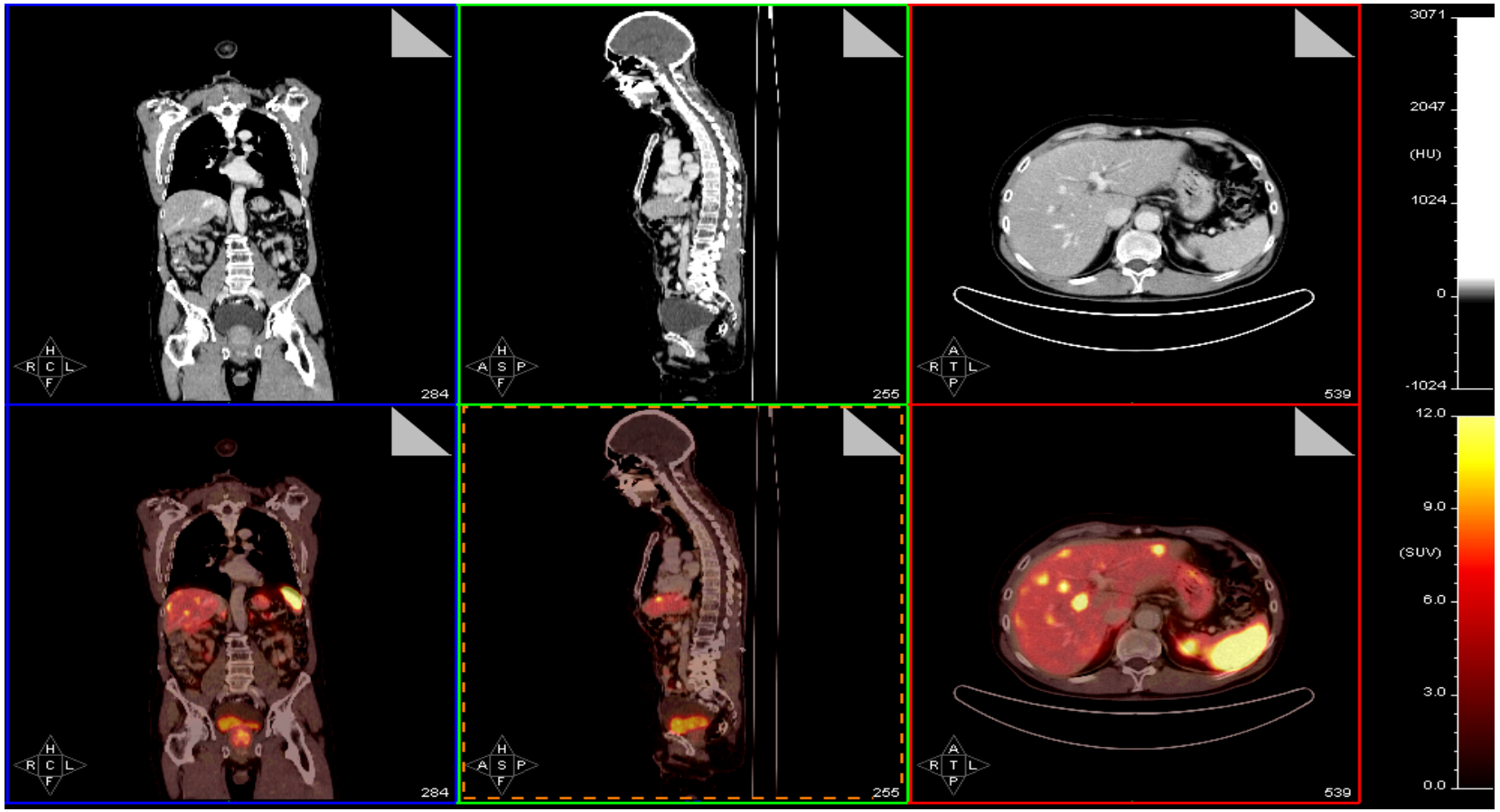

Male patient, 50 yrs, carcinoid with multiple metastases

Imaging of Neoangiogenesis

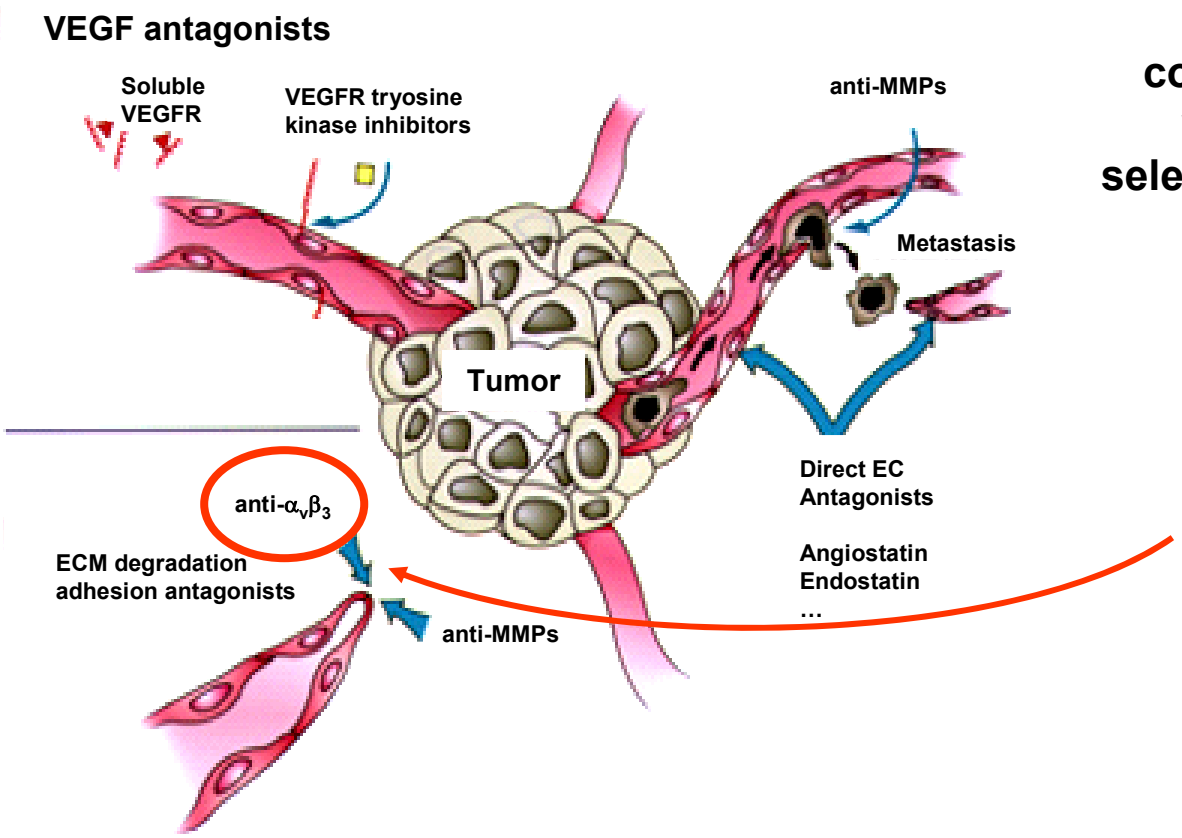

Arg-Gly-Asp (RGD)-containing pentapeptides with high affinity and selectivity to the $\alpha_v\beta_3$-integrin

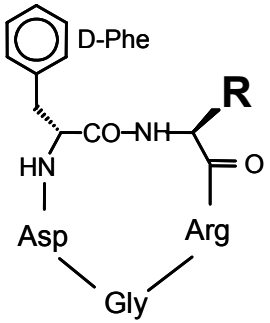

Carbohydrated RGD-Peptide : [^{18}F]Galacto-RGD

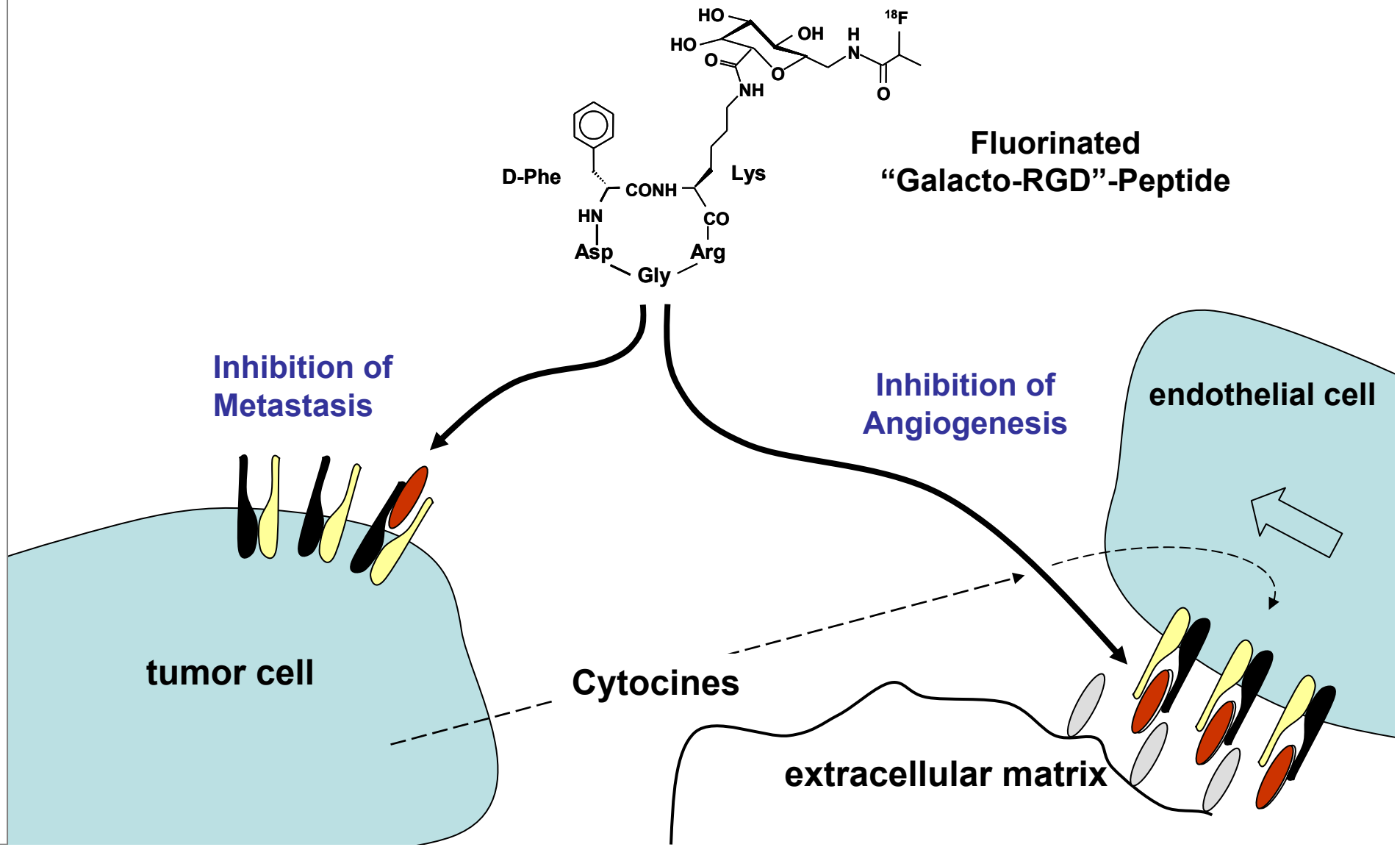

Carbohydrated RGD-Peptides with Improved Pharmacokinetics

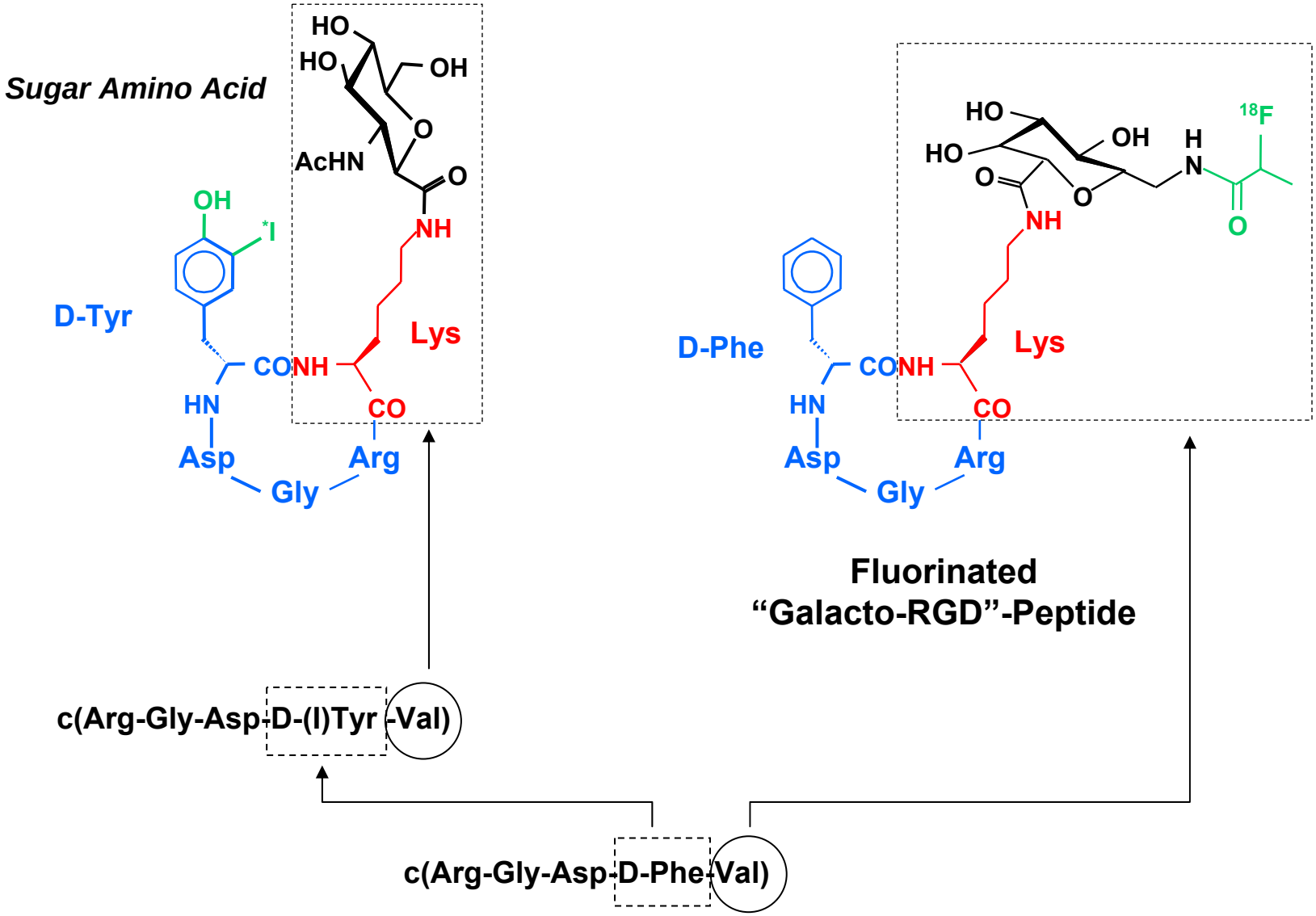

Comparison of the Pharmacokinetics in Selected Tissues

- *c(Arg-Gly-Asp-D-(l)Tyr -Val*): **Log P = -1.89**
- l-Gluco-RGD: **Log P = -2.45**

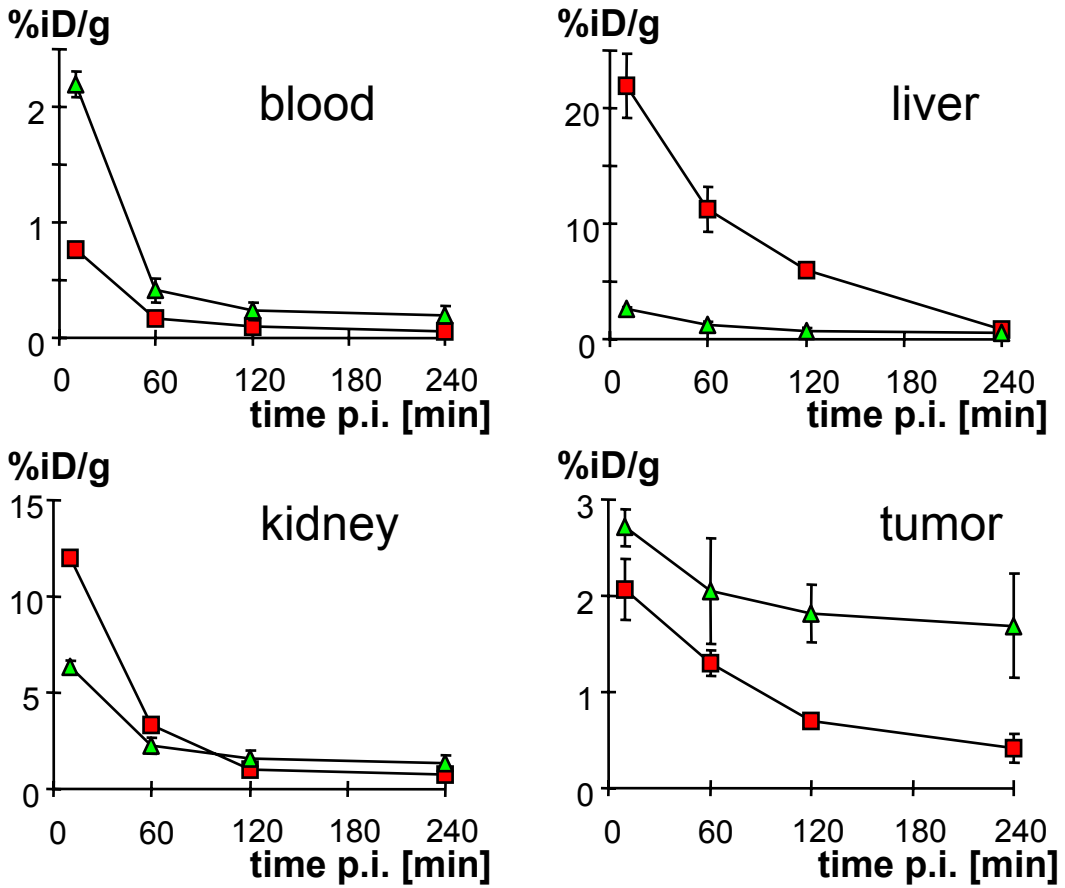

BALB/c mice, osteosarcoma model; comparable data obtained with M21melanoma bearing mice

Non-invasive Monitoring of $\alpha_v\beta_3$ Expression on the Tumor Vasculature

nude mouse bearing a *human* squamous cell carcinoma at the right shoulder

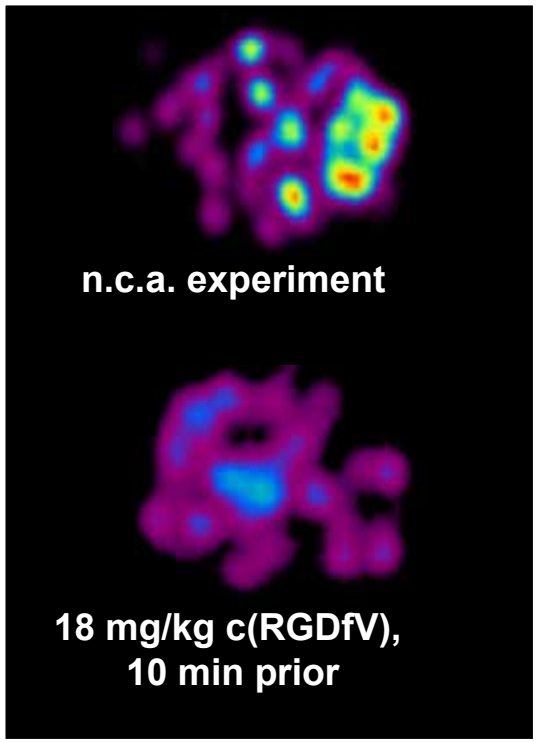

1.5h p.i

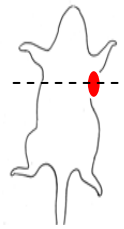

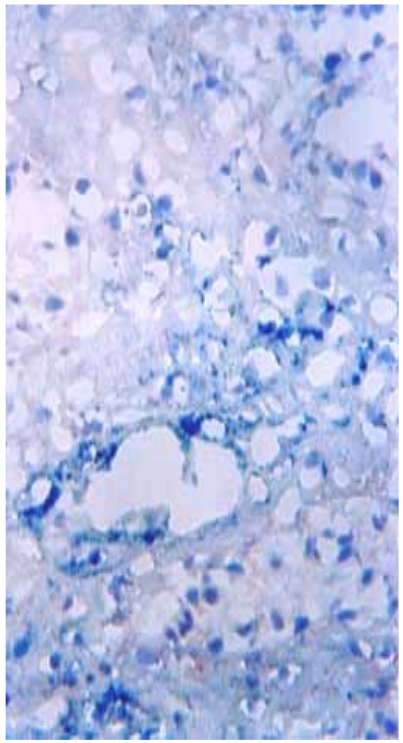

anti human αvβ3
MAb LM609

no expression of αvβ3 on cells

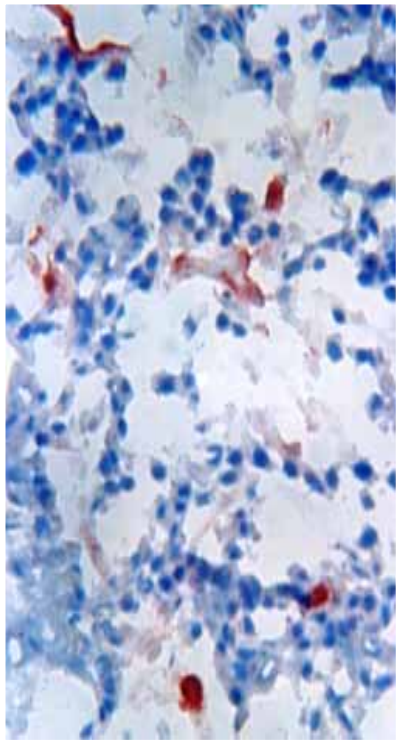

anti murine β3
MAb 2C9.G2

expression of murine β3 on vasculature

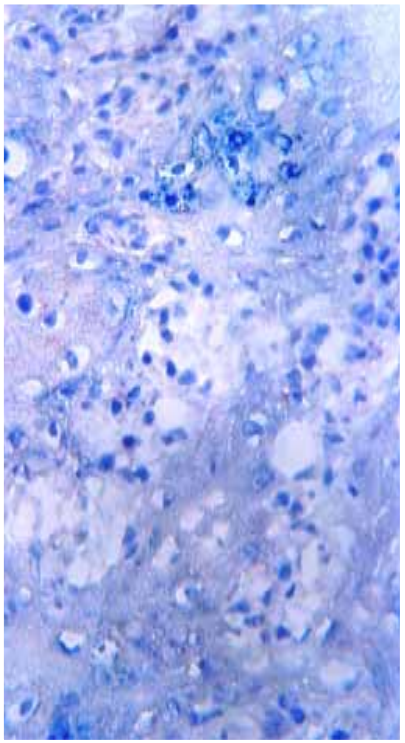

control
(**unspecific** MAb)

Determination of $\alpha_v\beta_3$-Expression in vivo

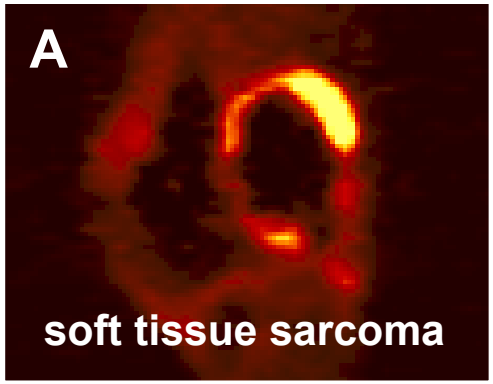

sagittal section, 170 min p.i. ,
circular tracer uptake,
max. SUV=10

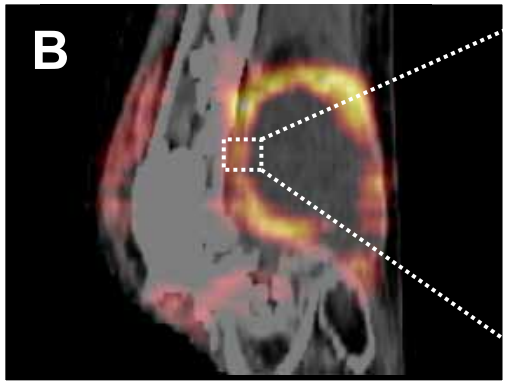

PET/CT image fusion;
uptake corresponds with
the tumor-wall

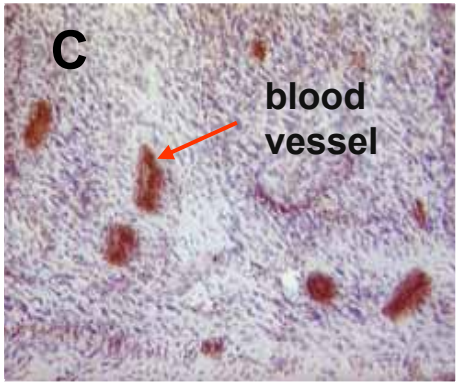

Immunohistochemistry,
MAb LM609, staining of
blood vessels

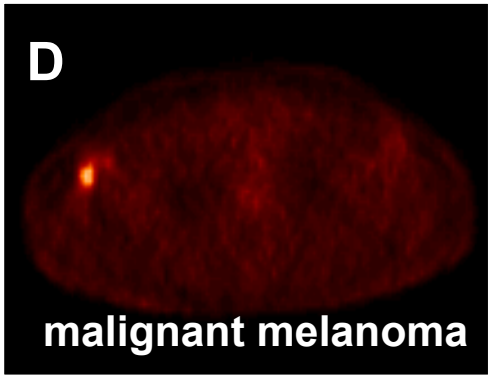

axial section, 140 min p,i,
uptake in the lymph node

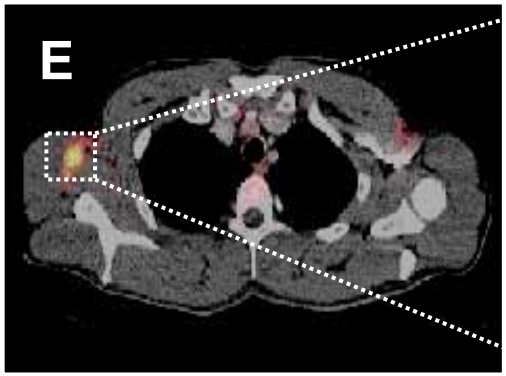

PET/CT image fusion

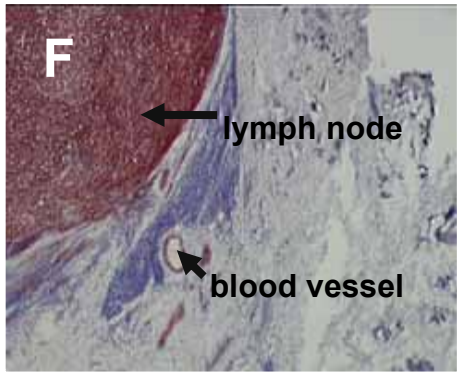

Immunohistochemistry, focal
MAB LM609, staining of
tumor cells and blood vessels

Multiple-Ligand-Tumortargeting (MLT)

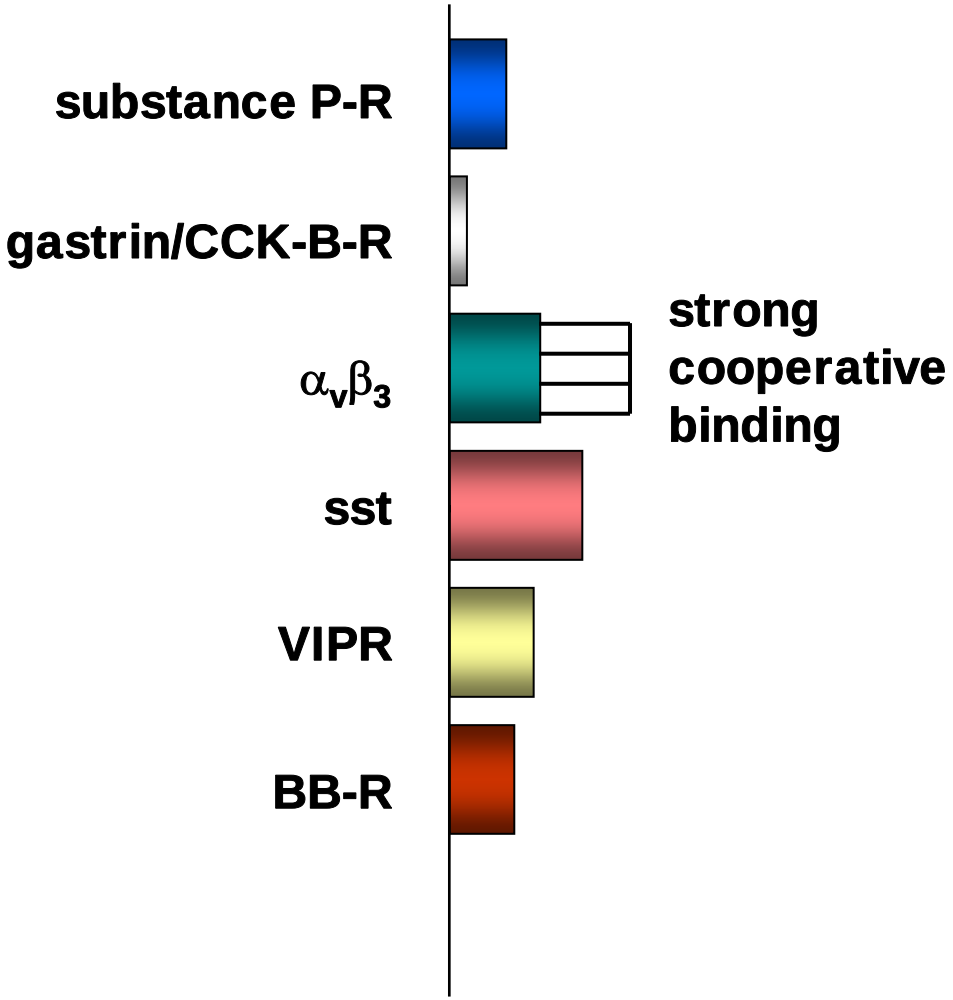

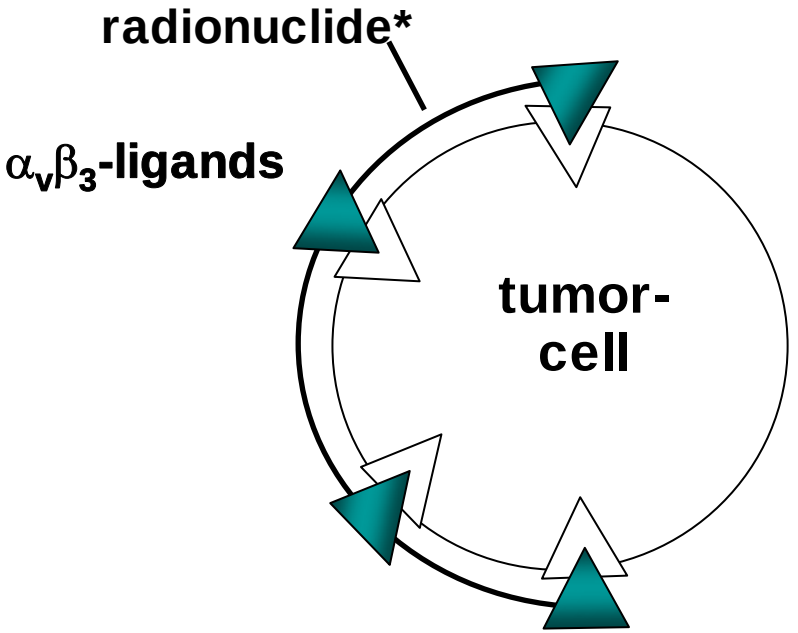

Structure of the Extracellular Domain of $\alpha_v\beta_3$

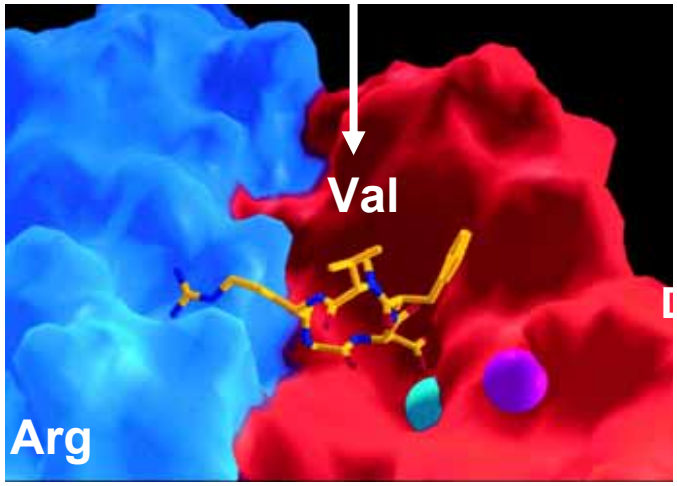

J.-P. Xiong, et. al, Science **2001**.

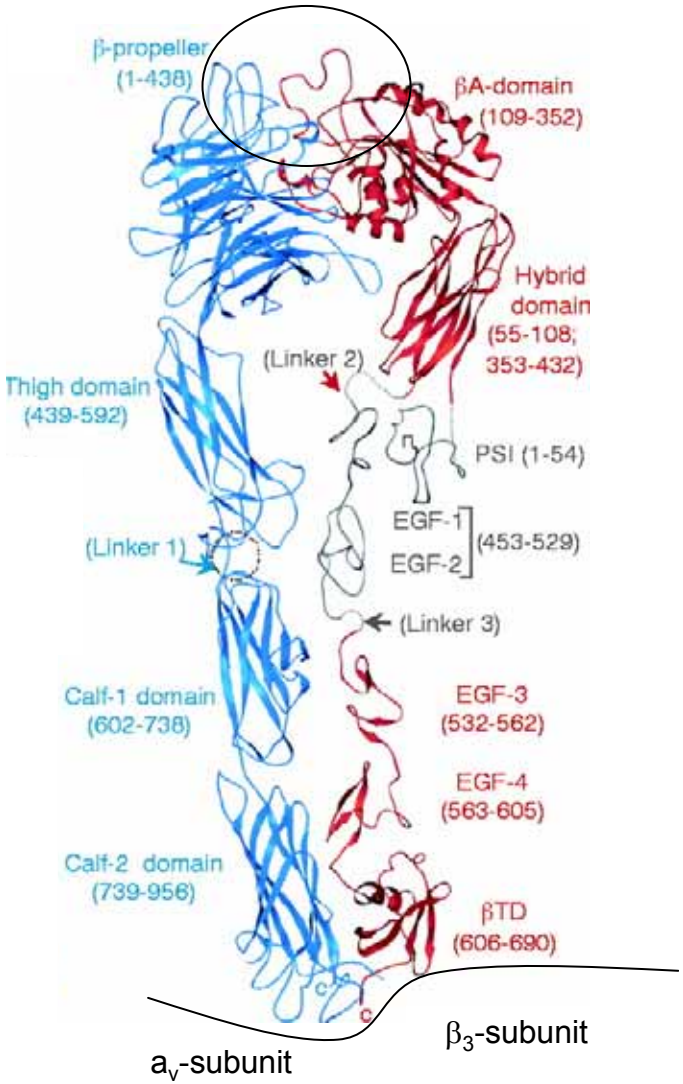

Multimeric [^{18}F]c(RGDfE)-Peptides

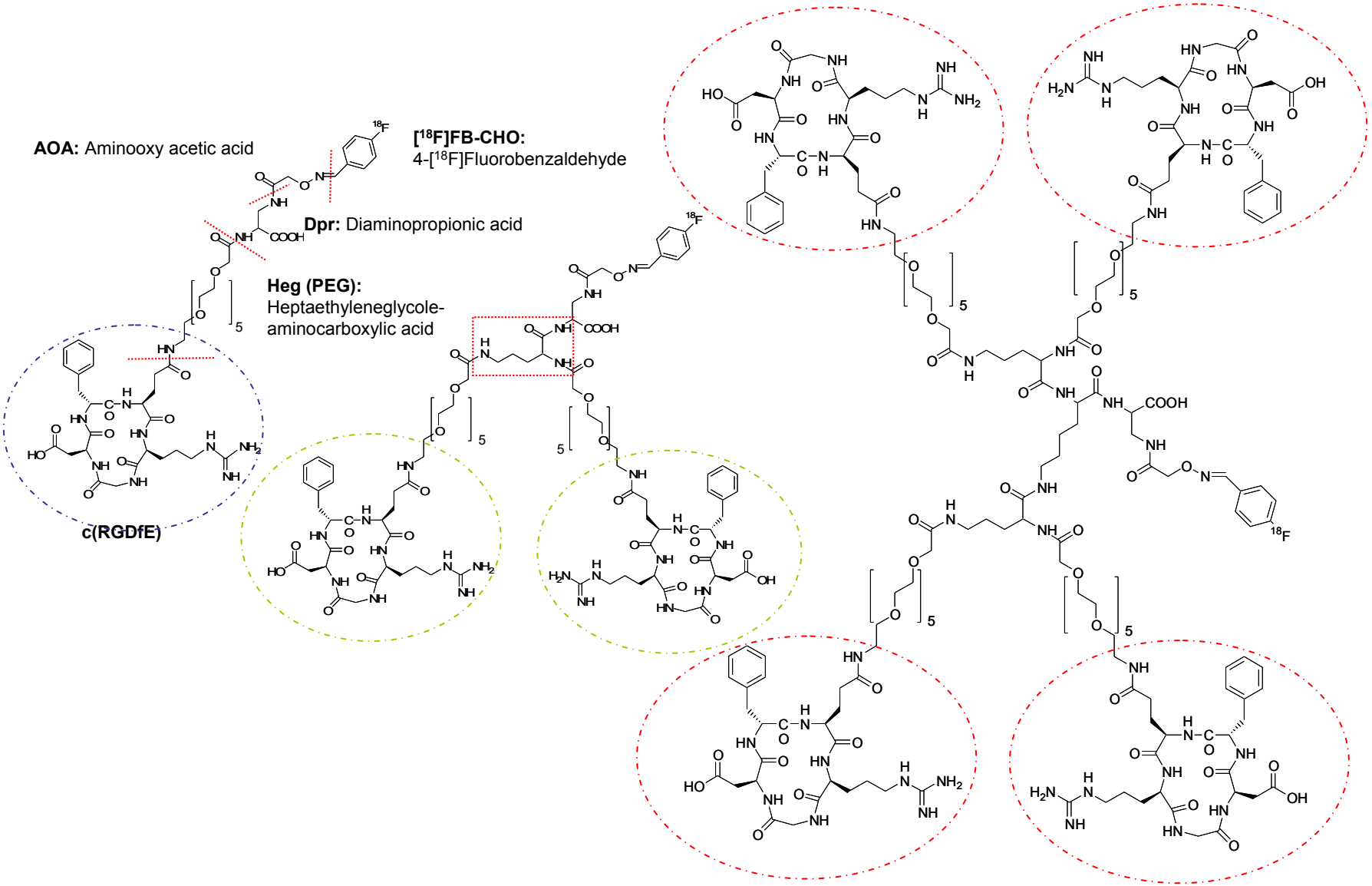

^{18}F-Labeling via Oxime Formation

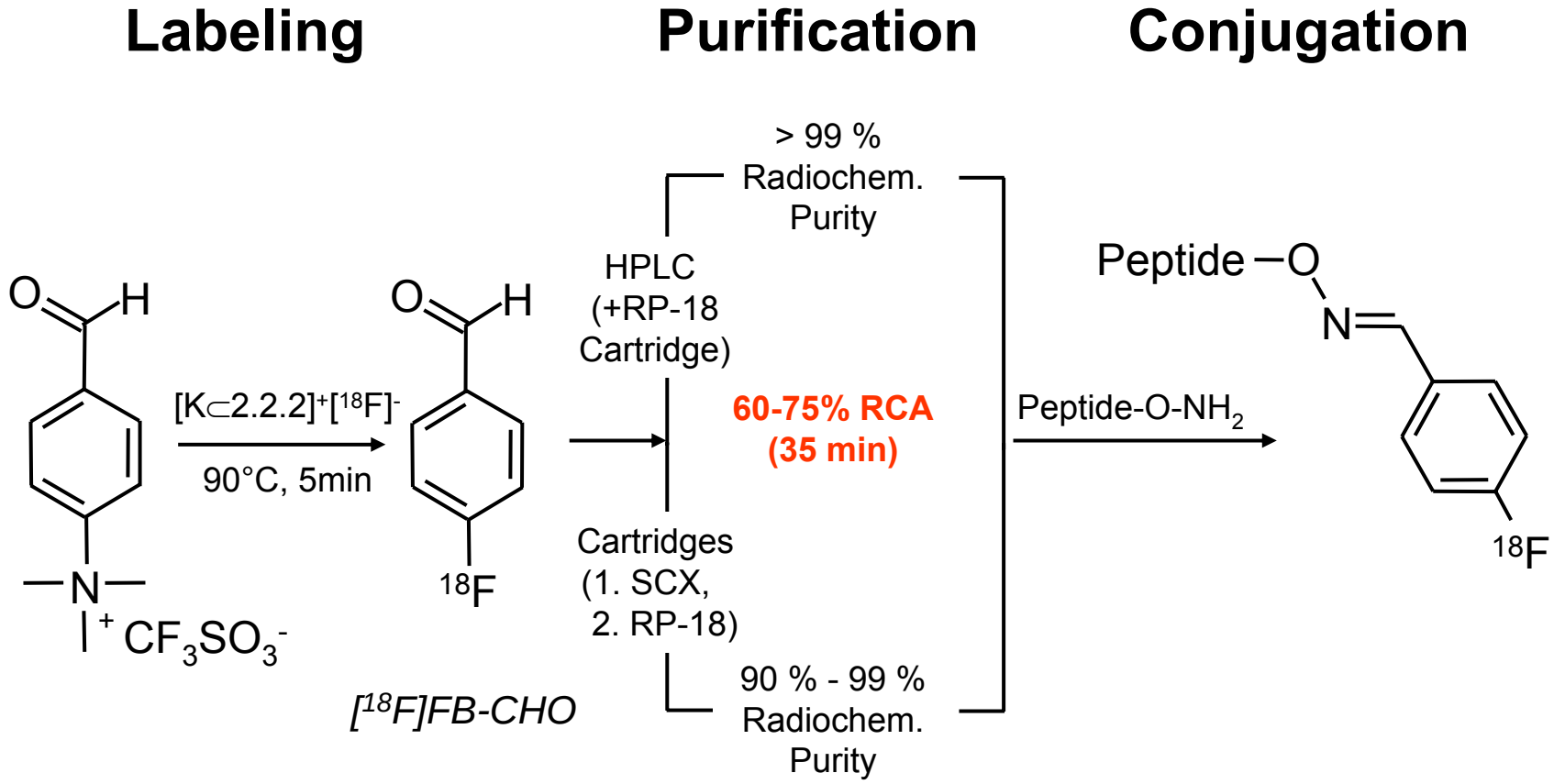

Route suitable for a variety of radiolabeled aldehydes and ketones

Binding Affinities of Multimeric RGD-Peptide Constructs

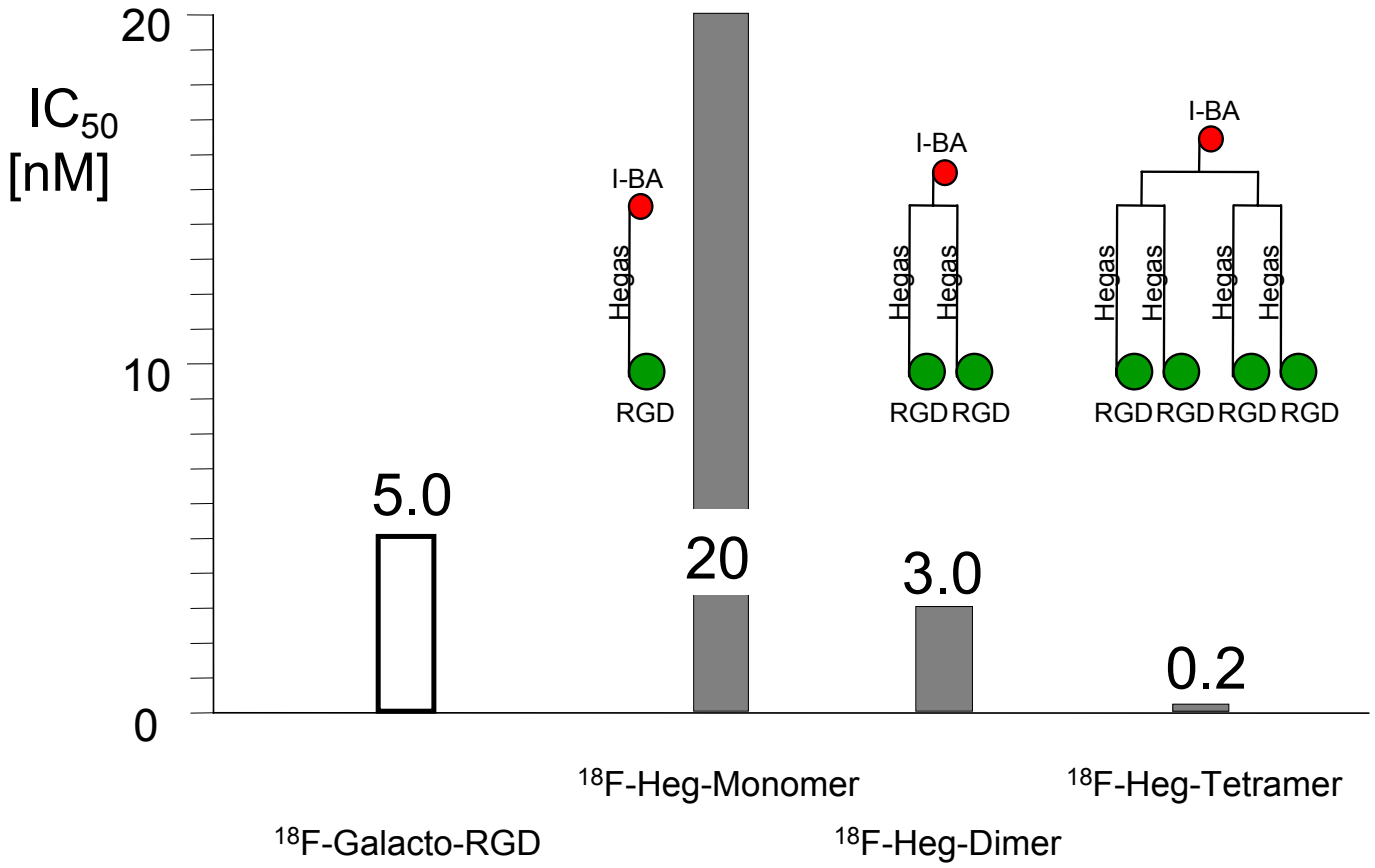

Tumor to Organ Ratios

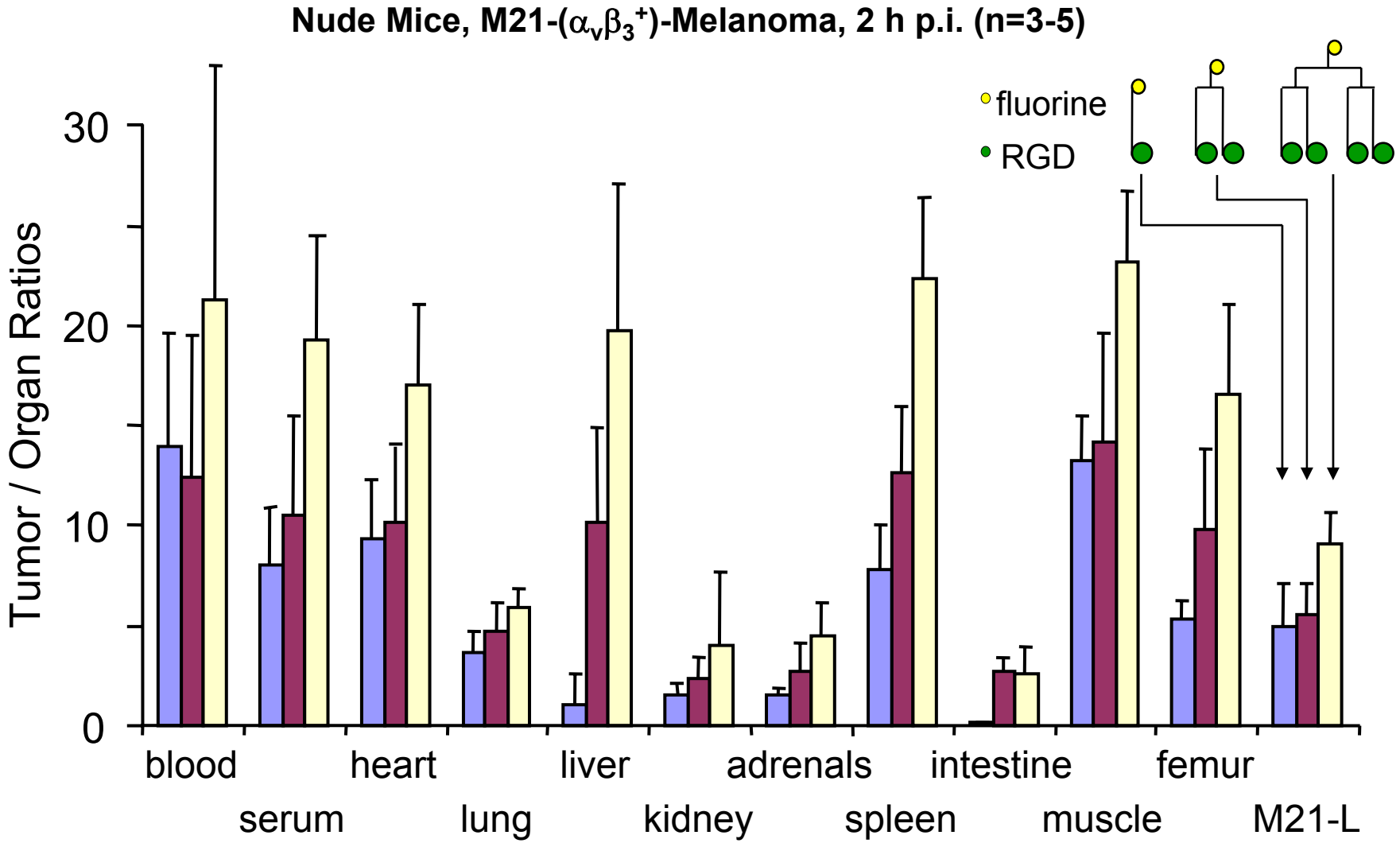

PET Imaging of [^{18}F]RGD-Mono-, Di- and Tetramers

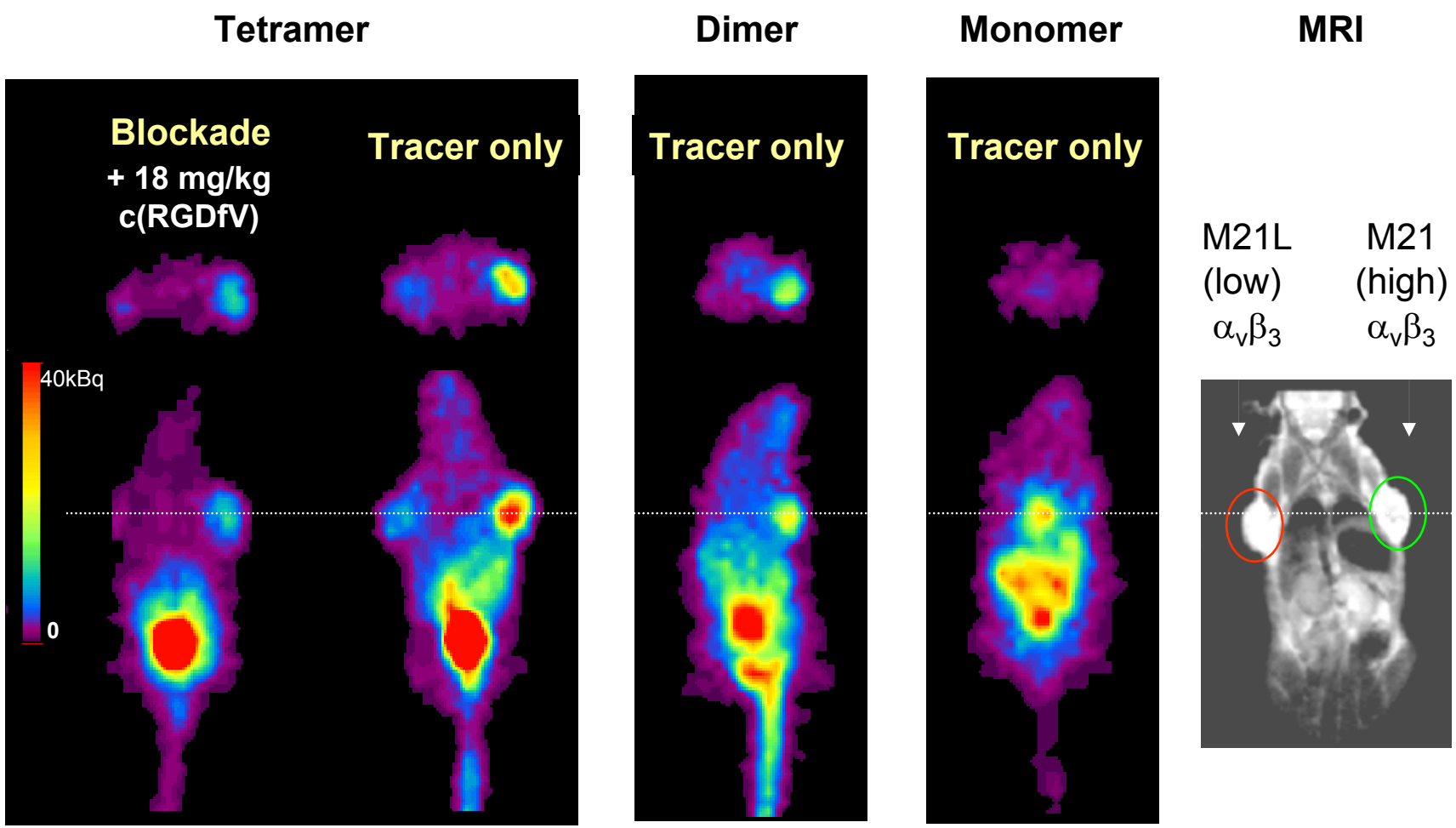

ECAT Exact HR$^+$, 90 min p.i.

Affinities of Multimeric RGD-Peptides with/without RAD-Sequences

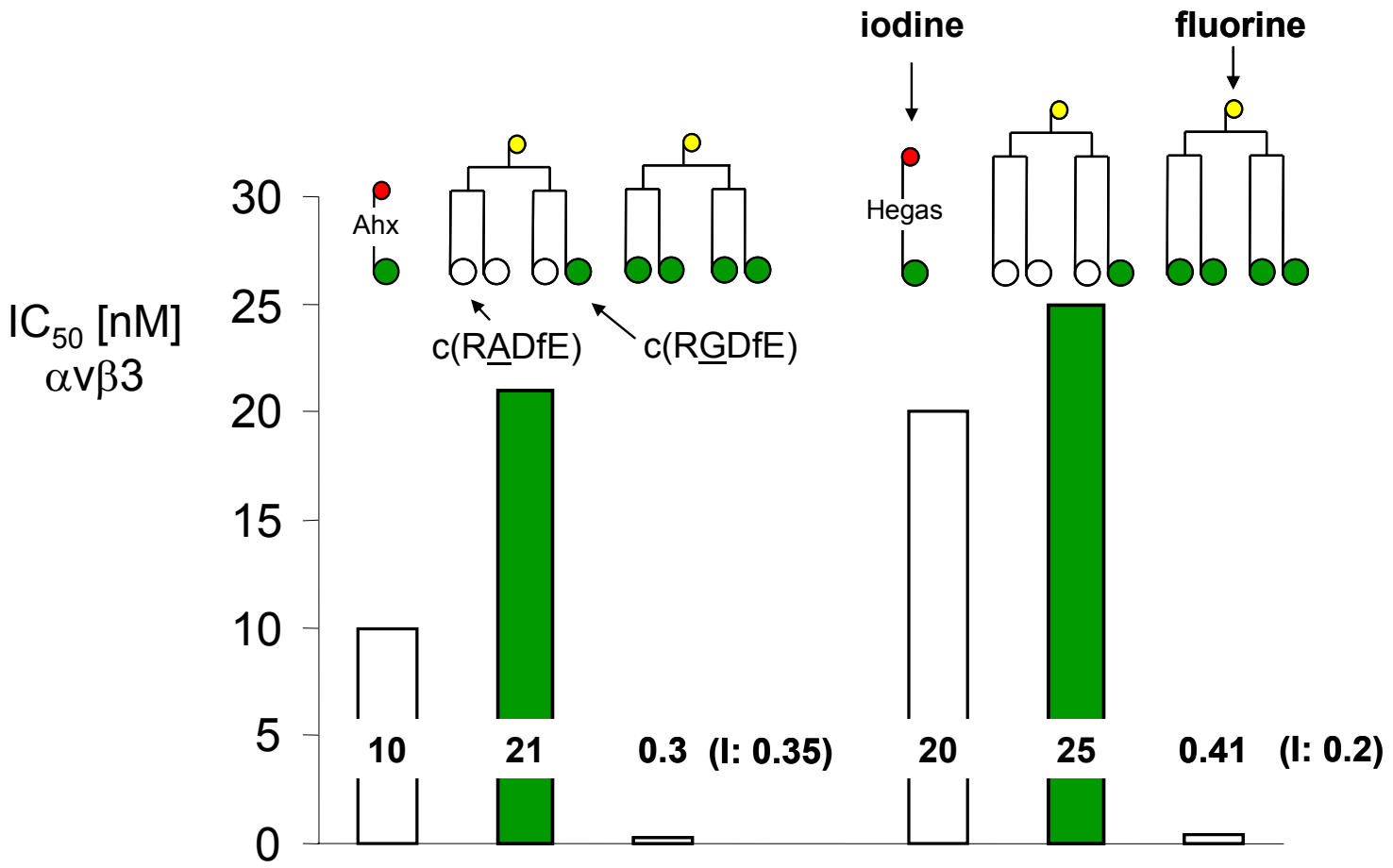

Thumshirn et al. Eur Chem. 2003

PET Imaging of Tetrameric [^{18}F]RGD with and without „Knockout“ Sequences

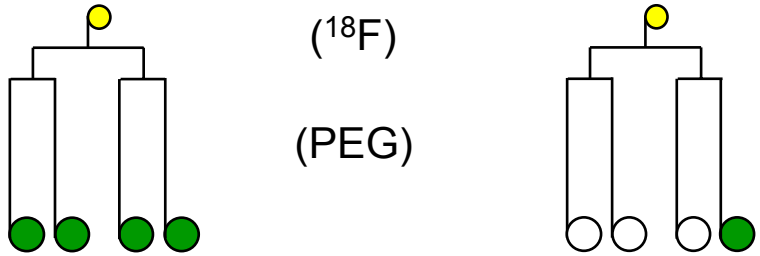

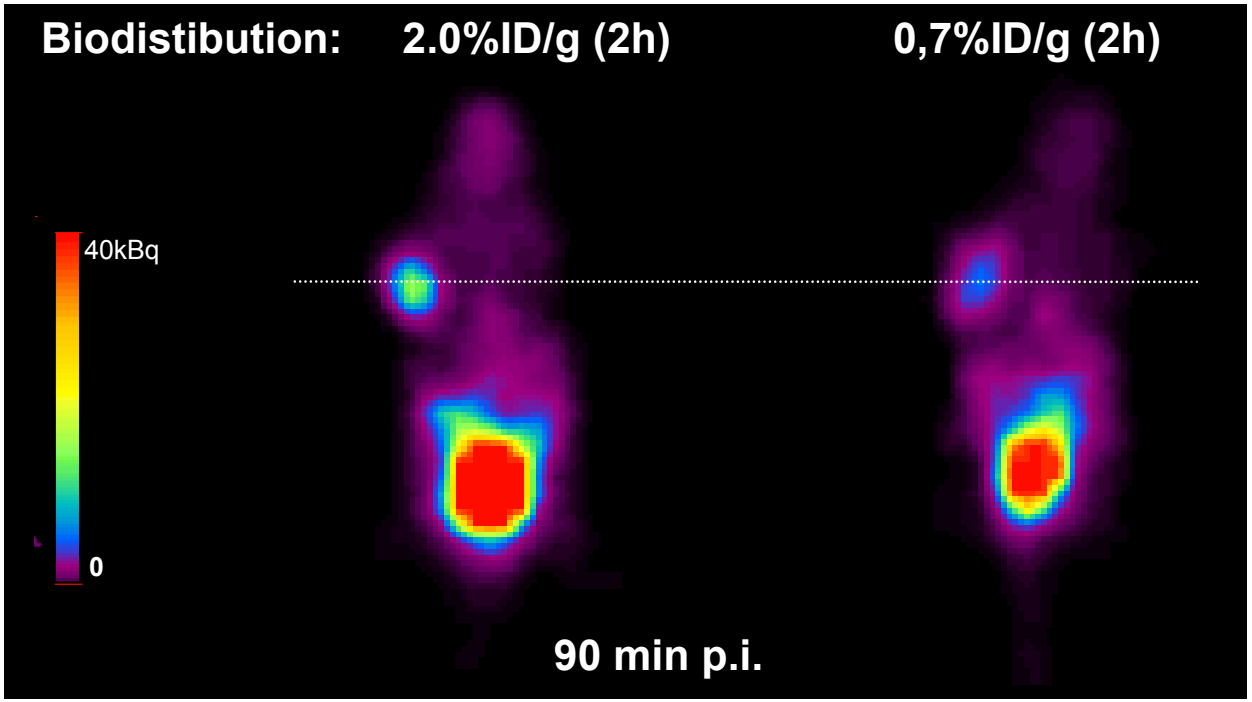

ECAT Exact HR^{+}, 90 min p.i.

Poethko et al. Radiochimica Acta 2004

Radiopharmaceutical Chemistry and Development of Radiopharmaceuticals